The Thesis Committee for Leila Dolce Donn
Certifies that this is the approved version of the following Thesis:

Long-Term Human Impact on a Neotropical Fluvial System in the Belize-Guatemala Transboundary Area

APPROVED BY
SUPERVISING COMMITTEE:

Timothy Beach, Supervisor

Sheryl Luzzadder-Beach

Carlos E. Ramos Scharrón

Long-Term Human Impact on a Neotropical Fluvial System in the Belize-Guatemala Transboundary Area

by

Leila Dolce Donn

Thesis

Presented to the Faculty of the Graduate School of

The University of Texas at Austin

in Partial Fulfillment

of the Requirements

for the Degree of

Master of Arts

The University of Texas at Austin

December 2018

Acknowledgements

I would like to thank Tim Beach, my graduate advisor, for providing me with guidance throughout this project. I would like to thank Sheryl Luzzadder-Beach and Carlos E. Ramos Scharrón, my thesis readers, for providing additional advice. I would also like to thank Jason Yaeger and Kathryn Brown for helping me with the fieldwork necessary for completion of this project, and for letting me stay at their field camp. Finally, I'd like to thank the other graduate students in my lab group, as well as the Department of Geography and the Environment at the University of Texas at Austin. They provided me with the support and resources necessary to produce this thesis.

Abstract

Long-Term Human Impact on a Neotropical Fluvial System in the Belize-Guatemala Transboundary Area

Leila Dolce Donn, MA

The University of Texas at Austin, 2018

Supervisor: Timothy Beach

Humans have played a significant role in the geomorphic evolution of the Belize River Valley in western Belize over the past 4,000 years, and this anthropogenic landscape still influences land use and flooding regimes today. Using LiDAR and GIS, fieldwork and lab analyses, I have studied the ways in which ancient Maya construction and agriculture affected the sediment budget thereby influencing geomorphic evolution of the river system. Soil geochemistry and radiocarbon dating have identified potential paleosols characterized by high levels of phosphorus, calcium, and potassium. These horizons are also composed of clay-sized particles, abundant organic matter and elevated magnetic susceptibility values. These buried soils are often overlain by a deposit of coarse, non-local sandy material that was transported from the Maya Mountains some 50 km away. These results may suggest that Maya activity caused changes to the Belize River's sediment budget, thus contributing to the geomorphic evolution of the fluvial landscape. More research is required to further test this hypothesis.

Table of Contents

List of Tables

List of Figures

Chapter 1: Introduction

By 2050 over half of the world's population will live in the tropics (Roberts et al. 2017), however we have a poor understanding of tropical watersheds. This is despite millennia of human interaction and land use. Evidence exists for human use of the Belize River Valley watershed across the last four millennia, from the Maya Archaic to the present. The Belize River Valley watershed is a clay fluviokarst floodplain located in a tropical wet-dry climate. This thesis focuses on a subset of the watershed: a 3-km stretch of the Mopan River with an average slope of less than 5° (Figure 1.1). Some of the largest and most enduring Maya cities in Central America were located in this watershed, and today intensive agriculture supports modern populations throughout the valley. I have studied the sediment record to identify and quantify markers of landscape changes to floodplain aggradation and erosion, both human and natural, over the past 4,000 years during which the landscape has been humanized. I hypothesize that as the Maya were deforesting their landscape for construction and for agriculture, they were causing large-scale erosion and thus altering the Mopan River's sediment budget. This altered the river's flood frequency, shaping the landscape as it exists today. This thesis tests this hypothesis.

This kind of research can inform environmental management systems and resource use today. To quantify rates of landscape change, we need to understand linkages between climate, flood regimes, and human activity through time. I have studied landscape formation in the Belize River Valley using a combination of approaches that include mapping with GIS and LiDAR imagery, fieldwork, and lab analyses, using methods from geography, geoscience, and geoarchaeology. These are the first steps necessary to develop a conceptual model of landscape formation.

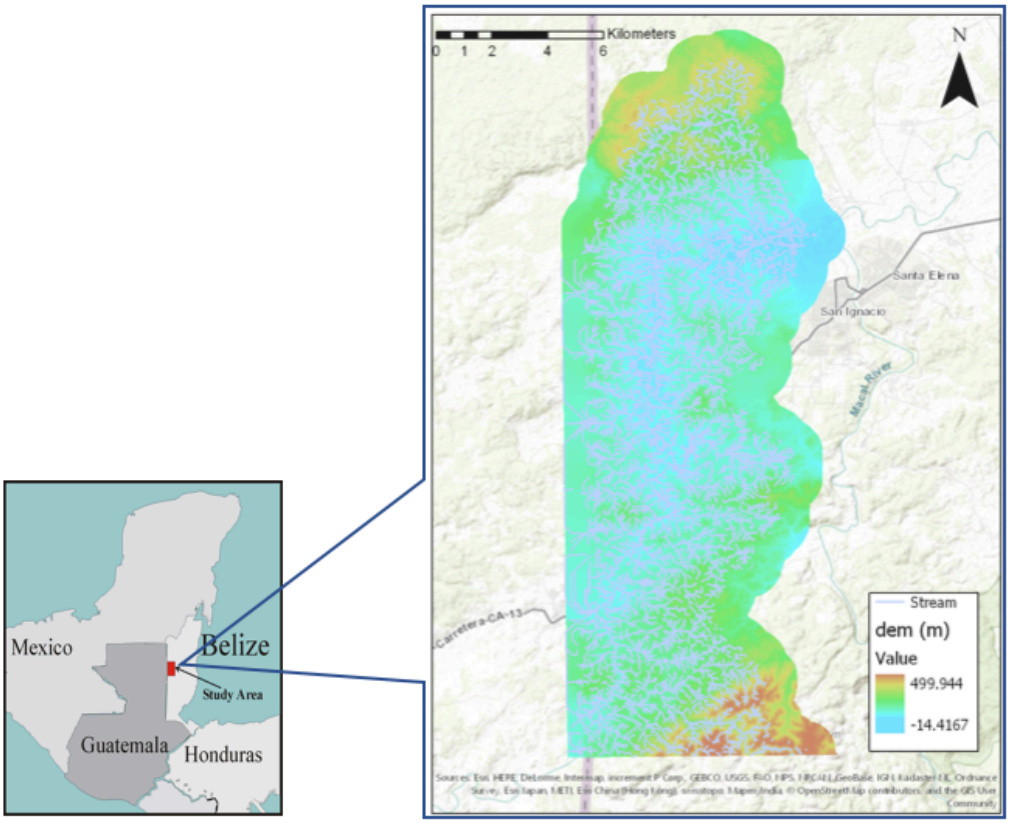

Figure 1.1: Study area

ADDRESSING RESEARCH GAPS

This thesis addresses two key research gaps in this region: geomorphic mapping of the river system and developing a record of geomorphic and hydrological change in the watershed. The Belize River Valley has a continuous history of human occupation and flooding over the past 4,000 years, but it still lacks even a rudimentary recurrence interval for predicting floods and for hazard planning. Geomorphological, geoarchaeological, and remotely sensed data can provide some of the flood planning information that we do not yet have for developing nations like Belize.

There is very limited and sometimes inaccurate river stage gauging data available for the Mopan River near the study area. The Belizean government sporadically maintained several gauging stations across the country from 1981 to 1997, but recent data are not available. Trigg et al. (2016) checked the reliability of some of these outdated data against a high-fidelity Regional Flood Frequency Analysis (RFFA) model created by Smith et al. (2014). They found that the extant discharge data for the Mopan River shows a mean annual flood that is 578 m^3/second less than the RFFA's estimated flood volume. This suggests that gauging data necessary for flood prediction is incomplete. Additionally, the publicly available watershed map for the Belize River Valley (Meerman and Clabaugh 2017) that Trigg et al. (2016) use for flood prediction does not agree with the stream network shown in our LiDAR dataset. This is likely because Meerman based his stream delineation on a 10-meter resolution digital elevation model from the Shuttle Radar Topography Mission, but the LiDAR we use for this study has a resolution of 1-meter. Accurate stream network delineation is the first step in flood prediction.

In terms of paleofloods, Muhs et al. (1985) present data based on soil profiles for the Macal floodplain, another key tributary of the Belize River. These data indicate, based on down-profile organic matter content (Soil Survey Staff 1975), that the Macal floodplain has not experienced frequent high-magnitude flooding since at least the Maya Late Classic (1350-1050 BP). Holley et al. (2000) present a slightly earlier date for what they describe as "catastrophic" Mopan flooding, suggesting that this has not occurred since the Maya Early or Middle Classic (1700-1350 BP). Modern discharge data from 1982 to 1994 for the Macal and Mopan Rivers show infrequent high-magnitude flooding, with only four annual maximum flood discharges exceeding 400 m3/s for the Macal River and no floods exceeding 300 m3/s for the Mopan River (Smith 1998). Since Muhs et al. (1985) and Holley et al. (2000) show that high-magnitude flooding occurred with some

frequency in ancient history, Smith suggests that both rivers have undergone significant changes in discharge and flooding behavior over the last few thousand years (Smith 1998). My work provides an opportunity to study both past and present flood patterns through soil profiles and identification of paleo floodplain features visible in LiDAR imagery.

Chapter 2: Background

MAYA CHRONOLOGY

The first traces of human landscape modification in the Maya Lowland Region begin to show up during the Archaic period, around 5000 BP (Table 2.1; Beach et al. 2009). The Archaic period extends from around 5000-3000 BP. It is defined by early forms of agriculture, followed shortly thereafter by erosion as documented in the regional sedimentary record. Most early agriculture was swidden, but Pohl et al. (1996) suggest that wetland agriculture began during the Archaic. The Preclassic follows the Archaic, extending from 3000-1700 BP. During the Middle Preclassic, from 2900-2300 BP, a small Maya population continued to practice swidden agriculture. Evidence from lake cores indicates that soil erosion increased in some places during this time. Then, in the Late Preclassic, from 2300-1700 BP, both population and agricultural intensity increase. The Maya begin to create agricultural terraces and practice wetland farming (Fedick 1991; Pohl et al. 1996; Luzzadder-Beach and Beach 2009; Luzzadder-Beach et al. 2012).

Cultural Time Periods of the Maya (after Beach et al. 2008)			
Years BP	**Years BC/AD**	**Cultural Period**	**General Human-Environment Patterns**
9000+	8000 BC +	Paleoindian	Hunter-gatherer
9000-4200	8000 BC-2000 BC	Archaic Period	Stone tools, early agriculture
4200-3000	2000 BC-1000 BC	Early Preclassic	Agriculture, deforestation
3000-2400	1000 BC-400 BC	Middle Preclassic	Agriculture, deforestation, increased erosion
2400-1850	400 BC-AD 159	Late Preclassic	Agriculture, deforestation, increased erosion, population increases
1850-1700	AD 159-AD 250	Terminal Preclassic	Continued erosion
1700-1350	AD 250-AD 550	Early Classic	Less erosion, population increases, increased agriculture
1350-1180	AD 550-AD 800	Late Classic	Less erosion, population peak, wetland agriculture increases
1180-1050	AD 800-AD 900	Terminal Classic	Wetland agriculture increases
1050-700	AD 900-1200	Early Postclassic	Limited/opportunistic use of some agricultural systems
700-450	AD 1200-AD 1511	Late Postclassic	Reforestation
450-present	AD 1511-present	Colonial/Modern	Reforestation

Table 2.1: Cultural periods and transitions of the Maya. From Krause 2018.

The Maya Classic period follows the Preclassic, beginning in 1700 BP and continuing through 1050 BP. It is characterized by higher populations, intensive agriculture, and hydraulic manipulation. Evidence for soil conservation, such as terracing, becomes much more common during this period. Agricultural terraces are a significant water management feature because they increase soil depths and soil moisture, as well as enable diversion and redirection of water flows. These modifications likely allowed the Maya to more readily adapt to changing environmental

conditions. Intensive wetland agriculture with canals and fields also expanded in several key wetland zones of the region (Chase and Chase 1998; Dunning et al. 1999). Erosion actually decreases toward the end of the Classic, during the Late Classic (1350-1050 BP, Krause 2018). Toward the end of the Late Classic, a significant dry period and a series of droughts shows up in the sedimentary record, but it is not clear how the drought affected the Maya. It is clear, however, that around 1100 BP, the beginning of the Postclassic, the Maya began to abandon many of their sites. Some evidence exists for an Early Post Classic drought as well (Hoggarth et al. 2017). During the Postclassic, populations were more dispersed and centered around water bodies. Pollen evidence indicates reforestation and less intensive cropping and sediment evidence shows a decrease in lake deposition rates. We also see a corresponding erosion rate decrease in the sedimentary record, which is likely due to the decrease in agriculture and associated reforestation.

Below I present a Maya chronology that is specific to my study area, the Belize River Valley. Early settlement within the Belize River Valley began during the Archaic period (8000-900 BC; Stemp et al. 2016). Populations expanded during the ensuing Middle Preclassic period, and there is evidence of multiple-household settlements at several sites in this region, including nearby Xunantunitch (Yaeger 1997; Figure 2.1). Several Middle Preclassic settlements also have pyramid shrines, including Actuncan (McGovern 1993) and Xunantunich (Robin et al. 1994). The Middle Preclassic population in the upper Belize River Valley was small and agrarian, but there were differences in power dynamics among sites with several sites possessing ritual importance (Yaeger 2000). The Middle Preclassic Maya also maintained long-distance trade networks with other parts of Mesoamerica. The Late Preclassic is not as well documented as the Middle Preclassic, but regional archaeology suggests that there was a sizeable population in the upper Belize River Valley at this time. Late Preclassic architecture was more elaborate, and many sites

clearly served as centers of ritual power. It is likely that centers of ritual power were also politically important. Over the next 300 years, during the Early Classic period (cal AD 250-600), sites throughout the Belize River Valley began to grow in size (Ebert et al. 2016). Settlement and construction data from Barton Ramie (Awe and Helmke 2005), Cahal Pech (Awe and Helmke 2005), Buena Vista (Ball and Taschek 2004), and Pacbitun (Healey et al. 2004) indicate that populations were also increasing throughout this period.

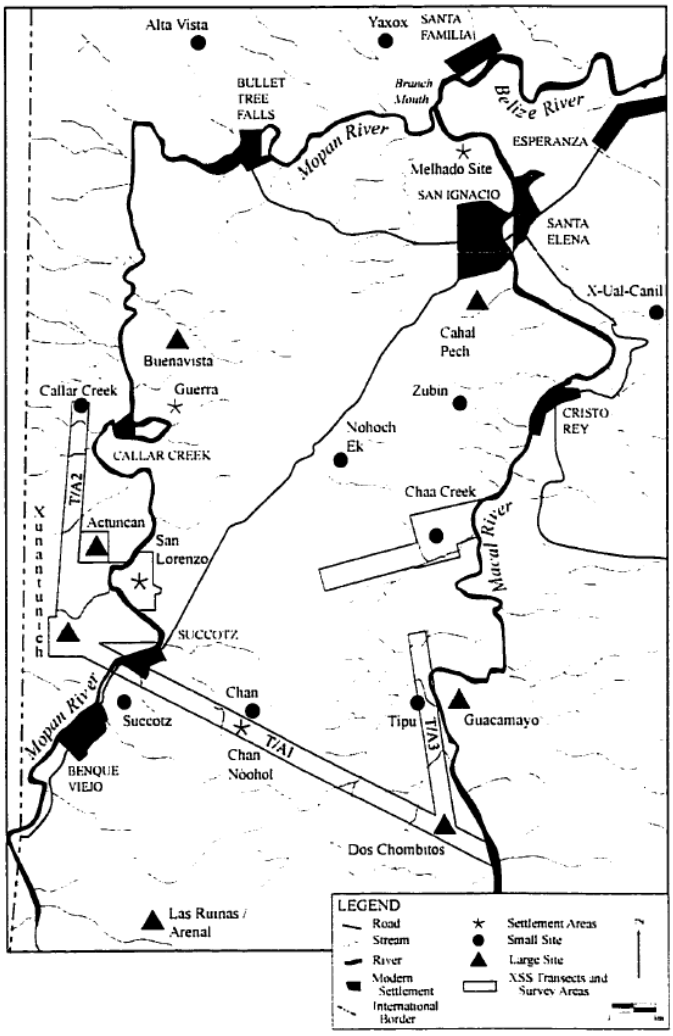

Figure 2.1: Archaeological sites and modern settlements in thesis study area. From Yaeger 2000.

The Late and Terminal Classic periods experienced continued population growth (Yaeger 1997). The population of the valley expanded substantially, indicated by the intensity of residential construction and ceremonial architecture at both old and new polities. During the Late Classic, a number of important polities existed concurrently within close proximity. Then, at the end of the Terminal Classic, there was a massive population decline in the region that occurred at the same time as significant socio-political changes. Most of the region's large centers became abandoned by the end of the Terminal Classic, if not earlier (Yaeger 2000). A much smaller population with few centers of importance characterized the Postclassic. Even the centers that retained some importance experienced large population declines. Actuncan, Buena Vista, Xunantunich, and Baking Pot (Hoggarth et al. 2014) remained unoccupied during this period. Outside of the Belize River Valley, however, some polities did persist through Spanish contact. This includes Lamanai in northwestern Belize (Graham 2004). During the Spanish Colonial period of the mid-1500s, Spanish conquistadors attacked many Maya centers (Yaeger 1997). The upper Belize River Valley, however, was at the edge of the area controlled by the Spanish crown. Therefore, the Maya that lived in this area were able to maintain contact with still-independent Maya centers in other parts of Mesoamerica. This connection may be what enabled the success of the Maya rebellion against the Spanish in 1648, ousting the Spanish from the region. During the 18th century, small Maya villages still survived, just beyond the reach of the weak Spanish frontier. British lumber extraction expanded into the Belize River Valley during this period. Over the first half of the 20th century, logging activity declined and small- and large-scale agriculture arose. Agriculture still plays an important part in the region's economy. It is accompanied by a growing tourism industry (Kwan et al. 2010).

In summary and with regard to this thesis, small populations and forested landscapes characterized the area through the Archaic period (ending 2000 BC). We see little evidence of erosion in the sediment record. Beginning in the Early Preclassic (2000 – 1000 BC) and extending through the Terminal Preclassic (AD 159 – AD250), population increased and deforestation became widespread as agriculture intensified (Figure 2.2). During this period we see a significant increase in the evidence of erosion in the sediment record. In the Early Classic (AD 250 – AD 550) the Maya began to use methods of soil and water regulation, such as terracing and wetland farming. We see a corresponding decrease in the evidence of erosion in the sediment record. Population and agricultural intensity began to decrease toward the end of the Late Classic (AD 550 – AD 800) into the Terminal Classic (AD 800-AD 900). After this point, erosion rates slowly begin to decrease (Anselmetti et al. 2007). This gradual decrease in erosion may be because at the beginning of the Terminal Classic, as population began to decline, the landscape was still largely deforested. This meant that terraces and other methods of erosion control were not maintained, and runoff rates were high. By the Postclassic (AD 900 – AD 1511), however, the landscape had become reforested and erosion rates become very low.

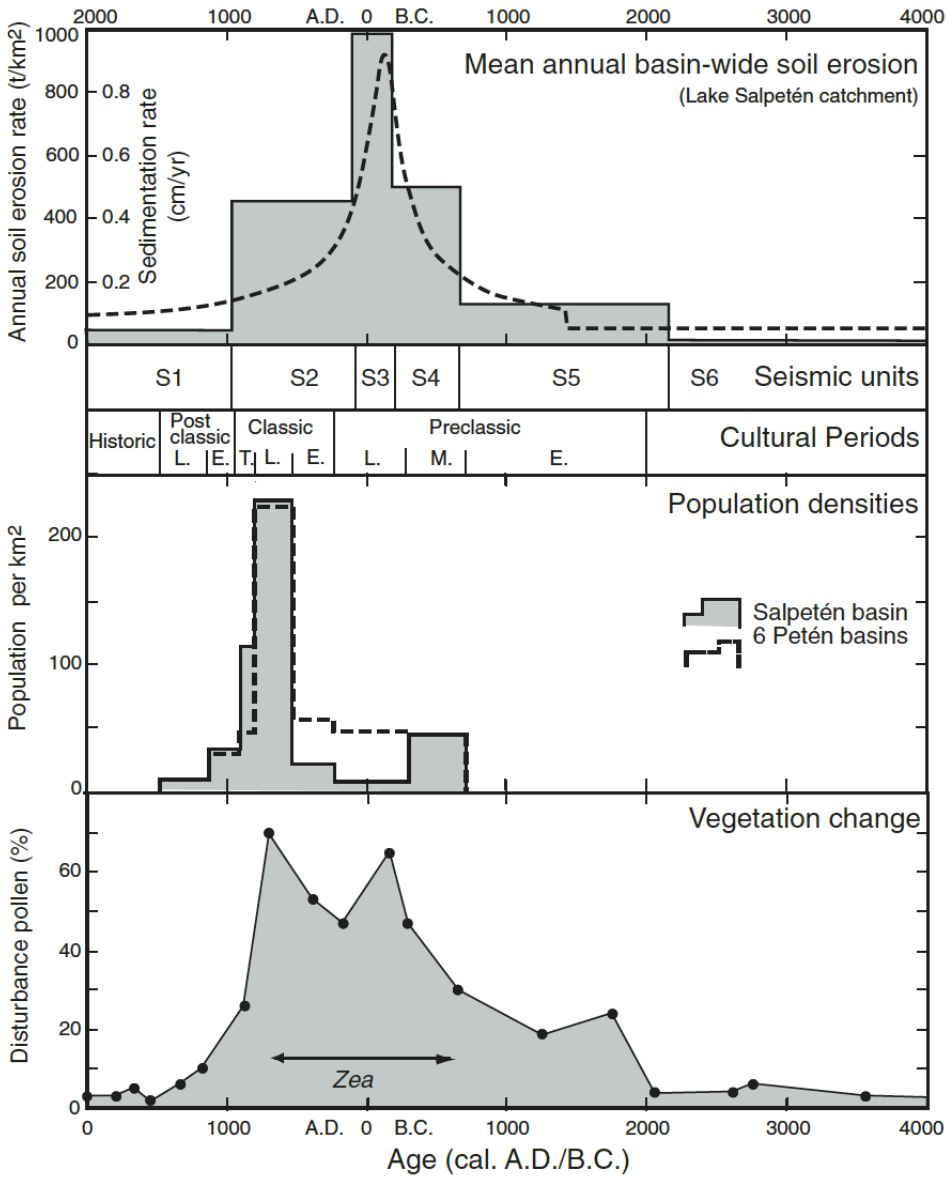

Figure 2.2: Erosion, population, and agriculture data from Lake Salpetén in northern Guatemala over the last 6000 years. For erosion graphic, the gray area represents annual soil rates over the entire catchment. The dashed line represents the lacustrine sedimentation rate at the coring site based on age modeling (Rosenmeier et al. 2002a, 2002b). The population graphic shows the population densities corresponding with different Maya periods based on both Salpetén alone as well as five other sites in northern Guatemala. The disturbance pollen graphic represents the percentage of non-natural tropical forest vegetation, including abundant Zea (corn), and may indicate deforestation and associated agriculture. From Anselmetti et al. 2007.

LEGACY SEDIMENTS

Karl Butzer, the founder of the field of geoarchaeology, stressed the importance of understanding the ways that human-environment interactions can affect the landscape (Butzer 2008). Humans have become a powerful geomorphic force, and one of the most obvious ways to understand potential human impacts on our environment is to study the nature, scale, and timing of alluvial sedimentation. Studies of sediment generated from human activities, known as 'legacy sediment,' have been carried out across the world over the past century. It is important to note that no such study exists for the Belize River Valley.

Evidence of agriculture-related erosion is present in soil profiles across the world and throughout time. Research on the Dust Bowl of the 1930s demonstrated that alluvial stratigraphy can provide a complex record of the intertwined effects of humans and climate on landscape formation (Happ et al. 1940). In their 2013 paper, Brown et al. studied a series of sites with histories of agriculture around the world and found that the profiles at these sites showed a clear sedimentary boundary associated with the advent of agriculture. At sites in northern Africa, Faust et al. (2004) and Schuldenrein (2007) found primarily climate-driven sedimentary changes that were then exacerbated by agricultural activities. The resultant stratigraphic signature was, therefore, as it was during the Dust Bowl, a complicated product of human-environment interaction (Cordova and Porter 2015). Beresford-Jones et al. (2009) came to a similar conclusion in their paper discussing long-term landscape changes in the Ica Valley of Peru. Today the Ica Valley is an unpopulated desert, however extensive archaeological remains indicate that it used to be highly populated. This suggests that at some point the region had the natural resources to support a large population. Beresford-Jones et al. (2009) conclude that a mega-flood initiated these extreme

regional environmental changes. These changes were then magnified by the combined influence of poor floodplain management and changes to precipitation patterns.

Areas characterized by extensive land clearance associated with long histories of farming in North America generally have very distinct profile characteristics with floodplain soil covered by rapid overbank sedimentation (Beach 1994; Walter and Merritts 2008). These profiles represent frequent floods and show both associated aggradation and erosion. Beach (1994) and Walter and Merritts (2008) hypothesize that these floods are the result of deforestation and decreased infiltration due to agriculture increasing sediment supply and runoff to rivers. Knox's (2006) research demonstrates that human activity over the past approximately 200 years in the Upper Mississippi Valley has had more of an impact on floodplain geomorphology and sedimentation than anything natural that took place over the past 10,000 years. Related research about the relationship between the intensity of human disturbance and the scale of fluvial change highlights the complexity of this type of work. Verstraeten et al.'s (2017) work at a number of sites across Europe, the eastern Mediterranean, and the eastern United States, at sites ranging in age from 200 years to 5,000 years old, shows that there are no similar identifying characteristics associated with sediments following anthropogenic disturbance. Dotterweich (2013) also finds evidence of soil erosion across a range of Old and New World sites, since the beginning of agricultural activity. In northwestern Belize and the Petén of northern Guatemala, the 'Maya Clays' may provide a regional agriculture-related erosion signature (Anselmetti et al. 2007). These sediments are hypothesized to be the product of Maya land use, reflecting erosion and then deposition in wetlands, floodplains, and other types of sinks (Beach et al. 2006).

ANTHROPOGENIC LANDSCAPES OF MESOAMERICA

We know that the Maya altered their landscapes in many ways. For example, they adapted to changing environmental conditions through constructing complex systems of dams, diversions, and agricultural fields with canal networks (Luzzadder-Beach et al. 2012; Beach et al. 2015; Luzzadder-Beach et al. 2016). These adaptations in some cases enabled the Maya to persevere through centuries of environmental changes. The land uses of any civilization, however, are never perfect. The Maya built remarkable landesque capital; nonetheless, they eroded hillslopes and degraded soil and water quality (Luzzadder-Beach and Beach 2008; Luzzadder-Beach and Beach 2009). In some places, this degradation may have even resulted in site abandonment. Such may be the case in the Maya heartland of the Peten, which popular and archaeological literature consider one of the world's important societal 'collapses' (Lentz et al. 2014).

At the large Maya center of Tikal in Guatemala's Petén, land cover and land use studies indicate that the Maya were continuously engineering their landscape, though even these intense alterations were not sufficient to meet the needs of the burgeoning population (Lentz et al. 2014). An estimated 850 km^2 of land was deforested at Tikal during the Late Classic period, equivalent to around 60-70% of the site's total area. It is hypothesized that the area of fertile land that was required to feed the large population meant that fields were only allowed to sit fallow for three years at a time, which is a relatively short fallow period compared to historical studies of swidden agriculture in this region. This practice would have likely led to erosion and degradation of soil fertility. At the same time, we know that the residents at Tikal were aware of the detrimental effects of soil erosion because archaeological excavations have revealed chert-lined terraces that would have reduced hillslope erosion. Nonetheless, as aforementioned, one of the explanations for the decline of Tikal is directly connected to natural resource demand exceeding supply.

In the Maya Lowlands of northern Belize there is also clear evidence of Maya landscape alteration. These alterations variably resulted in erosion and aggradation of sediment, sometimes leading to degradation of modern soils, while at other times enhancing soil fertility and moisture holding capacity. Agricultural terraces and canal field systems in northern Belize at Chan Cahal (Beach et al. 2015; Luzzadder-Beach and Beach 2009), Birds of Paradise (Beach et al. 2015; Luzzadder-Beach et al. 2012), Chawak But'o'ob (Beach et al. 2015; Luzzadder-Beach et al. 2012), and Colha (Jacob 1995) provide information about the range of Maya landscape alterations and their lasting modern impacts. A great diversity of Maya wetland field systems exist across the Maya Lowlands through time and space, from simple drained fields that appear to have random ditches dug across them, to raised fields with extensive, linearly oriented canals that would have required significant planning (Beach et al. 2015).

Wetland agroecosystems provide some of the best examples of landscape formation through human-environment interaction. At the site of Chan Cahal, located in the Rio Bravo watershed, the geomorphic evolution of the wetland field system includes contributions from both human and natural drivers (Beach et al. 2015). Sea level rise and an attendant increase in the water table meant that the Maya had to adapt their field system to handle the increased amount of water and changes to soil and water chemistry(Luzzadder-Beach and Beach 2008; Luzzadder-Beach and Beach 2009). Birds of Paradise, located in the same watershed, has a more extensive canal system (Beach et al. 2018b). Evidence indicates that this system was formed through a mix of human and natural drivers. At Chawak But'o'ob, also part of the Rio Bravo watershed, research shows that floodplain aggradation rates increased during the period of intense Maya land use. The influx of sediments came from field construction, overbank floodplain sedimentation, and hillslope erosion. In Cobweb Swamp at the site of Colha, Jacob (1995) presents clear evidence of Maya wetland

modification, though the nature, chronology, and extent of modification is unclear. Research at the swamp suggests that the Maya altered the topsoil at the edge of the wetland area and the wetland margin, modifying it through a small range of changes from ditch digging to channel straightening. This canal and field system are not well-organized, indicating lack of pre-planning.

In addition to wetland fields, sinks and lakes serve as sediment traps and therefore can provide important records of sediment aggradation generated by geomorphic change. Beach et al. (2008) have found increased aggradation rates in these sinks beginning in the Preclassic, coincident with increasing Maya populations. They hypothesize that aggradation rates increased due to deforestation-related erosion as the Maya cleared land for agriculture. Fields closer to the coast, however, experienced aggradation due to sea level rise that caused groundwater, rich in calcium and sulfate, to precipitate gypsum (Luzzadder-Beach and Beach 2008; Luzzadder-Beach and Beach 2009). This natural aggradation mechanism can produce sediments that looks similar to those produced through human-driven processes, providing yet another example of how difficult it can be to untangle human versus naturally driven landscape change. Bajos can present interesting examples of complex landscape change. Data collected from agricultural bajos near La Milpa in northwestern Belize and Yaxha and Tikal, Guatemala, show that both human- and naturally-driven environmental changes resulted in the transformation of several bajos from perennial wetlands to seasonal swamps (Dunning et al. 2002).

All of these landscape alterations result in changes to the chemical signatures of the associated sediments. Altered fields frequently show changes to phosphorus levels and carbon isotope signals (Terry et al. 2004, Wells 2004). Phosphorus is an important indicator of human land use because it captures activity related to fertilization and waste. Additionally, the ratio of carbon isotopes present in the soil can be indicative of either naturally-occurring tropical rainforest

vegetation with a C_3 isotopic signature, or vegetation with a C_4 signature that includes non-naturally occurring maize. Analyzed soil profiles throughout the period of Maya occupation show high levels of C_4 vegetation isotopic signatures, which may represent the cultivation of maize or other tropical grasses or weeds associated with agriculture.

Closer to the Belize River Valley several kilometers north of my research area, Fedick (1994) studied a system of ancient Maya agricultural terraces. The terracing appears to be restricted to areas of low slope angle where Mollisols are present on consolidated limestone bedrock. Fedick associates terracing with the most fertile land in areas with the densest populations; he hypothesizes that terracing is an effort to conserve and improve agricultural resources rather than moving farming activity to lower quality land. Since the terraces at the site are all relatively small and associated with residential units, however, it seems likely that they served more to enhance soil development and moisture retention in small home gardens, than to reduce erosion from large-scale agricultural activity. There is also limited contour terracing in areas of moderate slope, which indicates agricultural expansion into land that required erosion-prevention measures.

Kirke (1980) studied a human-modified floodplain-wetland system in the Belize River Valley at Norlands Farm, also slightly north of my research area. He identified three different types of canals, two of which he postulates are human-modified. He hypothesizes that these human-modified canals were constructed for agricultural purposes: probably for control of water passing from the high ground to the river to supply more or less water as the situation demanded. Other functions may have included nutrient transport to the fields. At the site of San Lorenzo, where I studied several profiles discussed in this thesis, Holley et al. (2000) studied a buried Preclassic site using remote sensing. They hypothesized catastrophic flooding occurred sometime after the Preclassic Period, likely initiated upstream from San Lorenzo as a product of land clearance for

construction of major Maya centers and associated agricultural fields before and during the Early Classic. Then, at some point during the Late Classic the hillslope above the river channel at San Lorenzo was terraced, and erosion stabilized, perhaps decreasing flood frequency and/or flood magnitude.

LIDAR TO STUDY ARCHAEOLOGY AND LANDSCAPE CHANGE

Roering et al. (2013) find that the use of LiDAR for the study of landscape evolution and associated natural hazards has completely revolutionized the way we look at both modern and paleo landscape formation. LiDAR enhances geomorphic research in multiple ways: by providing a detailed base map for field mapping and sample collection, by enabling the efficient and accurate description of large-scale landscape features, and by permitting the identification of unknown and sometimes unanticipated landforms. LiDAR is particularly well suited to research in Mesoamerica, whose societies evolved in a densely vegetated environment where the canopy often obscures the land surface. For example, LiDAR surveys have recently offered a new interpretation of Caracol as a highly-connected, large ancient Maya center located within a human-modified landscape (Chase et al. 2011, Chase et al. 2012). Identification of nearly continuous agricultural terracing suggests that the ancient Maya of Caracol were highly concerned with soil and water sustainability. In the Belize River Valley, and across Mesoamerica, LiDAR helps to provide spatiotemporal information about anthropogenic landscape formation.

I have used LiDAR imagery to identify paleochannels of the Mopan River that are also located near to archaeological sites, studying soil profiles located near these channels. These profiles enabled me to test my hypothesis: that as the Maya were deforesting their landscape for construction and agriculture, they were causing increased erosion and sediment supply to the

Mopan River. This in turn altered the region's flood frequency and thus should be reflected in the sediment record of the modern floodplain. I therefore expected to find soil horizons from the Preclassic and Classic periods that showed characteristics of human use and long-term stability followed by horizons composed of course flood sediments.

Chapter 3: Setting

Regional Environment

There has been limited environmental research completed related to the Belize River Valley, which leaves large knowledge gaps. There are few sources of information about both geology and soils, and these are 30-50 years old. This older research was conducted when the region was much less deforested, making the area physically difficult to access and work in. Flores (1952) acknowledges difficult working conditions in his partial geologic characterization of the area, citing problems including few well-defined contacts, thick vegetation, carbonate precipitate concealing lithology, and presence of few fossils. Over the past three decades, however, the area has experienced an increase in population leading to mass-deforestation associated with agriculture and ranching activities (Cherrington et al. 2010). While large-scale deforestation is certainly not a good thing, it means that the area is now much easier to study, and as such, we hope to see an increase in regional environmental research. For now, we must use what sources we have available.

The Intertropical Convergence Zone (ITCZ) and the Easterly Trade Winds dominate modern climate in Belize and across the Maya Lowlands (Lachniet and Patterson 2009). The climate is warm year-round, with a mean average temperature of about 25 degrees Celsius (The World Bank Group 2018). Belize has a tropical wet-dry climate; the wet season occurs from June to December and the dry season extends from January to May. Rainfall increases from north to south, as a function of latitude, rainshadow, and elevation. Rainfall averages around 1350 mm in the north and 4500 mm in the south in the Maya Mountains (Fleming et al. 2011). Convective storms are common and are responsible for much of Belize's precipitation. Hurricanes also occur relatively frequently and can be devastating to the 300-km-wide country. Denommee et al. (2014)

found that a mean of 12 hurricanes occurred per century over the last 1200 years. Elevations across Belize range from less than 100 m amsl near the coast to about 500 m in the Vaca Plateau (Day 1993). The region has both Udic and Ustic soil moisture regimes and has an Isohyperthermic temperature regime (Van Wambeke 1987).

Prehistoric climate data derived from lake cores and speleothems from the Maya Lowlands indicate oscillating precipitation during the Archaic and Preclassic, transitioning into more stable conditions during the Late Preclassic (Beach 2015; Luzzadder-Beach et al. 2016), followed by climate stability until the advent of very severe drought during the Late to Terminal Classic. Severe drought appears in the record throughout the region during the Terminal Preclassic. A review of lake core, speleothem, and leaf wax data from the Maya Lowlands suggest that droughts occurring from 900 to 1100 CE were unprecedented in severity (Douglas et al. 2016). This dry phase also shows up in lacustrine records from Central Mexico, indicating that drought occurred between 700 and 1000 CE (Metcalfe and Davies 2007). Climate records from the northern Yucatan indicate that drought events between 800 and 950 CE resulted in a 20 to 65% decrease in rainfall (Douglas et al. 2016.). Records also indicate that there was another earlier period of drought between approximately 250 and 500 CE.

GEOLOGY

Geologic study of Belize has been limited. Geologists first described Belizean geology in the early to mid-1900s (Ower 1928; Flores 1952; Dixon 1955). Beginning in the 1960s and extending through the 1990s, oil companies researched reservoir potential in Belize's karst features, both on land and offshore (Miller 1966; Chevron Overseas Petroleum Company 1975; Belize Natural Resources Ltd. 1995). Work during the 2000s has focused on the reef system (Purdy et al. 2002;

Gischler 2003; Purdy and Gischler 2003; Gischler and Hudson 2004). There has also been some more recent work focusing on cave exploration, which I will discuss later. Deforestation continues to increase across Belize, and as infrastructure within the country expands even the more rugged parts of the country become increasingly accessible. Therefore, there is now opportunity, as well as need, for renewed geological study as population growth and climate change put Belize's natural resources under increasing stress.

The geology of Belize consists of low-lying, young sedimentary rocks surrounding the ancient, fault-bounded non-carbonate Maya Mountains (Figure 3.1; Miller 1996). The sedimentary rocks of Belize are primarily carbonate, the majority of which show some degree of karstification. The most intensely karstified carbonates occur primarily at the base of the mountains, which is due to runoff from mountain waters undersaturated in calcite (Miller 1996). When these aggressive waters encounter the carbonates at the base of the mountains, they create a wide range of intensely dissolutional features. Cretaceous carbonates in northern and central Belize make up the Barton Creek Formation (Pope et al. 1999). The Maya Mountains are an uplifted block of Paleozoic and Triassic metasedimentary, igneous, and sedimentary rock. Evolution of the range played an important role in the future deposition of carbonate rocks. A massive deposition event during the Cretaceous left a thick layer of evaporites and marine carbonates in the Caribbean (Miller 1996), which grade into reef facies that surrounded the then-extant Maya Mountains islands (Dillon and Vedder 1973). In northern Belize, a blanket of impact ejecta sediment from the late Cretaceous Chicxulub impact crater overlies the Barton Creek Formation, outcropping on Albion Island (Pope et al. 1999). The Albion Formation is characterized by a clay and dolomite spheroid bed overlain by an >10 meter thick eroded diamictite bed.

At the end of the Cretaceous, the western edge of the Maya Mountains was submerged and covered by Tertiary limestone and dolomite (Bateson 1972). The western portion of the range today remains obscured (Miller 1996). Slow subsidence and associated carbonate deposition has occurred in northern Belize throughout the Tertiary and into the Quaternary (Miller 1996). These soft carbonates compose the low elevation, seasonal swampy coastal plain of Belize. This region is less dramatically karstified than southern and western Belize, but still nonetheless exhibits a range of smaller scale dissolutional features. Karst landscapes are complex interconnected systems of surface channels and subsurface conduits that can rapidly transport water and any associated pollutants throughout the watershed. Therefore, it is important that we understand the karst landscapes of Belize so that we may work to efficiently manage water resources and plan for the future.

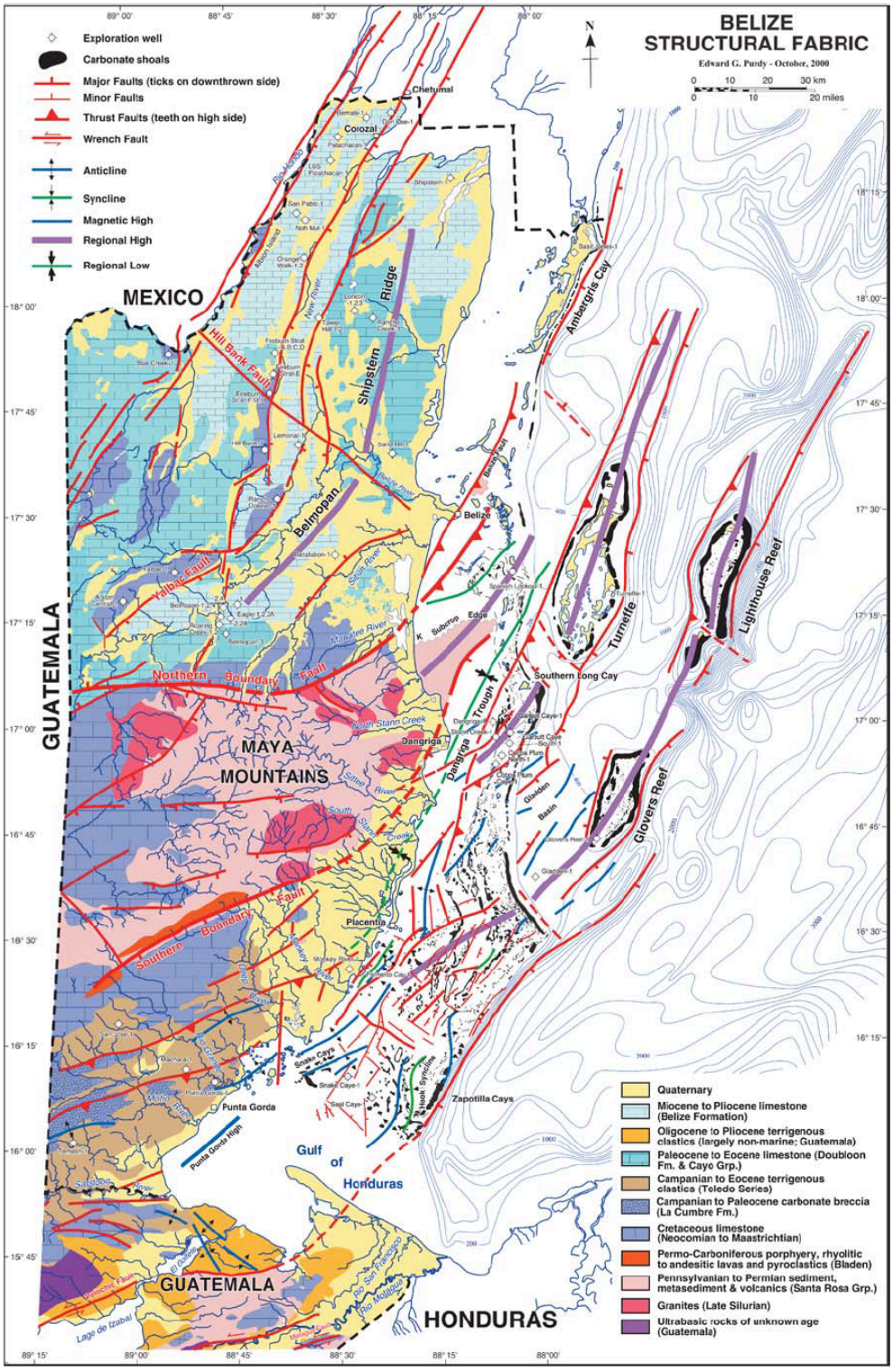

Figure 3.1: Belize geologic map. From Purdy et al. 2003.

Previous work provides a variety of estimates of the area of karst topography in Belize. Based on fieldwork and high-resolution LiDAR imagery, I believe that karst geology underlies most of Belize, though dissolutional features are the largest and most extensive in south-western and central Belize. Day (1996) suggested that karst in central Belize covers an area of about 200 km^2 over an 85-km-long east-west belt that is located north and west of the Maya Mountains and south of the Belize River Valley (Figure 3.2; Day 1993). Day (1996) also suggested that overall, carbonate bedrock underlies 50% of Belize's 23,000 km^2, around 22% of which he called karst. Both Day's estimate of area of carbonate bedrock and karst topography are likely too low, though more geological fieldwork is needed to accurately quantify Belizean karst. There are fewer dramatic dissolutional features, such as conduits and other types of voids, in northern Belize. However, the Tertiary limestones in the Rio Bravo area in the northwestern portion of the Orange Walk District and in the Yalbac Hills of the Cayo District show more intense dissolutional features than other northern locations (Day 1996). Additionally, fieldwork in northwestern Belize has identified numerous cenotes, some of which are quite large, such as the 30-meter-deep Laguna Verde (Hammond 2016; Luzzadder-Beach and Beach 2008; Luzzadder-Beach and Beach 2009). Further south, the Cretaceous limestones that flank the Maya Mountains show much more intense dissolutional features. Karst in this region covers about 2,000 km^2 north and west of the Maya Mountains, and includes the area south of the Belize River Valley. There is also a high concentration of highly developed karst features south of the Maya Mountains in the Toledo District.

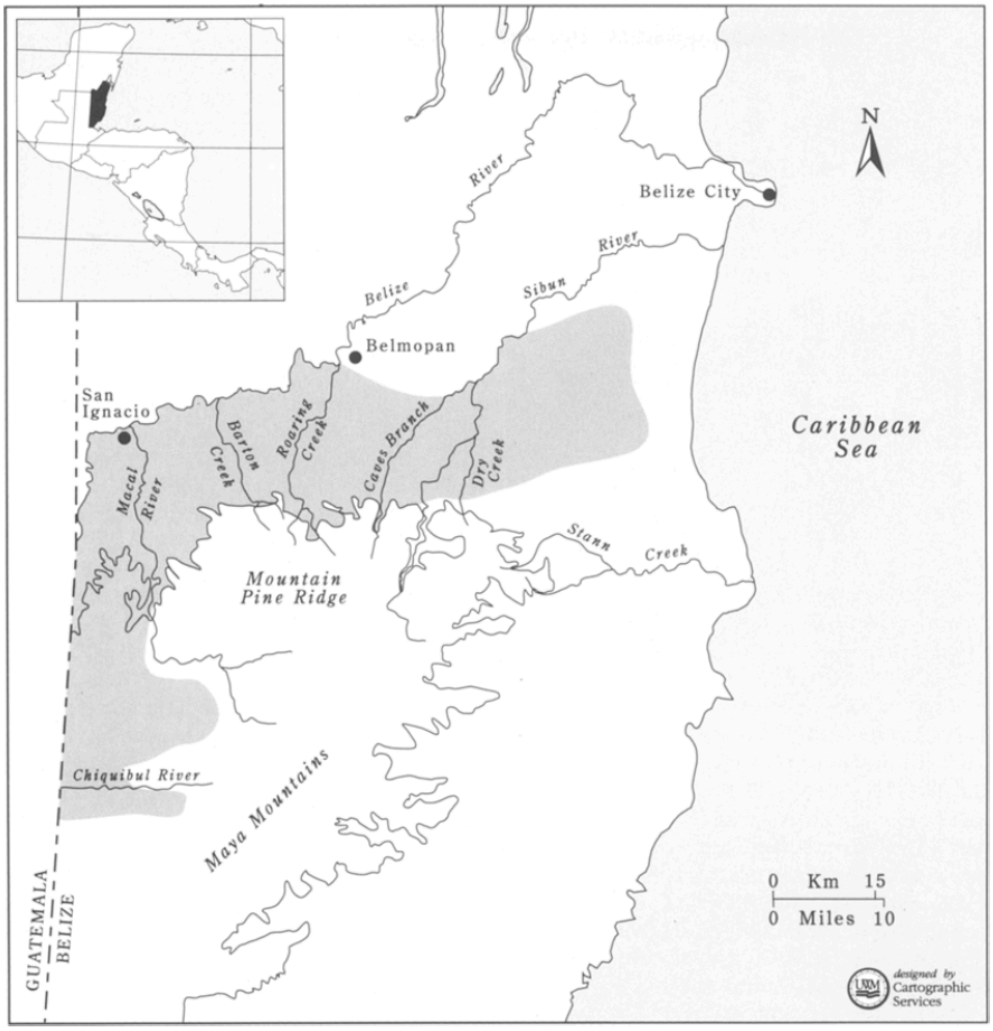

Figure 3.2: Central Belizean karst. From Day 1993.

Karst features that are common across Belize include sinking allogenic streams, dry valley networks of fluvial origin, hanging valleys, poljes, and abundant closed depressions (Miller 1996). Miller (1996) divided Belize into eight loosely defined, sometimes overlapping karst areas (Figure 3.3). Miller based his divisions on dominant dissolutional features, limestone composition, topography, and presence of caves. Much of the work focusing on karst in Belize in the 1990s and

2000s has focused on cave exploration in the extensive cave systems of western and southern Belize (Miller 1996, Williams 1996, Miller 2006). A small group of individuals has carried out most of the systematic cave mapping and exploration for non-archaeological purposes. The oldest caves in Belize are isolated chambers and passages of phreatic origin (Miller 1996). Trunk conduits are always found in association with sinking chemically aggressive allogenic waters originating in the Maya Mountains. Caves are generally multi-storied, which Miller (1996) attributes to the near-absence of bedding planes in the carbonate, providing little resistance to vertical flow in the heavily jointed rock. Vertical relief within caves may also be connected to episodes of tectonic uplift in the Maya Mountains. Most caves in Belize show archaeological evidence of Maya use either inside or nearby, and therefore many caves are given Maya names. Cave names often contain the word "Actun," which is the Mayan word for cave ("ac" means hollow and "tun" means stone; Williams 1996). The karst regions closest to my research area in the Belize River Valley are the Yalbac Hills and the Vaca Plateau, neither of which contain any known caves of significance. Here I summarize characteristics of these karst regions.

The Yalbac Hills are located in the northern third of Belize, which is composed of rocks that become increasingly younger in age with distance north from the Maya Mountains (Miller 1996). The hills rise to elevations of 200-250 meters with most drainage occurring on the surface. There is a high density of mapped dolines north of San Ignacio, but none of these have been found to open into caves (Albert and MacLeod 1971).

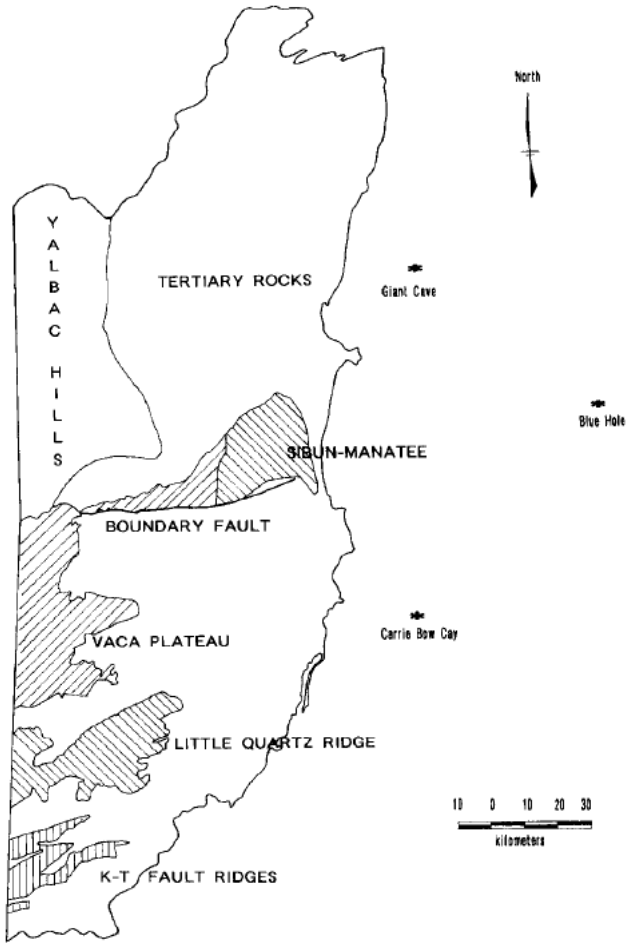

Figure 3.3: Karst regions. From Miller 1996.

The Vaca Plateau, located in west and central Belize, is the largest karst region in Belize (Miller 1996). The northern two thirds of this region is fluviokarst, whereas the southern area is composed of a karst that is heavily pitted. This morphologic difference may be because the southern area receives aggressive allogenic discharge from the Maya Mountains, whereas the deep incision of the Macal and Raspaculo Rivers buffer the northern plateau from the aggressive water. Additionally, fluviokarst may be present throughout most of the Vaca Plateau as a result of

deforestation. The river valleys in this region have alluvial floors and cliffed margins (Day 1993). This region lies at the eastern end of a broad platform of Cretaceous carbonates that spread out from central Guatemala (Miller 1996). To the north, the plateau blends into the non-Cretaceous carbonates and clastic sediments of the plain of the Belize River.

SOILS

Birchall and Jenkin (1979) completed a soil survey of the Belize River Valley from 1969-1971. The report assigned a few well-defined suites of identifying characteristics to soil. There is also a second, less comprehensive soil survey along the Macal River (Muhs et al. in 1985). Muhs et al. (1985) completed their soil survey as part of a project to identify feasibility of ancient Maya cacao cultivation at a variety of sites along the Macal River, located about five kilometers away this thesis's study area

Birchall and Jenkin (1979) used the FAO soil classification to identify the recently deposited alluvial terraces in the Belize River Valley as the Garbutt and Branch Mouth Series of the Quamana Subsuite. They classify both these series as Eutric Fluvisols, and neither has a type profile ascribed. These soils are subject to flooding and have very deep profiles with almost no horizon differentiation or mottling in the upper 90-centimeters. The deep profiles indicate that floods are high enough to rise to the terraces and above the floodplain. We would expect, however, that A and B horizons would have developed in these sediments over time. The lack of these horizons suggests either large-scale erosion or deep burial. These series are greyish, brownish, or yellowish-brown in color with a basic pH that becomes more alkaline in soils that are prone to flooding. Soils have high cation exchange capacities and base saturations near 100 percent, resulting in high fertility. Calcium and magnesium content is high, and phosphate levels in

unfertilized soils are low. Clay and silt content is generally around 30-40 percent; permeability is therefore relatively low.

The Garbutt Series includes a gravel phase that occurs infrequently and only in association with fine gravel deposited in paleochannels. The alluvial gravel is generally overlain by a thin layer of brownish sandy loam. The series also includes a sand phase that is much more common, associated with the higher parts of the recently deposited terraces. Profiles associated with the sand phase typically are characterized by an approximately 1-meter deep A-horizon composed of sandy loam to sandy clay loam on top of sandy to loamy alluvium. The Garbutt wet phase is the least common of the three phases of the series and tends to occur only in the lowest parts of the terraces. This phase is characterized by greyish-brown clay with weak subsoil mottling. The Branch Mouth Series is similar to the Garbutt Series in both morphology and chemistry, with the main difference being that the Branch Mouth series is paler and greyer in color with sand-sized nodules of calcium carbonate that may be pedogenic. Textures are generally loam to clay, and soils are well drained, friable, and moderately blocky. This series also has a common sand phase, which like the Garbutt, is characterized by sandy loam to sandy clay loam textures.

Muhs et al. (1985) classify soils using the USDA Soil Classification of the modern floodplain as Typic Hapludolls and Typic Argiudolls. The Argiudolls have argillic horizons and occur farther away from the river, as we would expect for clay-rich floodplain soils. Additionally, these soils are weathered. Most of the floodplain soils show only a cambic B-horizon with well-developed soil structure and weak clay films on ped surfaces. The soil does not show any indication of poor drainage, so Muhs et al. inferred that it drains well despite the clay textures. The solum extends to a depth of approximately 1.5 meters and has an angular blocky structure with a silt loam texture that has a high moisture retention rate. Organic matter decreases with depth in these soils,

which is mirrored by a decrease in total nitrogen. These soils have a high cation exchange capacity throughout all horizons. X-ray diffraction indicates that clay mineralogy is dominated by kaolinite and mica. The pH was consistently higher than expected (7-8). This may initially seem unexpected since the Macal flows through igneous and metamorphic rocks at its head; however, many of the streams that flow into the Macal have their heads in carbonate bedrock. Additionally, subsurface throughflow from the surrounding carbonate slopes likely also contributes to the basic pH of these floodplain soils.

Birchall and Jenkin (1979) identify the higher terraces in the Belize River Valley as the Young Girl and Barton Ramie Series. The Young Girl Series is similar to the Garbutt but is less common. There is a sand phase that, like the Garbutt's sand phase, is made up of sandy clay or sandy clay loam textures. The Barton Ramie Series looks like the Branch Mouth Series; however, these soils exhibit weak gleying in the subsoil because of moderately poor drainage. The Morning Star Series is a Gleyic Cambisol that occurs on the lowest parts of the highest elevation terraces, predominantly near Buena Vista and Clarissa Falls. Soils in this series have very deep profiles and dark grey, mottled topsoils that overlie grey to brown subsoils with red-brown or yellow-brown mottling. The C-horizon of these soils is still more strongly mottled with grey, orange, and yellow coloration. Manganese nodules are common in the subsoil. Soil texture is a poorly drained silty clay or clay.

Muhs et al. (1985) classify soils located on the terraces above the floodplain as Aquic Tropodalfs. These soils are more weathered than the floodplain soils because of their greater age. The well-developed argillic Bt-horizons are reddish in color and show clay films on peds. Solum depth, as with floodplain soils, is around 1.5 meters. Textures are silt loam and show mottling in the subsoil that indicates seasonally wet conditions. Organic matter and nitrogen content are

slightly lower in the terrace topsoil than in the floodplain topsoil. The cation exchange capacity is low, and x-ray diffraction suggests a similar kaolinite and mica clay mineralogy to the floodplain soils. Soil pH is higher here than the floodplain soils. Additionally, extractable phosphorus is relatively high, which is probably due to modern fertilization.

Birchall and Jenkin (1979) describe the Redbank Subsuite as soils that occur on the old alluvium in the lower Belize River Valley. These soils are probably located several miles to the north of my study area. Compared to the previously described Quamina Subsuite, these soils contain older and more weathered horizons that show greater profile development. Most of the soils in this subsuite are poorly drained, excluding the well-drained Central Farm Series. This is due to low-lying topography that floods regularly. Because of the drainage qualities of these soils, they generally show some kind of greyish to greyish-brown hue in the topsoil, with red-brown or yellow-red, unmottled subsoils. The well-structured, friable soils range in texture from clay loam to silty clay. There is a sand phase within this subsuite, identified as the Listowel Phase, which has only been mapped in the Central Farm/Norland area where it seems to be related to paleo channel and paleo levee deposits that are at slightly higher elevations. Muhs et al. (1985) describe small areas of alluvial fan deposits that could possibly be the same well-drained soils that Birchall and Jenkin describe as part of the Redbank Subsuite. The alluvial fan soils described by Muhs et al. overlie some of the terrace soils and seem to be derived from the local upland limestone bedrock. The solums overlying the fan deposits are very thin. The fan deposits are made of gravelly sediments interbedded with sand. Calcium carbonate content is high, but there is still some clay present.

Birchall and Jenkin (1979) identify one other soil that occurs near my research area: the Norland Series of the Creek Subsuite. Soils of the Creek Subsuite occur along streams that cross

the floodplains of rivers, and as such, are not constrained to certain terraces. The Norland Series appears to be the most common soil of this subsuite occurring in my study area and is classified as a Mollic Gleysol. It occurs predominantly in creeks and back swamps. It is characterized by a dark grey to black topsoil over a poorly drained olive to grey subsoil with yellow-brown mottling. The texture is typically silty clay to clay and manganese nodules are common in the subsoil. Soils of this series generally have basic pHs, medium to high cation exchange capacities, high base saturation, high calcium levels, medium magnesium levels, low phosphate levels, and low to medium sodium content. Muhs et al. (1985) describe one other soil unit that is limited to upland limestone bedrock surfaces, where soil type varies with slope angle. Soils located on very flat topography are Typic Argiaquolls, whereas steep slopes are generally dominated by Lithic Rendolls. The solum is usually less than 1 meter deep in areas with Argiaquolls and is dominated by clayey textures in the lower B and C horizons. These horizons also show evidence of gleying and slickensides, both of which indicate presence of shrink-swell clays. The characteristics of both the alluvial fan and bedrock soils described by Muhs et al. include organic matter decreasing with depth and attributes associated with the limestone parent material: very high soil pH and low values of extractable phosphorus.

Chapter 4: Methods

I applied a diverse group of methods to address my hypothesis: that the ancient Maya were shaping their landscape by altering the watershed's flood frequency through deforestation and associated erosion. I have used the following methods to identify and quantify the most significant long-term anthropogenic drivers of landscape change and associated flooding in the watershed. This work addresses two key research gaps in this region: geomorphic mapping of the river system and developing a record of fluvial and hydrological change in the watershed.

FIELD METHODS

In spring 2017, I used sub-meter accuracy LiDAR imagery (acquired by the University of Texas at San Antonio) to conduct a preliminary study of Belize River Valley geomorphology. First, using the imagery, I identified paleofloodplain features such as paleochannels. Next, I identified areas that lay on the floodplain in proximity to significant, ancient Maya centers and their attendant landscape manipulation for settlement and agriculture (Yaeger 2000). Over 10 weeks of summer 2017 fieldwork, I studied 11 soil profiles, collecting soil samples from 9 of these and carbon samples from 7 of these. Sample sites were chosen based on either presence of an already exposed soil profile (due to erosion and/or quarrying activities) or permission from a landowner to dig a backhoe trench on their property. A backhoe dug four trenches that provided profiles that were 3 – 5 meters in depth. The other 7 profiles were already exposed. I cleaned up and made several of these already-exposed profiles deeper. These cleaned profiles were around 2 meters in depth.

I described each profile, characterizing moist soil colors using the Munsell Soil Color Chart (2010), manual texture, soil structure, magnetic susceptibility, and horizons. I later revised field

descriptions with laboratory-based observations and analyses, as appropriate. I measured magnetic susceptibility of soil horizons (Dalan, 2006) in the field by placing an SM20 magnetic susceptibility meter (at a resolution of 10−3 SI units) flat against the soil profile and collecting measurements at 5- or 10-cm increments down the profile. Magnetic susceptibility assesses the concentration of ferromagnetic minerals in the soil. Burning activities, such as those involved in large-scale deforestation for construction and agriculture, as well as long term exposure of sediment, result in elevation of magnetic susceptibility values. Therefore, elevated magnetic susceptibility values can indicate presence of an A horizon. After in situ data characterization, I collected soil samples of approximately 100 g for further analysis from all horizons. I collected carbon for AMS dating wherever possible, but I found limited samples.

LAB METHODS

Following the summer 2017 field season, I shipped our samples to UT Austin Soils and Geoarchaeology Lab. Upon arrival, I logged and processed the samples. Then I air-dried, disaggregated, and powdered samples using mortar and pestle. I subsampled soils to send to Cornell Nutrient Analysis Laboratory (CNAL) for geochemical analyses. International Chemical Analysis Inc. ran all the samples of organic materials and charcoal from soil layers, which they calibrated by INTCAL13 Radiocarbon Age Calibration. Geochemical analyses provide information about sediment formation conditions. CNAL also completed particle size and analysis and quantified cation exchange capacity. Particle size analysis provides information about sediment origin through large-scale flooding or local deposition from valley side erosion. Cation exchange capacity provides a measure of soil fertility. Radiocarbon dating helps us to understand the timing and rates of sediment deposition. I also completed loss-on-ignition and phosphate

analysis. Loss-on-ignition quantifies the percentage of organic matter in sediment samples as an indicator of sediment and top soil formation. Elevated values of phosphate in soil indicate that humans fertilized the soil for improved agriculture.

The CNAL used hot plate-assisted 2-acid digestion, Inductively Coupled Plasma-Atomic Emission Spectroscopy (ICP-AES), and Mehlich III extraction for macro- and micronutrients to determine concentrations of 26 elements for the 30 soil samples. This gave us total element concentrations for elements such as K, Ca, and P. Phosphorus is the most useful element for assessing human inputs into soils (Schlezinger and Howes 2000, Holliday and Gartner 2007). The CNAL determined soil texture, pH, and soil cation exchange capability (CEC) following methods from the Soil Survey Laboratory Methods Manual (Burt et al. 2014) developed by the National Soil Survey Center (National Resources Conservation Service, United States Department of Agriculture).

I used Mehlich II methods to determine the easily extractible concentration of P in the soils (after Mehlich 1984). I diluted the Mehlich II extractant by mixing 500 mL with 4500 mL of distilled water. Then, I weighed 2 grams ± 0.2 of each soil sample into 30 mL jars attached to a wood board, running 10 samples at a time. I added 20 mL of Mehlich II extraction solution to each jar. Then I capped the jars and shook them for five minutes, after which I filtered them through 15-cm filter papers, collecting the filtrate in a second series of 10 30-mL jars attached to wood boards. Next, I used a pipette to aliquot 1 ml of the solution from each jar into a colorimeter vial and diluted it to 10 mL using deionized water. I added a packet of PhosVer 3 Reagent (Hach PhosVer 3, Phosphate Reagent for 10 mL sample, Hach Cat. 21060-69) to each vial, individually shaking each vial for 60 seconds immediately after adding the reagent. If the reagent is not immediately shaken to dissolve, it will auto-react to form blue color. Then I let the vials rest four

minutes for color development. Last, I measured the samples with a Hach DR/850 Colorimeter using the % Transmittance function (Hach DR/850 Procedures Manual). First, I set the 100% Transmittance value with a blank sample that consisted of a vial filled with 10 mL of deionized water, mixed with a packet of reagent and shaken for 60 seconds. Then I inserted each of the vials into the colorimeter and recorded the percent transmittance. Transmittance values were converted to mg/L and mg/kg soil by producing a standard curve for the Mehlich II P test. The procedure for producing a standard curve is as follows: First, prepare a 1.5 ppm KH_2PO_4 phosphorus standard. Pipette 1.5 ppm of the standard into 12 vials at volumes of 10, 8, 6, 4, 3, 2, 1.6, 1, 0.8, 0.6, 0.4, and 0 mL. Fill the vials up to 10 mL with distilled water. Add a packet of PhosVer 3 Reagent to each vial and shake for one minute. Then let stand for four minutes. Calibrate the colorimeter with a blank. Read percent transmittance for each of the vials and record in Excel. Use the Excel regression function to calculate the standard curve.

I used loss-on-ignition to determine the total carbon in our soil samples. I followed the method detailed in the Loss-on-Ignition Standard Operating Procedure by LacCore, National Lacustrine Core Facility (2013). I ran approximately 20 samples at a time. First, I numbered and weighed our approximately 20 crucibles, using tweezers to place them on a metal tray after weighing. I recorded crucible weight and number. Next, I weighed out approximately 5 g of each soil sample, recording this number before adding the soil to the crucibles. I then placed the tray with the crucibles in a drying oven and heated them overnight at 100 degrees C, to evaporate any water in the sample. The following morning, I weighed the samples as soon as they were cool enough to do so, recording weights. I then put the crucibles into the muffle furnace for 4 hours at 550 degrees C, which burns off organic matter. Once the samples were cool, usually the following day, I weighed them and recorded these weights. Last, I put the crucibles back into the muffle

furnace for 2 hours at 1000 degrees C. Once the samples were cool, usually the following day, I recorded these weights. The change in weight between each of these steps provides a measure of sample moisture and carbon content.

LIDAR AND GIS METHODS

LiDAR, or light detection and ranging, is a remote sensing technology that uses electromagnetic energy to detect an object, determine the distance between the target and the collection instrument, and gather information about physical properties of the object based on the interaction of radiation with the target through scattering, absorption, reflection, and fluorescence (Fernandez-Diaz et al. 2013). LiDAR survey systems derive measurements based on the speed of light, using laser pulses to measure distance and direction of the vector from the sensor to the surface of what is being scanned (Prufer et al. 2015). Lasers typically emit from 33,000 to 167,000 points per second in swaths that are 250 to 500 meters wide, which results in scan point densities of 5 - 15 point returns per meter squared. This high frequency of point collection enables laser penetration of dense jungle canopies through spaces in the leaf canopy. After the survey is complete, raw point cloud data are classified into categories such as vegetation, bare earth, buildings, and ground surface. We can then generate a highly detailed terrain model, showing the land surface, buildings, and canopy. LiDAR enables maximization of surveying efforts and collecting data over a much larger area in a much shorter amount of time than would be possible with traditional methods of field survey.

The expansion of LiDAR technology outside of government work over the last 15 or so years has revolutionized both archaeological and geomorphological work (Fernandez-Diaz et al. 2013, Chase et al. 2012, Gran et al. 2013). LiDAR imagery is particularly well-suited for work in

tropical rainforest environments (Chase et al. 2012) because imagery collection through thousands of laser data points enables canopy penetration by at least some of these points. An extremely accurate bare earth elevation model can them be generated from the point cloud generated by the laser points.

I developed a new way of applying the height above nearest drainage (HAND) method of flood mapping for my study area using a sub-meter accurate LiDAR DEM acquired by the University of Texas at San Antonio, in conjunction with ArcGIS Pro HydroTools. HAND analysis is a common way of calculating the land surface elevation in relation to height above the nearest drainage (Nobre et al. 2011), enabling inundation for floods of given stages above the streambed to be mapped. This method generally requires known stream channel elevation values, as well as flood stage values, which do not exist for the Mopan River. The LiDAR imagery had a number of no data values within the stream channel, which would have been a problem for delineation and mapping. I used the "Elevation Void Fill" tool to fill my DEM, which takes the average elevation of the eight cells closest to the cell with no data and assigns it that value.

I began my analyses by delineating the stream network shown in my LiDAR imagery using a procedure outlined in David Maidment's ArcGIS manual: *Arc Hydro: GIS for Water Resources* (2002). My LiDAR imagery does not include the entire watershed, so I delineated the streams shown in the LiDAR that are part of the Mopan River watershed. First, I manually determined the decimal degree coordinates of the outlet of the Mopan River and used these coordinates to create my point feature, from which I delineated my watershed using the "Ready-To-Use Watershed" tool. I made sure to set the projection of my point feature, and the projection of all the layers I created, to the projection of my DEM: WGS 1984 UTM Zone 16N. Then I added my void-filled DEM to the map and created a one-kilometer buffer around it. From there, I extracted only the

portion of the DEM that included my delineated streams using the "Extract by Mask" tool. From here, since there is no accurate available stream network dataset for Belize, I began hydrologic terrain analysis.

First, I ran the "Fill" tool on my DEM. Next, I ran the "Flow Accumulation" tool, which took three hours to run. From here, I defined my streams based on a flow accumulation threshold. First, I delineated my streams based on a threshold of 5,000. This threshold was too high and so it showed many streams that likely do not exist, so I reran my delineation using a flow accumulation threshold of 10,000. Then I clipped my streams to my basin. Last, I created a stream links layer that I then converted into a vector representation. The resultant stream network delineation has some edge contamination present at the western edge. This part of my method will need to be further refined.

At this point, I began my own method of HAND analysis. First, I added elevation information from my DEM to the stream network vector file just created. I did this by right clicking on "Map" at the top of the Contents pane and adding an elevation surface in "Properties." Then I ran a tool called "Add Surface Information" that allowed me to calculate elevation (Z) values for my stream network from my DEM. I had the option of calculating minimum, maximum, or mean Z values and chose to use mean Z values. Next, I ran the "Topo to Raster" tool, which converted the elevation values for my stream network into an elevation raster. I then subtracted this from my DEM. At this point, I generated a series of flood inundation maps by using the less-than-or-equal-to command in "Raster Calculator" to display a variety of stage values on the HAND map.

Chapter 5: Results and Discussion

I chose each of the following sample sites to gather data that would enable me to address my hypothesis: that the ancient Maya were shaping their landscape by altering the watershed's flood frequency through deforestation and associated erosion. These sites are floodplain environments that provide information about the last 4,000 years of sediment aggradation and erosion rates; method of deposition, either through local valley-side erosion or large-scale flooding, periods of landscape stability and instability; and landscape manipulation through agriculture and/or construction. I present all of my results as they relate to each of these areas. Loss-on-ignition, magnetic susceptibility, phosphorus, cation exchange capacity, and geochemical results provide us with information about landscape stability and Maya landscape manipulation. Particle size analysis tells us about the method of deposition. Radiocarbon dates give us a way to calculate aggradation and erosion rates, which relate to landscape stability and soil development. These data provide some of the information required to develop a conceptual model of landscape formation, which will be future work.

The San Lorenzo Sand Quarry (SL Quarry Pit) series of soil profiles are located adjacent to the prehistoric Maya site of San Lorenzo, and archaeological excavation is ongoing. The SL Quarry Pit area was quarried for sand in the last decade, removing the top ~ 100 cm of sediment. Therefore, all of our profiles actually begin ~ 100 cm below the surface. At the time of data collection the field was covered in planted Bahiagrass with many small Mimosa trees and surrounding larger stands of tropical forest. The top 15 cm of the field is regularly plowed, and the entire area is pasture land for cows. The Buena Vista (BVC) series of soil profiles are located just downslope from the archaeological site of Buena Vista in an active Mennonite field. Here I provide results from a total of eight sampled profiles.

B-SL QUARRY PIT

Profile B-SL Quarry Pit is located at coordinates N 17° 6’ 13.2’’, W 89° 7’ 43.8” (Figures 5.1, 5.2, 5.3). This profile is the only profile that includes the 100 cm of sediment that were elsewhere removed due to quarrying activitiy. It preserves a well-developed soil above a paleosol. LiDAR imagery suggests that this area may be an old channel complex or oxbow (Figure 5.4). This profile is 200 cm deep. Sediment descriptions and tentative horizon assignments follow (Table 5.1). The profile begins with approximately 12 cm of 10YR 2/1 very fine, loose sandy loam. I have called this an A1 horizon. Next is the A2 horizon, which extends from 12 to 25 cm and is composed of 10YR 3/2 coarse, loose granular sandy loam. The B horizon is below that, from 25 to 55 cm. It is 10YR 3/3-3/2 coarse, loose sandy loam. Beneath that there is a horizon that may be a C1 horizon, but it could also be a B or A horizon based on our lab results. This horizon begins at 55 cm and continues through 85 cm. Next is the C2, extending from 85-142 cm, composed of 10YR 6/4-6/6 coarse, loose sand. The C3 horizon is below that, from 143-160 cm. It is made up of 10YR 5/4 massive blocky loam-silt and loam that is mottled and has a white mineralization throughout that may be gypsum or calcium carbonate. The last horizon is the Ab, which occurs from 160-200 cm. It is a silt loam with slickensides that is 10YR 4/3 mottled with 10YR 4/1 and 10YR 3/6. The last 10 cm of this horizon show a color change to 10YR 3/3.

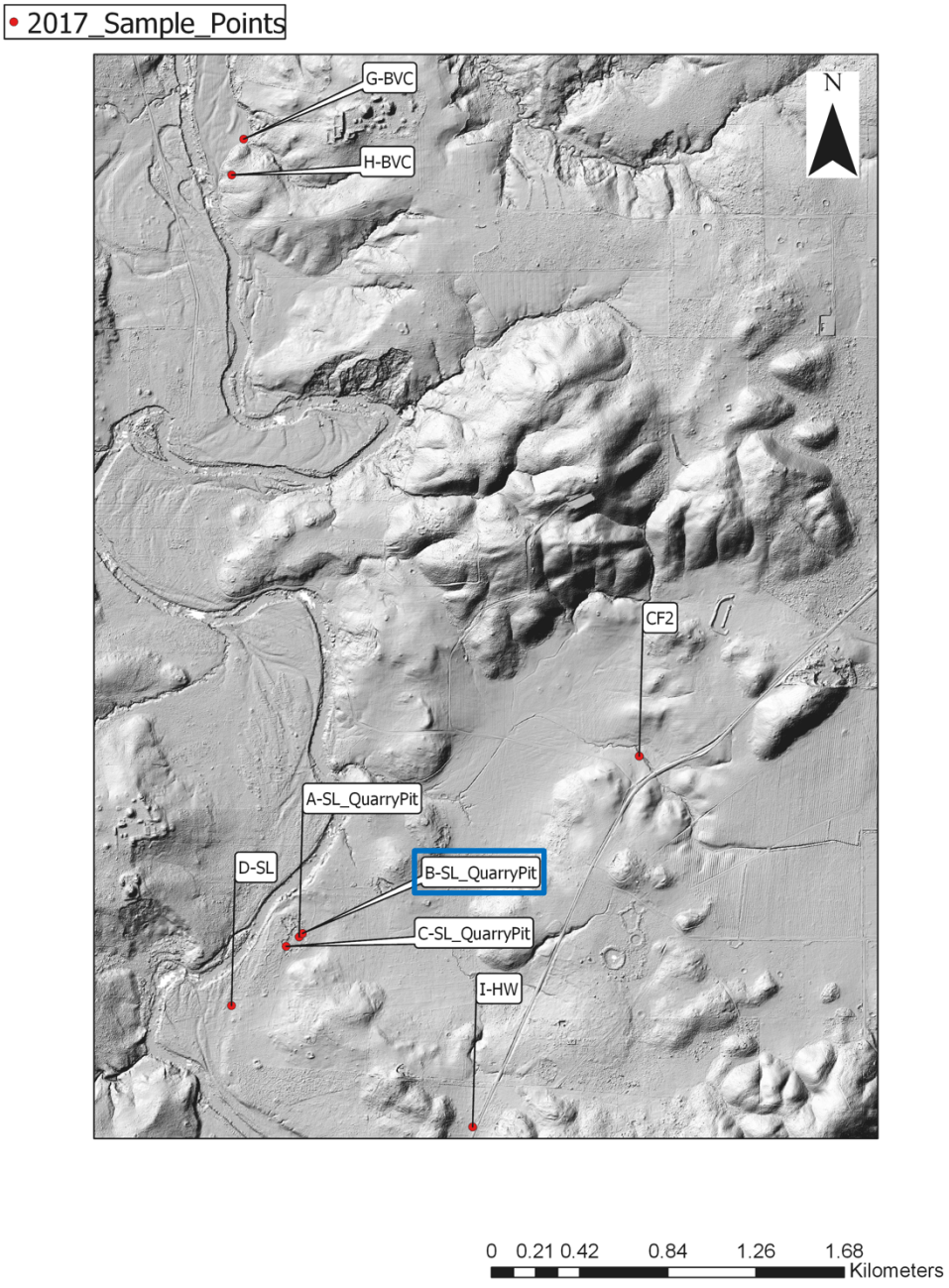

Figure 5.1: Profile B-SL location map.

Figure 5.2: Profile B-SL

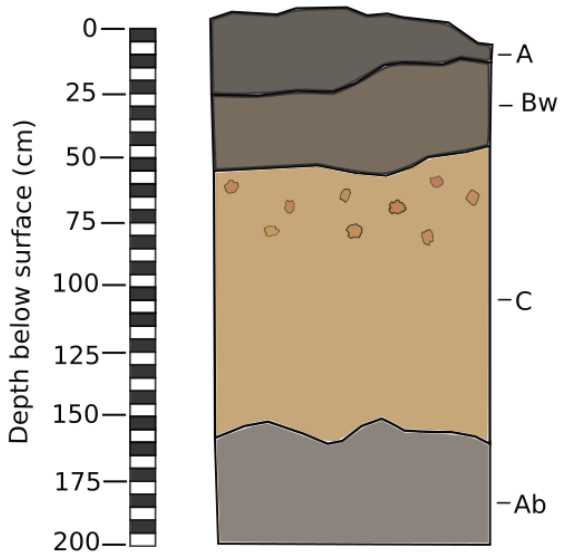

Figure 5.3: Profile B-SL

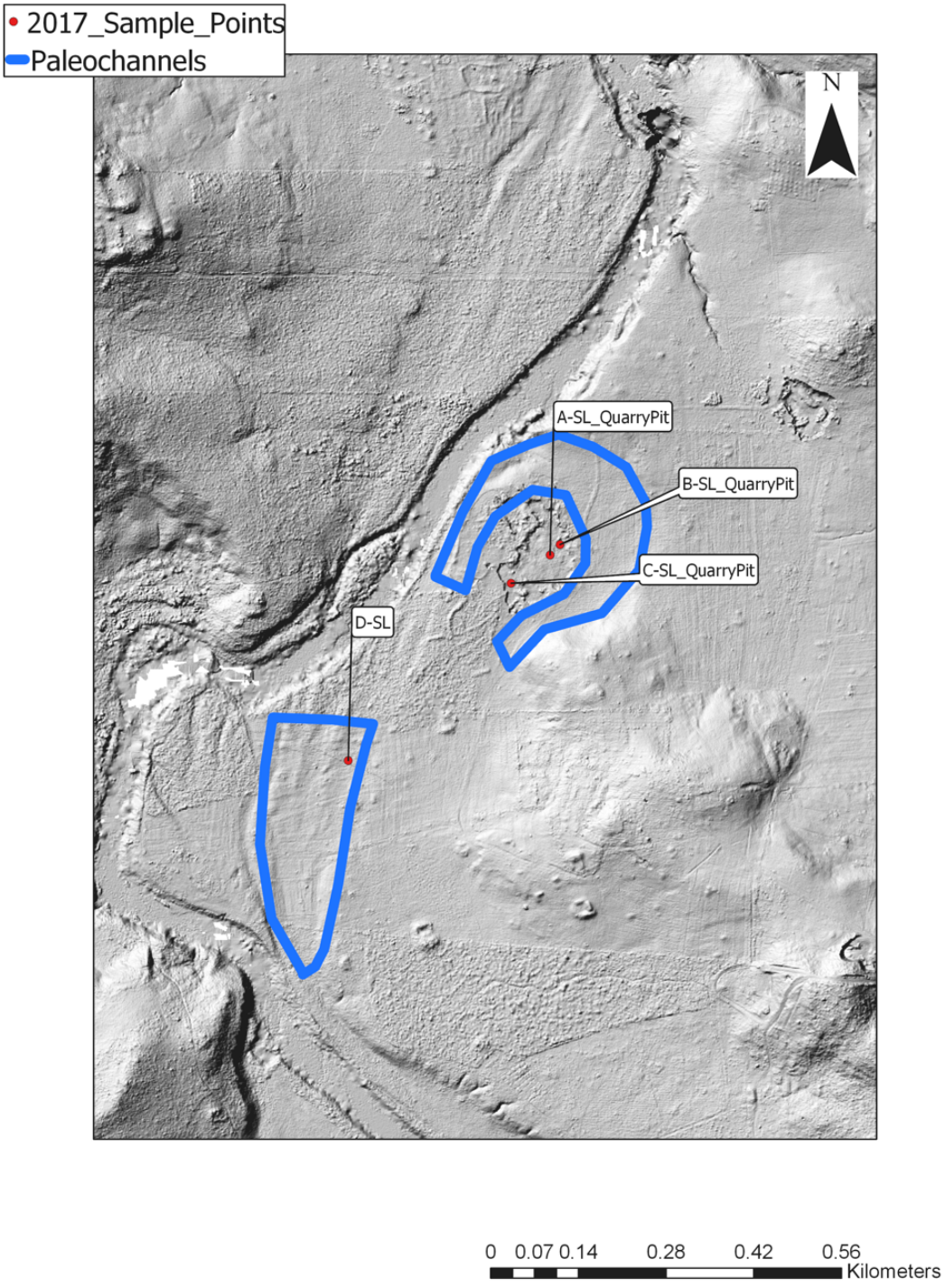

Figure 5.4: Paleofloodplain features visible in the LiDAR imagery near the San Lorenzo series soil profiles.

Depth (cm)	Horizon	Description
0-12	A1	Very fine sandy loam, soft, 10YR 2/1
12-25	A2	Coarse sandy loam, loose granular, many roots, 10YR 3/2
25-55	B	Coarse sandy loam, loose, many roots, 10YR 3/3-3/2
55-85	C1	Coarse sand and small cobbles, 10YR 3/4
85-142	C2	Coarse sand, loose, no structure, 10YR 6/4-6/6
143-160	C3	Loam-silt loam, some red and grey mottling, massive blocky, white mineralization, 10YR 5/4
160-200	Ab	Silt loam, red and grey mottling, slickensides, 10YR 4/3 mottled with 10YR 4/1 and 10YR 3/6; 170-180 is 10YR 3/3

Table 5.1: Profile B-SL log

Loss-on-ignition, magnetic susceptibility, and phosphorus values all increase from 160-200 cm (Figure 5.5), suggesting that this zone is an Ab horizon. This sediment in the zone is also visibly darker in color, supporting this hypothesis. Moreover, the loss-on-ignition, phosphorus, and magnetic susceptibility values from 160-200 cm are similar to those of the modern topsoil. Loss-on-ignition and phosphorus values are particularly similar. In general, loss-on-ignition and magnetic susceptibility values seem to be well correlated down the entire profile. The areas where these two values are high are hypothesized A or Ab horizons, where we would expect more well-developed soils. This long-term stability would result in both a higher percentage of organic matter and ferro-magnetic material. Cation exchange capacity (CEC) values for the modern topsoil and 190-200 cm, which we hypothesize to be a buried soil, are similar (Table 5.2).

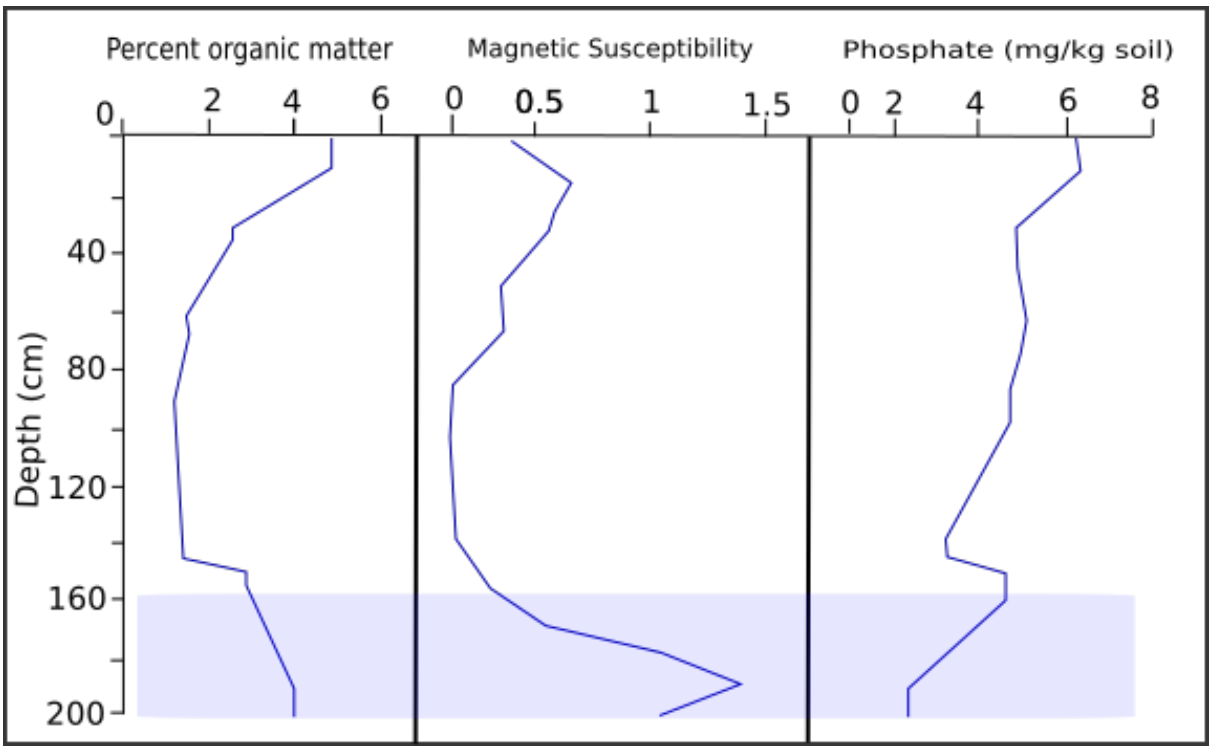

Figure 5.5: Profile B-SL loss-on-ignition, magnetic susceptibility, and phosphate results.

Depth (cm)	CEC (cmol/kg)
0-10 cm	18.72
190-200 cm	14.11

Table 5.2: Profile B-SL cation exchange capacity (CEC) results.

I have only one data point from CNAL for particle size analysis (Figure 5.6). Results are similar to profile A-SL Quarry Pit, showing a significant amount of clay. This could indicate presence of a buried soil. However, I cannot draw particularly valid conclusions with this limited data set. Further research will include additional particle size analysis. CNAL ICP-AES results show that most elements demonstrate a short, relatively abrupt increase at approximately 150 cm

(Figure 5.7). Iron and aluminum show a particularly pronounced increase here: I would expect these concentrations to be elevated in the phyllosilicate clays of the Ab horizon. Below this depth, most values remain consistently elevated. Calcium and phosphorus, however, decline. The increase at 150 cm correlates to the upper boundary of the hypothesized buried soil, but there may also be a groundwater component. Calcium, Magnesium, Sulfur, and Strontium show a slight decrease at 150 cm that continues through the end of the profile (Figure 5.8). This trend is the opposite of what all the other elements show through this zone. Lead is very high from 140-145 cm, directly above our hypothesized buried soil (Figure 5.9). These values occur in a zone that exhibits some redoximorphic features, so we may be seeing the result of groundwater-transmitted pollutants. The gleyed zone in this profile appears about 100 cm above that of nearby profile A. Based on field and lab data, LiDAR imagery (Figure 5.4), and Holley's previous study (2000), I hypothesize that this zone formed in an oxbow or abandoned channel complex where clay accumulated. This could explain why the gleyed zone occurs at a much shallower depth here. I don't have any dates for this profile. Further research includes identifying datable material in this profile, which would help to contextualize the buried soil and what role the potential paleochannel complex may have played in sediment deposition.

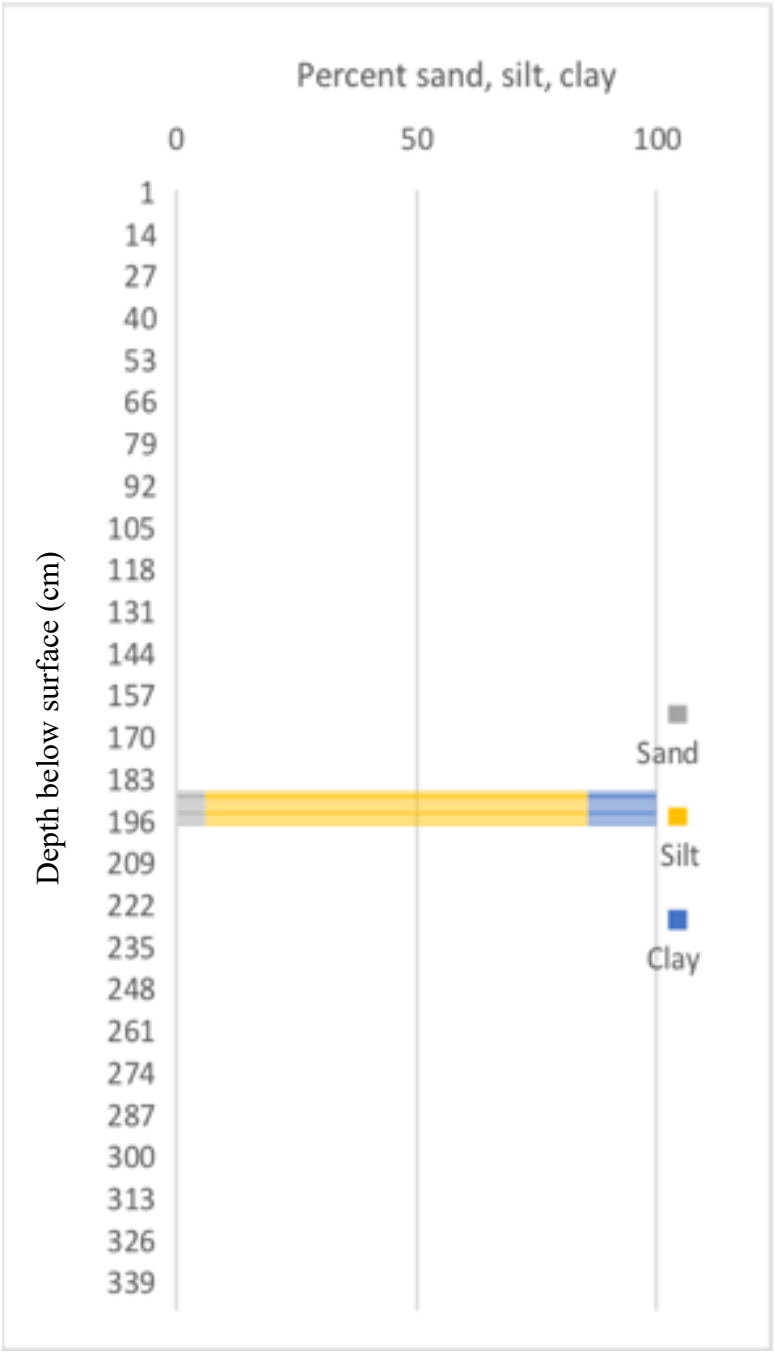

Figure 5.6: Profile B-SL particle size analysis results.

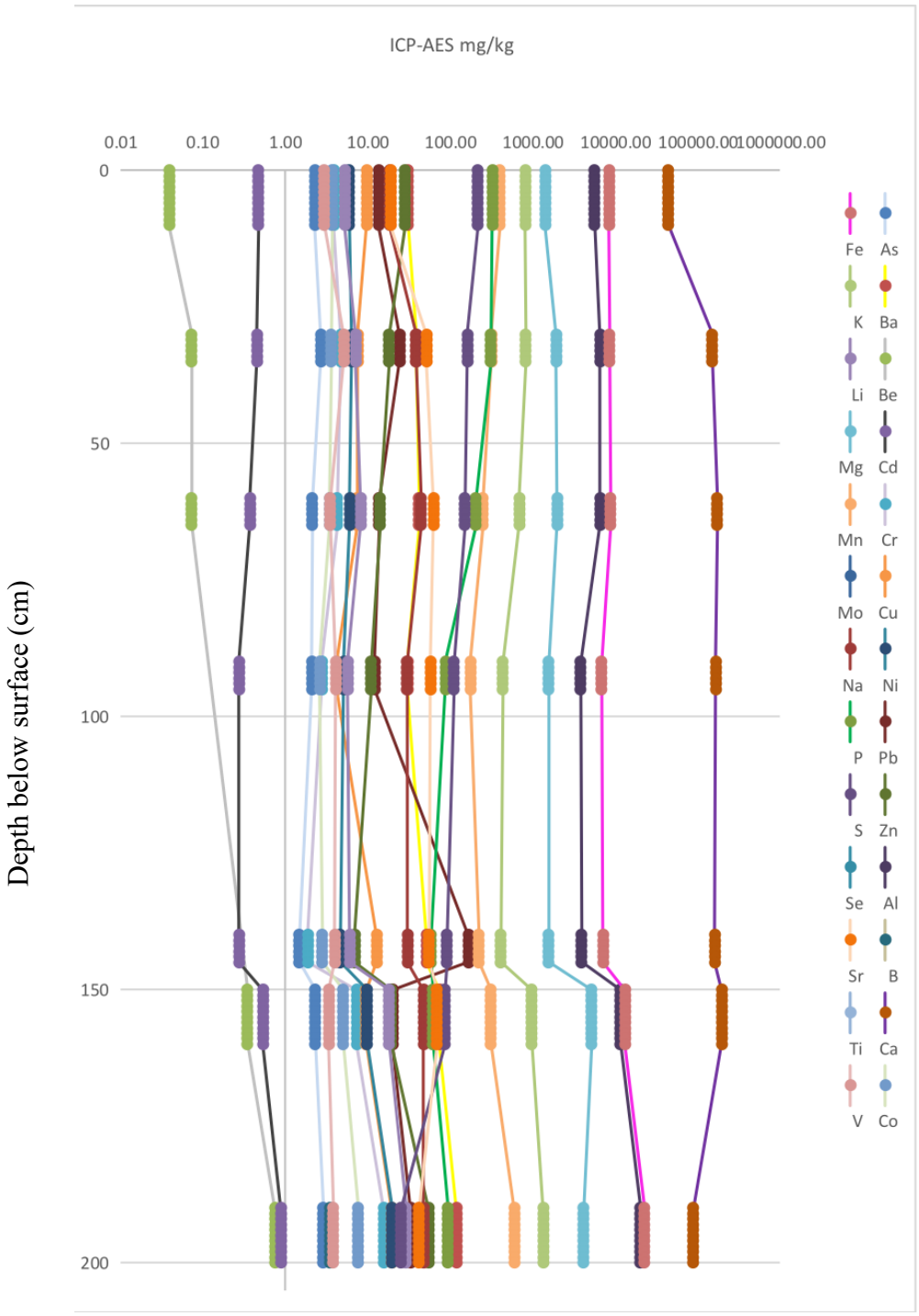

Figure 5.7: Profile B-SL ICP-AES results.

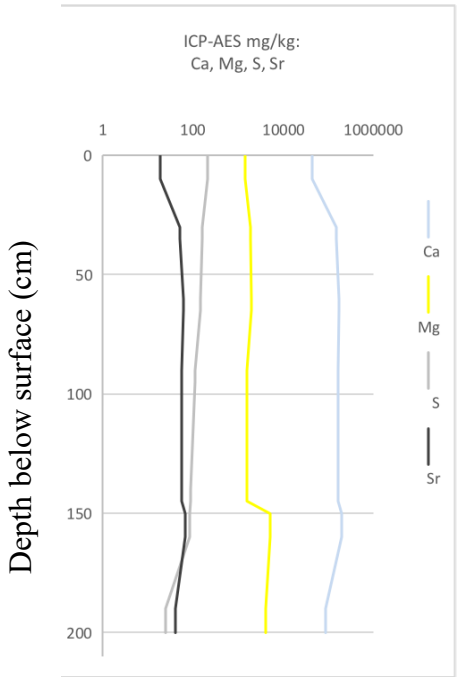

Figure 5.8: Profile B-SL ICP-AES Ca, Mg, S, and Sr results.

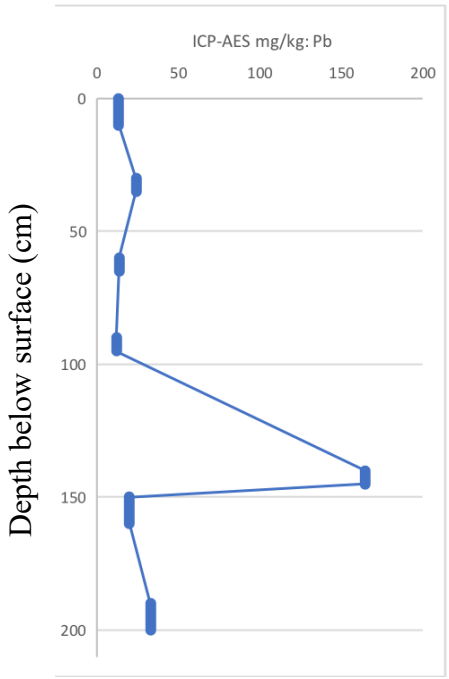

Figure 5.9: Profile B-SL ICP-AES Pb results.

D-SL

Profile D-SL Quarry Pit is located at coordinates N 17° 5’ 59.8’’, W 89° 7’ 56.7” (Figures 5.10, 5.11, 5.12). This profile is located in a slightly different area than profile B – SL Quarry Pit: closer to the river in a slight depression that lies to the east of a broader area that appears to contain some low mounds. This profile is not located in the area that has been quarried for sand and thus provides a nearly complete profile. Field observation and LiDAR imagery (Figure 5.4) suggest that the depression may represent a paleochannel. The profile extends from 10 cm to 185 cm below the surface (Table 5.3). The first 10 cm of the profile have been removed by plowing activity. Profile description follows, including tentative horizon assignments. The A horizon extends from 10 to 45 cm, but there are color and texture changes within this horizon. From 10-15 is a 10YR 2/2 loose granular loamy clay to loam. From 20-25 is a 10YR 3/2 granular loamy clay to loam. From 30-35 is a 10YR 3/1 subangular blocky loamy clay to loam with 5% coarse gravel. From 40-45 is a loam that is otherwise the same as the sediment directly above. Next is the Ac horizon, extending from 40-60 cm. It is a dark brown gravelly loam with ceramic smears throughout. Beneath that is the C horizon, which begins at 68 cm and continues through 125 cm. It is coarse sand to cobbles with some boulders. The Ab1 horizon extends from 125-137 cm. It is a very dark brown, subangular blocky to granular clay loam with 5-10% gravel and shell fragments throughout. The Ab2 horizon is beneath that, extending from 137-150 cm. It is similar to the Ab1, however it has less clay and is a loam, has increasing gravel with depth, and has a lightening color with depth. This is followed by a C horizon that begins at 150 and continues through the base of the profile at 185 cm. 150-160 cm is characterized by coarse sand to rounded cobbles and boulders, 160-180 cm is redoximorphic clay, and 180-185 is cobbles and boulders again.

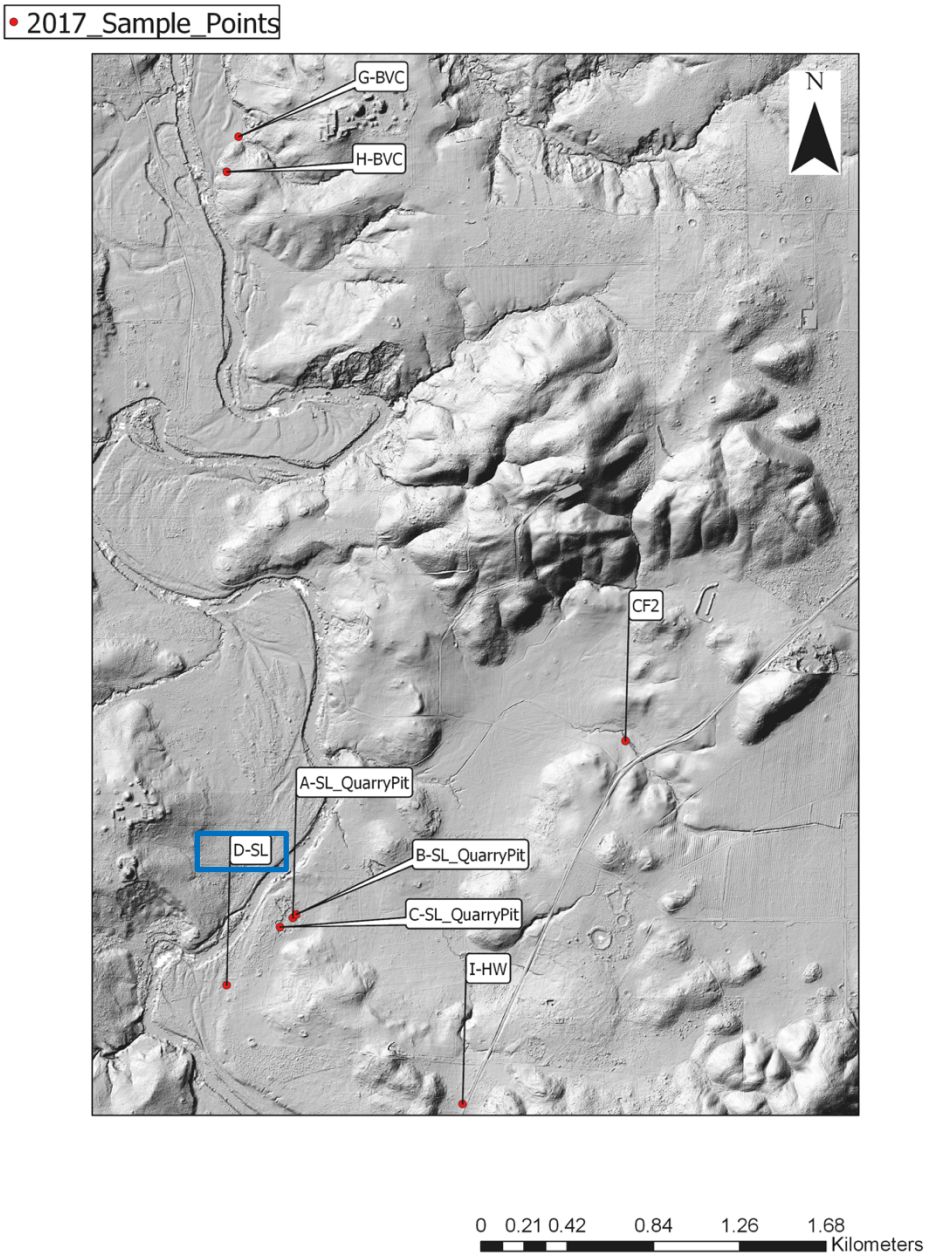

Figure 5.10: Profile D-SL location map.

Figure 5.11: Profile D-SL

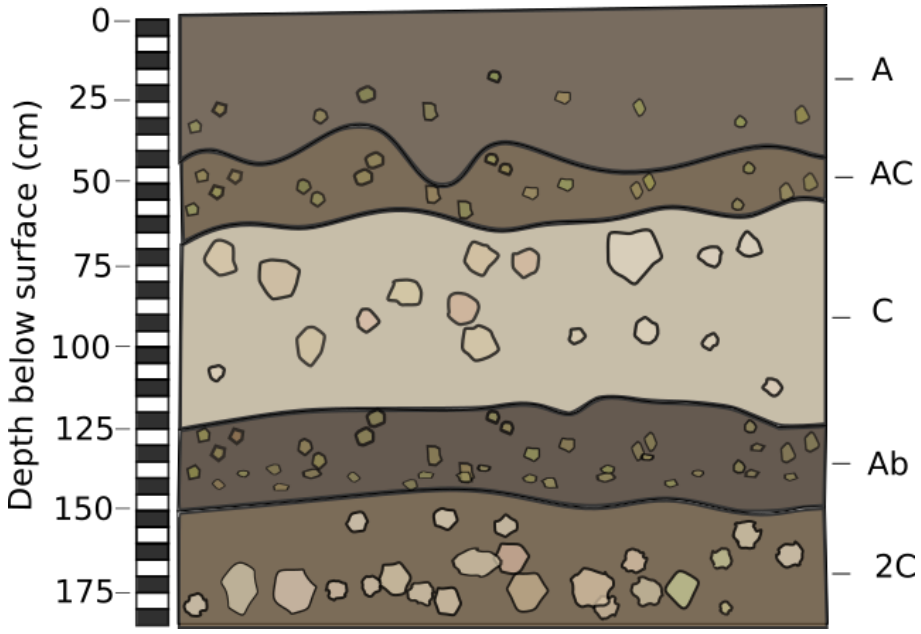

Figure 5.12: Profile D-SL

Depth (cm)	Horizon	Description
10-15	A	Loamy-clay loam, loose-granular, 10YR 2/2
20-25	A	Loamy-clay loam, granular, 10 YR 3/2
30-35	A	Loamy-clay loam, sbk, 5% coarse gravel, 10 YR 3/1
40-45	A	Loam, 10 YR 3/1
40-60	Ac	Gravelly loam, ceramic smears throughout, dark brown (10YR 3/3) with whitish streaks on surface from limestone
68-125	C	Coarse sand to cobbles with some boulders, 2.5Y 7/2
125-137	Ab1	Clay loam, sbk-granular, 5-10% gravel, shell fragments throughout, 10YR 2/2
137-150	Ab2	Loam, sbk-granular, gravel increases with depth, shell fragments throughout, color lightens with depth to 10YR 4/3
150-160	C	Coarse sand to rounded cobbles and boulders, 10YR 4/3
160-180	C	Clay, redoximorphic, 10YR 3/3
180-185	C	Cobbles and boulders

Table 5.3: Profile D-SL log.

Loss-on-ignition, magnetic susceptibility, and phosphorus results are less clear here than in some of the other profiles (Figure 5.13). I observed a dark colored soil in the field from 125-150 cm. In this zone, we see an increase in magnetic susceptibility, but phosphorus initially increases upon entering this zone before abruptly decreasing. There is no significant change down profile for loss-on-ignition. Values for all three of these tests are high near the top of the profile in the surface soil, as we would expect. We have a single cation exchange capacity value for this zone, measured in the top soil (Table 5.4). It is higher than any of the CEC values from profiles A and B SL-Quarry Pit, indicating that this is a very fertile soil. This makes sense because this profile is located closer to the modern river channel than either profiles A or B.

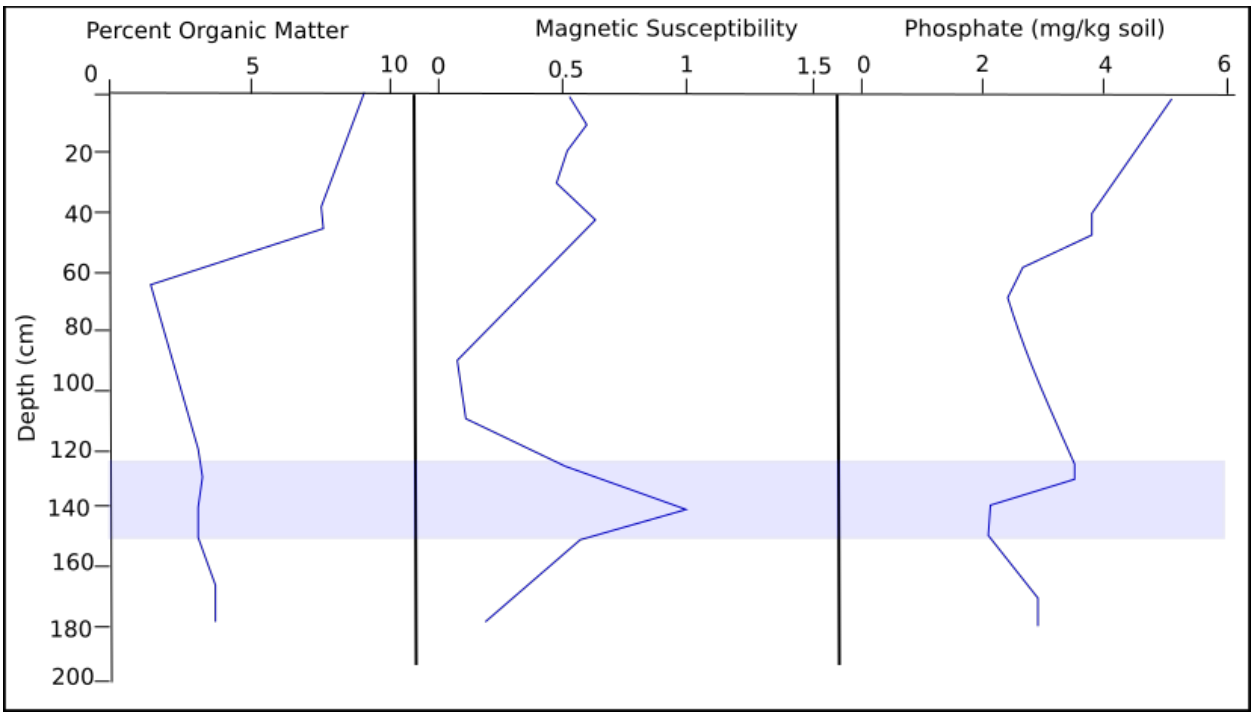

Figure 5.13: Profile D-SL loss-on-ignition, magnetic susceptibility, and phosphate results.

Depth (cm)	CEC (cmol/kg)
Surface	29.61

Table 5.4: Profile D-SL cation exchange capacity (CEC) results.

I have two data points from CNAL for particle size analysis (Figure 5.14), from which I can draw limited conclusions. Based on these two data points, clay appears to either increase with depth or to increase in the zone of the hypothesized buried soil. However, the abundance of large cobbles throughout nearly the entire profile indicates that overall this profile was deposited in a high energy environment. Since clays are characteristic of lower energy environments, it's more

likely that the clays that appear around 125 cm are indicative of a period of environmental stability during which this was not an active channel and there was not much flooding activity. CNAL ICP-AES results show that all elemental values seem to follow the same trend until about 140 cm (Figure 5.15). Below 140 cm, I have two samples from which I can draw conclusions: 137-150 cm and 170-180 cm. The upper zone falls within the area that I believe to be a buried soil. The lower zone is a redoximorphic soil. Most elemental values decrease at least slightly near the bottom of the profile coincident with the redoxomorphic zone that occurs around 160 cm. The elements that show a decrease in value are: beryllium, cadmium, arsenic, vanadium, cobalt, copper, nickel, zinc, strontium, sulfur, phosphorus, magnesium, and calcium. Elements that instead show an increase are far fewer, and include boron, sodium, barium and aluminum. Elements that decrease in the redoximorphic zone probably do so due to leaching from occasional saturation by the water table. Related research (Beach 2015) has shown that sulfur tends to accumulate near the top of the water table as a product of gypsum evaporation caused by a fluctuating water table. Sodium is likely deposited in a similar manner.

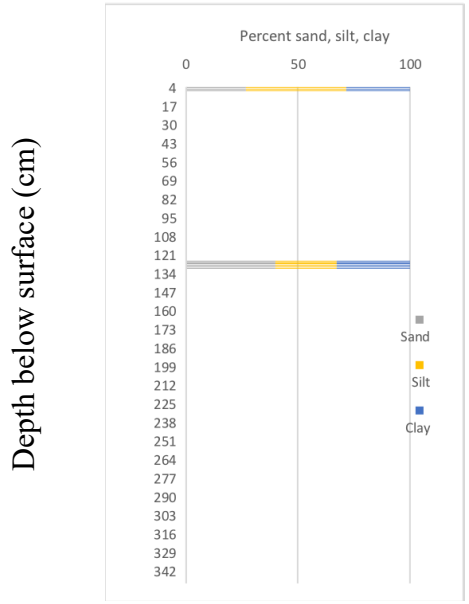

Figure 5.14: Profile D-SL particle size analysis results.

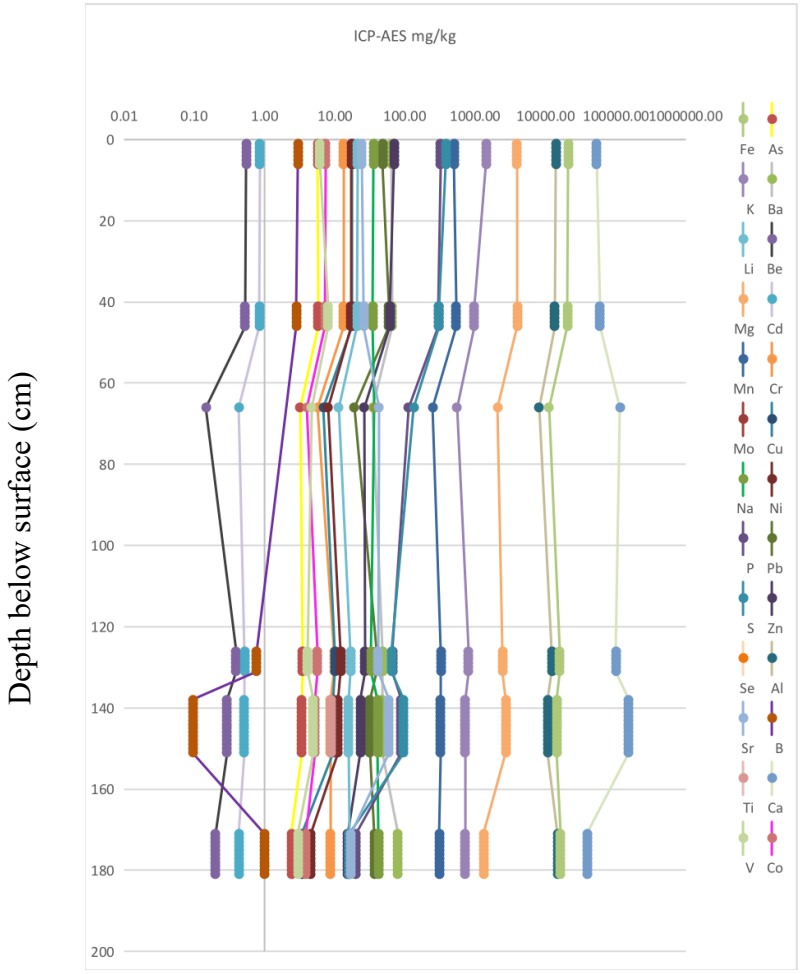

Figure 5.15: Profile D-SL ICP-AES results.

Most elemental values show only a slight decrease or increase between the samples collected at 137-150 cm and 170-180 cm, the last sample collected in the profile. Copper, nickel, strontium, sulfur, and phosphorus all show a moderately significant decrease between the samples collected at 137-150 cm and 170-180 cm (Figure 4.29). Copper decreases more than 50% between these two samples. Overall, it shows a greater than 75% decrease between the top soil sample and the sample collected from 170-180 cm. The top soil sample has the highest copper value in the entire profile, which may be related to application of fertilizer (Xiaorong et al. 2007). Nickel also decreases more than 50% between these two samples. It shows a similar value difference between the first and last samples, though there are other elevated values down the profile between these two samples. Strontium generally maintains a steady increase down the profile, except for the last value which shows a 75% decrease from the previous sample. Sulfur also steadily decreases, except for the sample collected from the buried soil. Between the last two samples, there is a nearly 85% decrease. Phosphorus shows a similar pattern to sulfur, with a value increase in the buried soil. Phosphorus decreases less dramatically between the last two samples. The periodic saturation of the redoximorphic zone has likely resulted in depletion of these elements through leaching. Sulfur and phosphorus are likely high in the buried soil due to Maya cultivation over a long period of time. Phosphorus is elevated as a reflection of soil fertilization. The higher sulfur concentration is probably a reflection of the presence of gypsum, produced at the water table boundary as a result of evaporation, like sodium. I don't have any dates for this profile. Further research includes identifying datable material in this profile. This profile likely represents a paleochannel, and dates would enable us to develop a chronology of channel activity based on presence of flood sediments and channel stability characterized by development of an A-horizon.

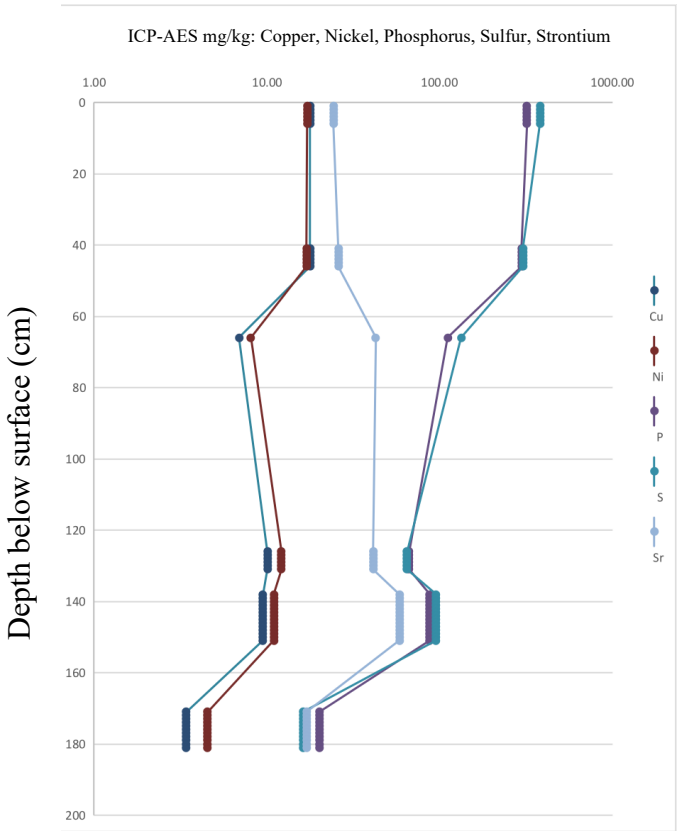

Figure 5.16: Profile D-SL ICP-AES Cu, Ni, P, S, and Sr results

A-SL QUARRY PIT

Profile A-Sl Quarry Pit is located at coordinates N 17° 6’ 13.2’’, W 89° 7’ 44” (Figures 5.16, 5.17. 5.18). This profile extends from 100-440 cm (Table 5.5) and is a truncated version of 4.1 B-SL Quarry Pit and 4.4 C-SL. This floodplain profile begins with about 50 cm (100-150 cm) of sandy C horizon, which could be alluvium from recent flooding or the leftover from the truncated soil sequence. From 150 to 180 cm is the Ab horizon, which gradually transitions into a Bt horizon from 180 to 215 cm since clay increased (by 20 %) from the Ab to the B horizon (Soil

Survey Staff 1999). The Ab horizon is composed of brown to dark brown subangular blocky clay. The Bt horizon gradually transitions into a C horizon that extends from 220 to 245 cm. It is a 10YR 5/2 subangular blocky silt loam with little evidence of pedogenesis. Another Ab horizon (2Ab) runs from 240 cm to 300 cm, which gradually transitions into another Bt horizon from 300-345 cm. This Ab horizon is reddish-brown subangular to angular blocky clay. Below this, from 350 to 440 cm are Cg horizons with silt loam textures and redoximorphic features, probably from overbank flooding. From 410 to 440 cm is likely a Cgk horizon because of pedogenic carbonate. Some sections at the bottom of the profile had elements of another Ab horizon with remnant organics, and in some areas this was on top of point bar or channel sands.

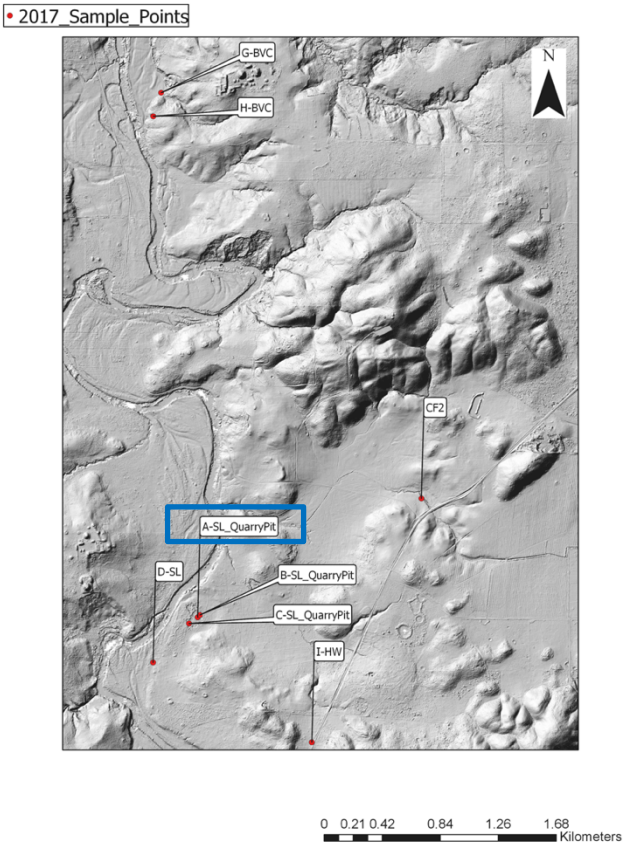

Figure 5.17: Profile A-SL location map.

Figure 5.18: Profile A-SL

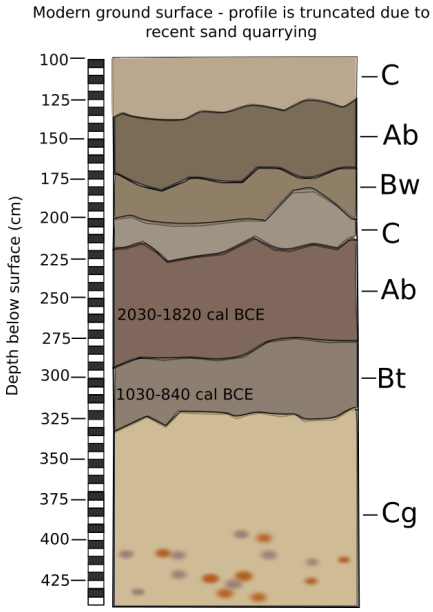

Figure 5.19: Profile A-SL

Depth (cm)	Horizon	Description
0-100	Truncated Soil	Two remnant soil profiles nearby suggest A, BW, C horizon truncated
100-150	C	Sand, 10YR 6/2
150-155	Ab	Clay, 10YR 3/3
160-165	Ab	Clay, 10YR 3/3, subangular blocky
170-180	Ab	Clay, 10YR 4/3, subangular blocky to angular blocky
180-185	B	Clay, 10YR 4/3, subangular blocky, manganese staining
190-195	Bw	Clay 10YR 4/3, subangular blocky
210-215	Bw	Clay, 10YR 4/3, subangular blocky
220-225	C	Clay, 10YR 5/2, subangular blocky
230-235	C	Clay, 10YR 4/3, subangular blocky
240-245	Ab	Clay, 5YR 3/3, chert throughout
252-256	Burn layer	Reddish-brown burn layer (5YR 3/3), subangular blocky
260-265	Ab	2.5YR 2.5/2 subangular blocky to angular blocky
270-275	Ab	5YR 3/3 clay, subangular blocky to angular blocky
290-295	Ab	Clay, melanized 10YR 5/2, subangular blocky
300-305	Bt	10YR 5/3, unmottled clay, subangular blocky
310-315	Bt	10YR 5/2 clay, subangular blocky
315-345	Bt	10YR 4/2, organic staining
360-380	Cg	Similar to above, but dominated by grey with red oxidation masses around pores
380-410	Cg	2.5Y 7/4 mottled with grey, redoximorphic, massive, no structure
410-435	Cgk	Similar to above, mottled orange and grey, no structure, small calcite nodules throughout
435-440	Cgk	Similar to above, mottled orange and grey clay, no structure, dense

Table 5.5: Profile A-SL log.

Both loss-on-ignition and magnetic susceptibility results seem to indicate presence of a buried soil (Ab horizon) from about 150 to 200 cm (Figure 5.19). Phosphorus, however, decreases in this zone. Phosphorus shows an abrupt increase around 320 cm, which is interesting because this is a redox zone so I would not expect elevated phosphorus values to occur here. The cation exchange capacity value in the buried soil is elevated (Table 5.6), which is what I would expect in an A or Ab horizon.

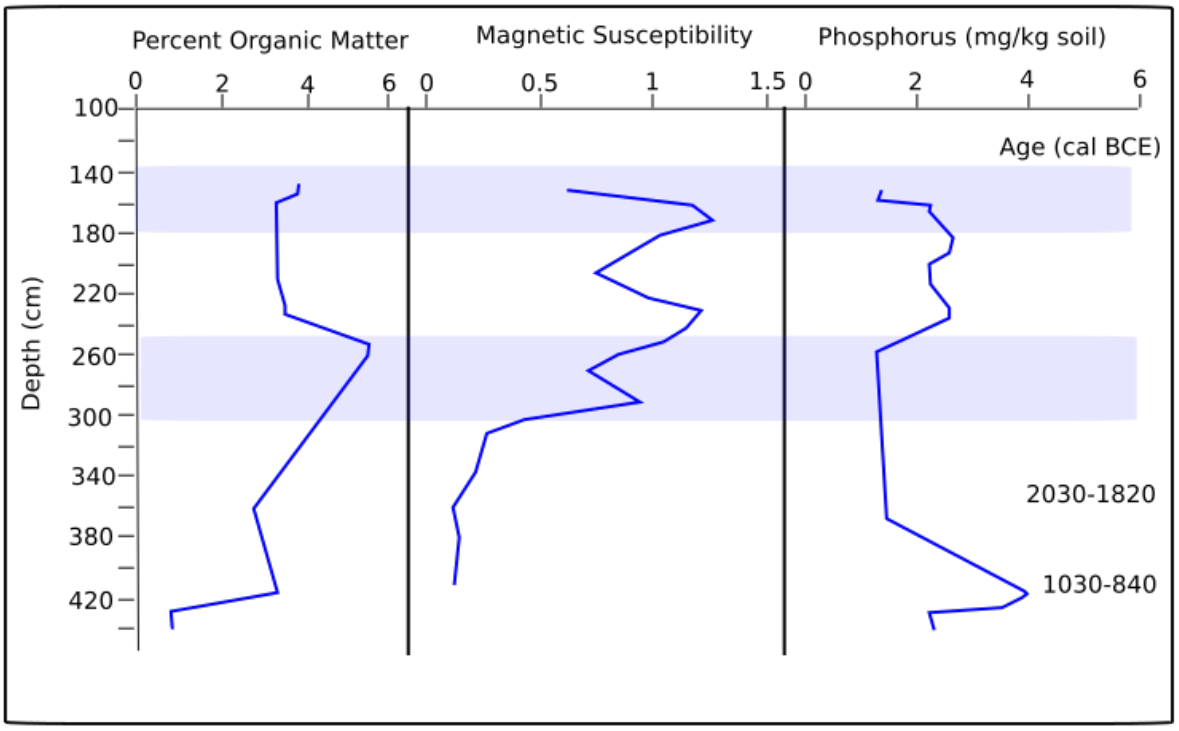

Figure 5.20: Profile A-SL loss-on-ignition, magnetic susceptibility, and phosphate results.

Depth (cm)	CEC (cmol/kg)
50-55	4.75
155-160	7.82

Table 5.6: Profile A-SL cation exchange capacity (CEC) results.

CNAL's particle size analysis shows mostly silts and clays throughout the entire profile, at relatively uniform distributions (Figure 5.20). However, it does appear that there is slightly more clay at 105 and 157 cm. Based on the log, 205 cm is a Bw horizon, so I would expect a lot of clay. At 157 cm is an Ab horizon, which would also be very weathered with abundant clay. CNAL's ICP-AES results show several well-defined trends (Figure 5.21). Excluding vanadium, calcium, and sulfur, all elements show a fairly dramatic decrease between 316 and 330 cm; however, due

to lack of data points in between these two depths it is difficult to tell how abrupt this transition is. This trend may be related to the redoximorphic environment that occurs at this depth. CNAL phosphorus trends in this profile show a similar increase after 260 cm (60 cm shallower than where our phosphorus lab results show an increase), which is interesting because soil in this zone shows a gleyed color and does not look like a typical dark-colored buried A horizon. It's difficult to draw a valid conclusion off of a single data point: this could be indicative of an outlier or this may reflect a gleyed, clayey soil from which all of the calcium has been leached out.

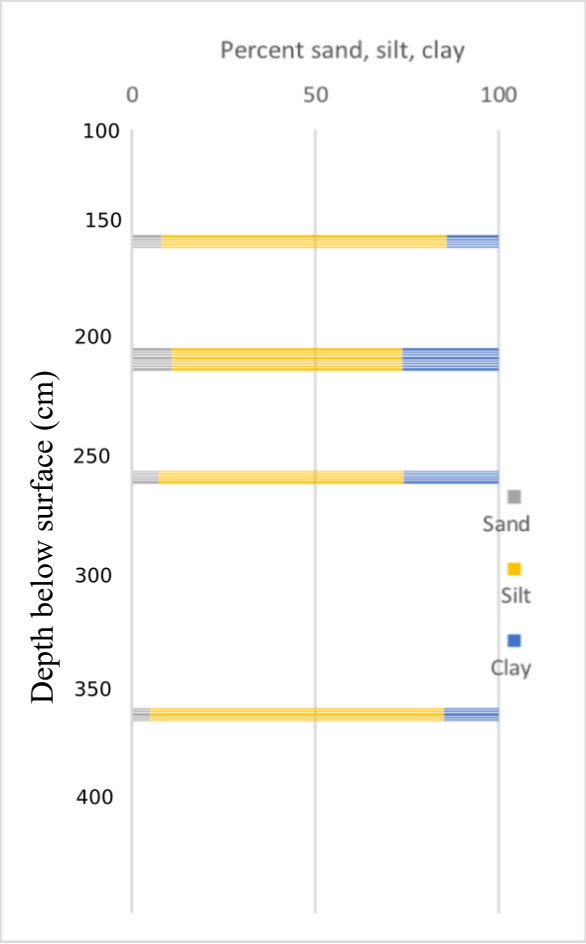

Figure 5.21: Profile A-SL particle size analysis results.

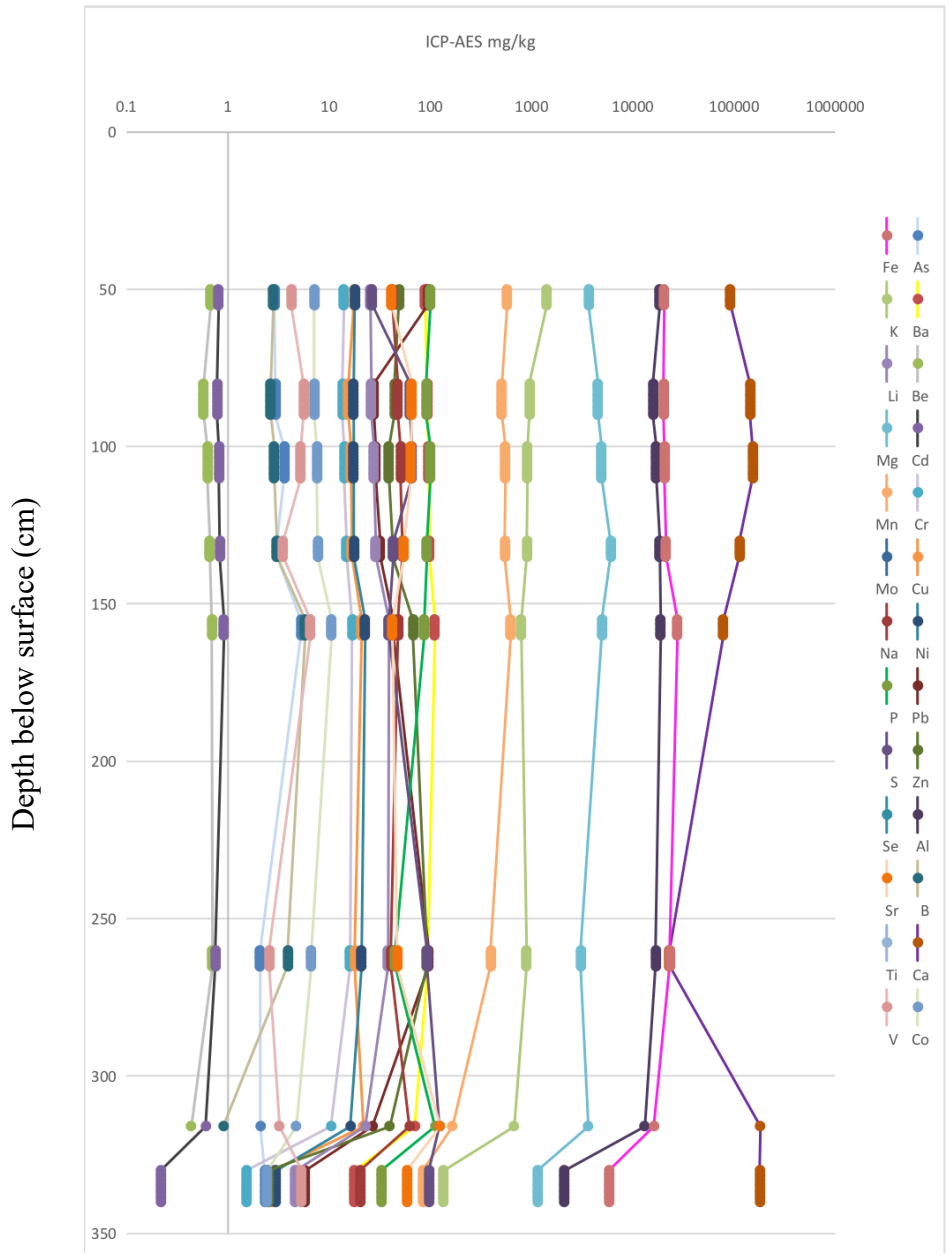

Figure 5.22: Profile A-SL ICP-AES results.

Calcium, like phosphorus, decreases in the buried A horizon (Figure 5.22). Sulfur shows an increase around 100 cm (Figure 5.22), which is the same place that lead decreases. Sulfur then increases near the bottom of the profile, as indicated by three data points. The sulfur could be from gypsum accumulation just above the water table, which is not uncommon in this environment.

Lead is high around 50 cm and increases abruptly at 260 cm (Figure 5.22). There are not enough data points to draw firm conclusions, but the samples above and below 260 cm seem to have significantly lower lead values, though I can't determine exactly where the elevated lead values begin. The high lead concentration occurs in gleyed soil, which means that this value is influenced by the water table and whatever may be dissolved in it.

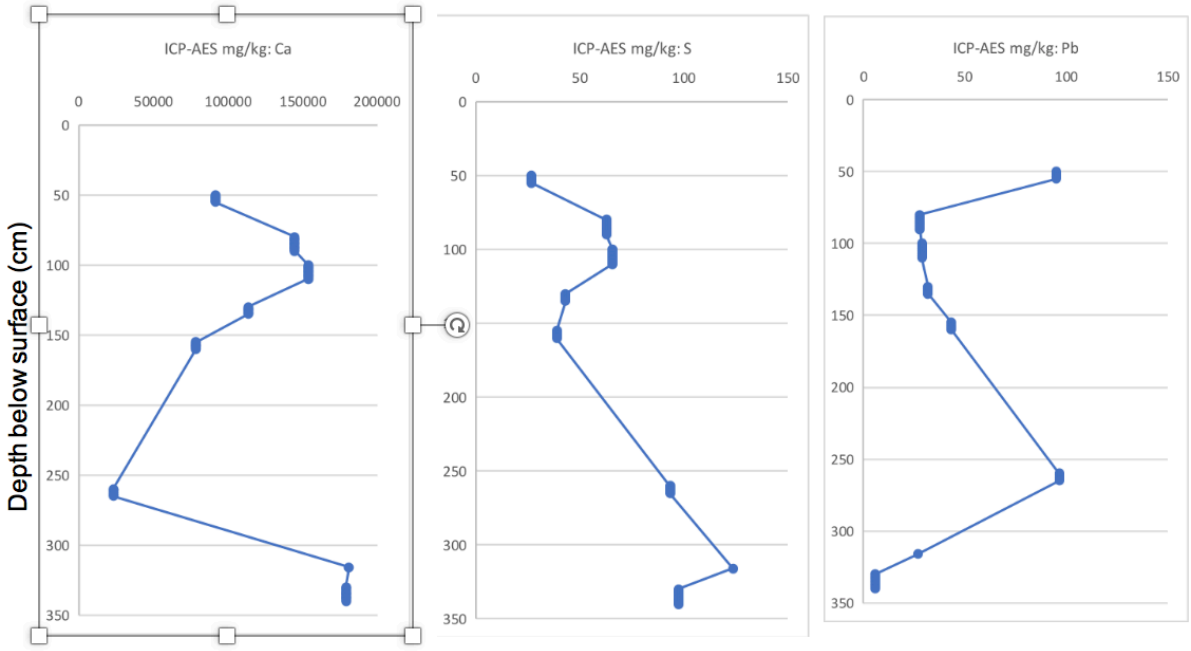

Figure 5.23: Profile A-SL ICP-AES Ca, S, and Pb results

I have two AMS dates for this profile (Figure 5.18, 5.19): 260 cm has been dated to 2030-1820 cal BCE, and 316 cm has been dated to 1030-840 cal BCE. These dates seem 1-2000 years older than what I would expect with an average sediment deposition rate of 100 cm per 1000 years. Additionally, the ages are reversed, with the younger age occurring at greater depth. More dates will help to refine and clarify this age-depth model.

C-SL QUARRY PIT

Profile C-SL Quarry Pit is located at coordinates N 17° 6’ 10.9’’, W 89° 7’ 46.9” (Figures 5.23, 5.24, 5.25 This profile may represent a paleochannel (Figure 5.4). It extends from 0 to 190 cm (Table 5.7) and is located across from B-SL Quarry Pit on the opposite edge of the sand quarry. The A1 horizon extends from 0 to 20 cm and is composed of 10YR 3/1 fine granular silt with pebbles and cobbles. This is followed by the A2 or Bw horizon from 20 to 36 cm. This is a 7.5 YR 3/2fine granular sandy silt with pebbles and gravel. The C1 horizon follows from 36 to 57 cm and is composed of mottled 10YR 5/4 and 10YR 6/6 coarse silty sand with abundant cobbles. The C2 horizon begins at 57 cm and extends through 100 cm. It is a mottled 10YR 6-row very coarse gravelly sand. The C3 horizon begins beneath that, extending from 100 to 122 cm. It is a 10YR 4/4 very fine silty sandy clay with ceramics and shells throughout. The Bb horizon extends from 122 to 160 cm and is a 10YR 5/6 very fine silty clay with a little bit of sand. The last horizon is the 2C, beginning at 160 and extending through the bottom of the profile at 190 cm. It is a 10YR 4/6 fine granular clayey silt with a little bit of sand.

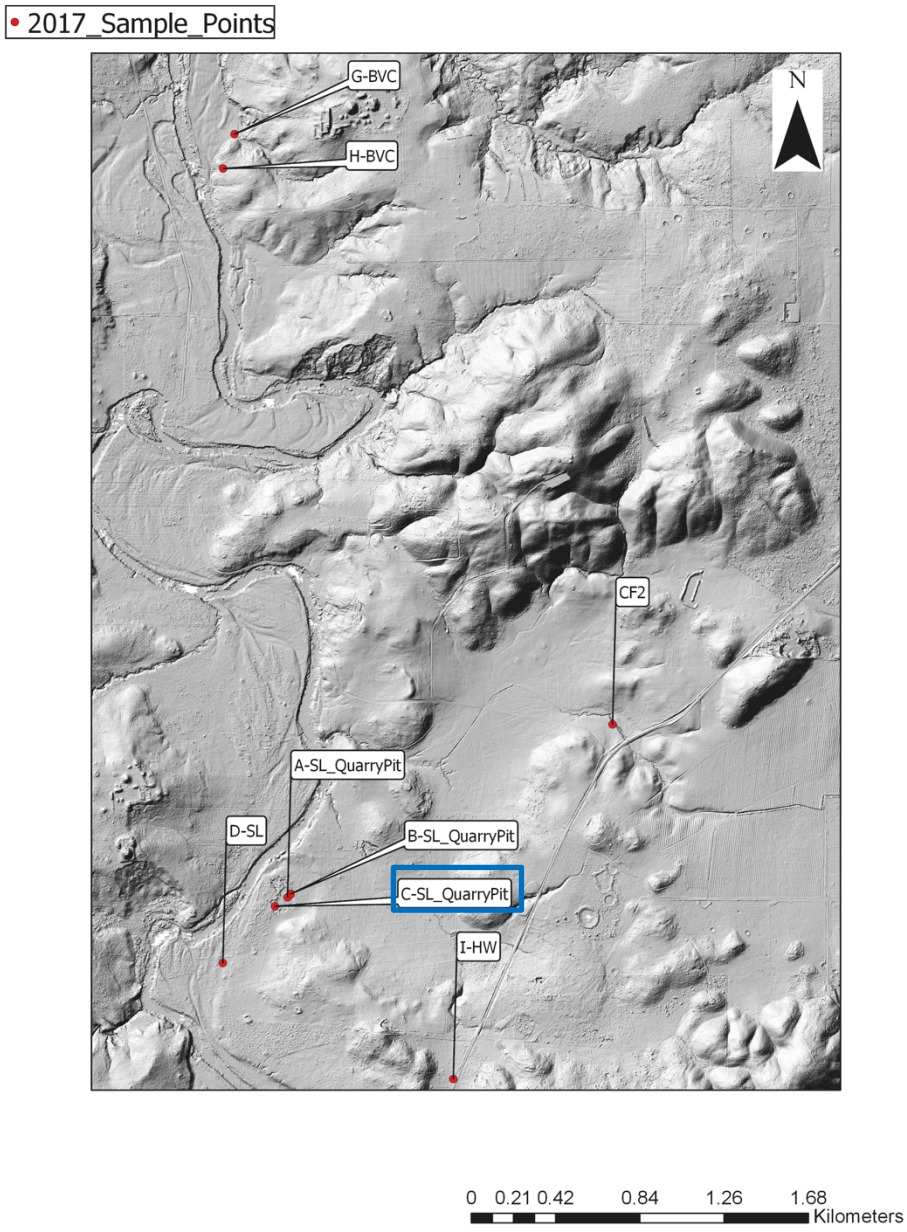

Figure 5.24: Profile C-SL location map.

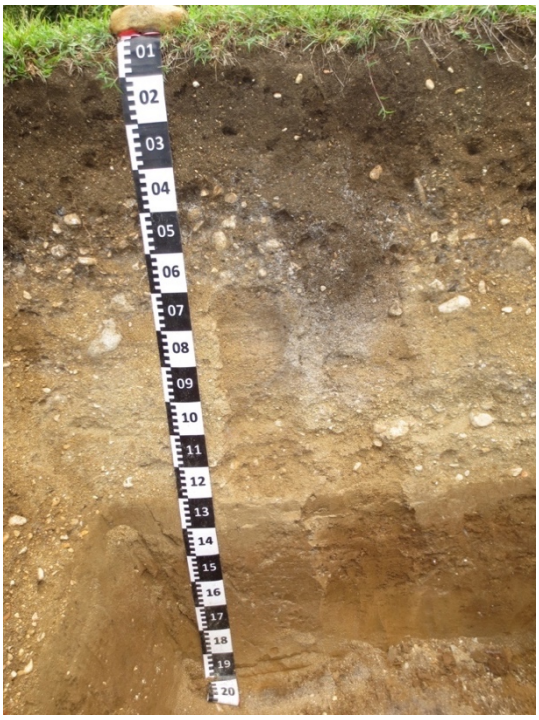

Figure 5.25: Profile C-SL

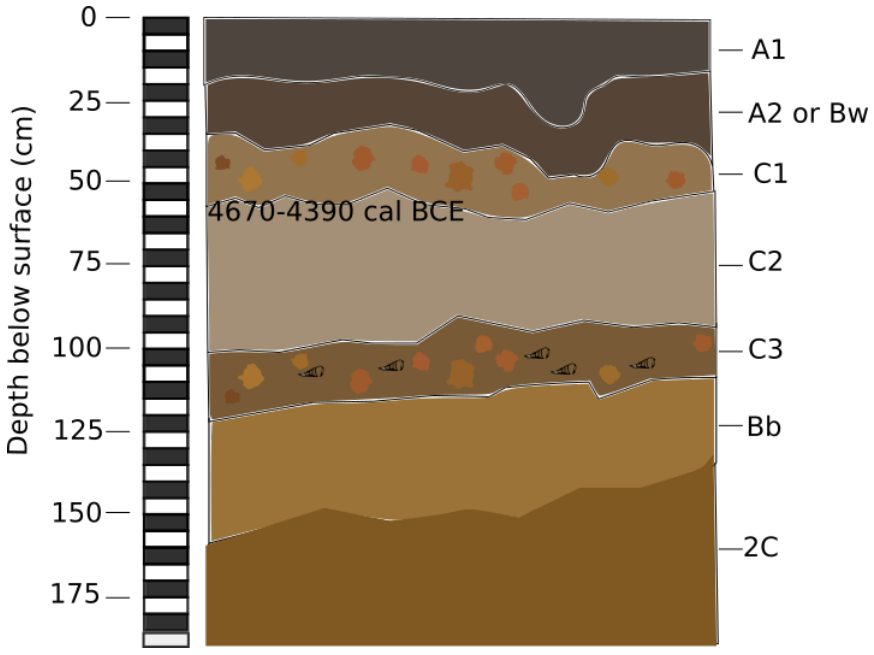

Figure 5.26: Profile C-SL

Depth (cm)	Horizon	Description
0-20	A1	Silt with pebbles and cobbles, fine granular, 10YR 3/1
20-36	A2 or Bw	Sandy silt with pebbles-gravel, fine granular, 7.5 YR 3/2
36-57	C1	Silty sand with abundant cobbles, coarse, mottled 10YR 5/4 and 10YR 6/6
57-100	C2	Gravelly sand, very coarse, mottled 10YR 6/ row
100-122	C3	Silty sandy clay, very fine, ceramics and shells throughout, gravel-cobbles, 10YR 4/4
122-160	Bb	Silty clay with little bit of sand, very fine, 10 YR 5/6
160-190	2C	Clayey silt with little bit of sand, fine granular, 10YR 4/6

Table 5.7: Profile C-SL soil log

No potential dark-colored Ab horizon was noted in the field (Figure 5.26). Magnetic susceptibility and phosphorus results indicate that there may be an eroded Ab horizon located between 100 and 160 cm, which I have here designated as a Bb horizon. The relatively light, orangey sediment color supports our hypothesis that this is indeed a Bb horizon, but it may be that this zone was affected over time by the now-eroded A horizon that it was at one point overlain by. Profile A-SL has a potential Ab horizon beginning at approximately 150 cm, and profile B-SL has a potential Ab horizon beginning around 160 cm. Therefore, is probable that profile C at one point had the same Ab horizon in this area, though all that now remains as indication of it is the Bb horizon. The cobbles, pebbles, and gravel in this profile indicate that this sediment was deposited in a very high-energy channel environment, which accounts for the potential erosion of the Ab horizon. We have an AMS date of 4670 – 4390 cal BCE at 55 cm, which is too old for this depth. This fits with the idea of this as a very high-energy, eroded deposition environment.

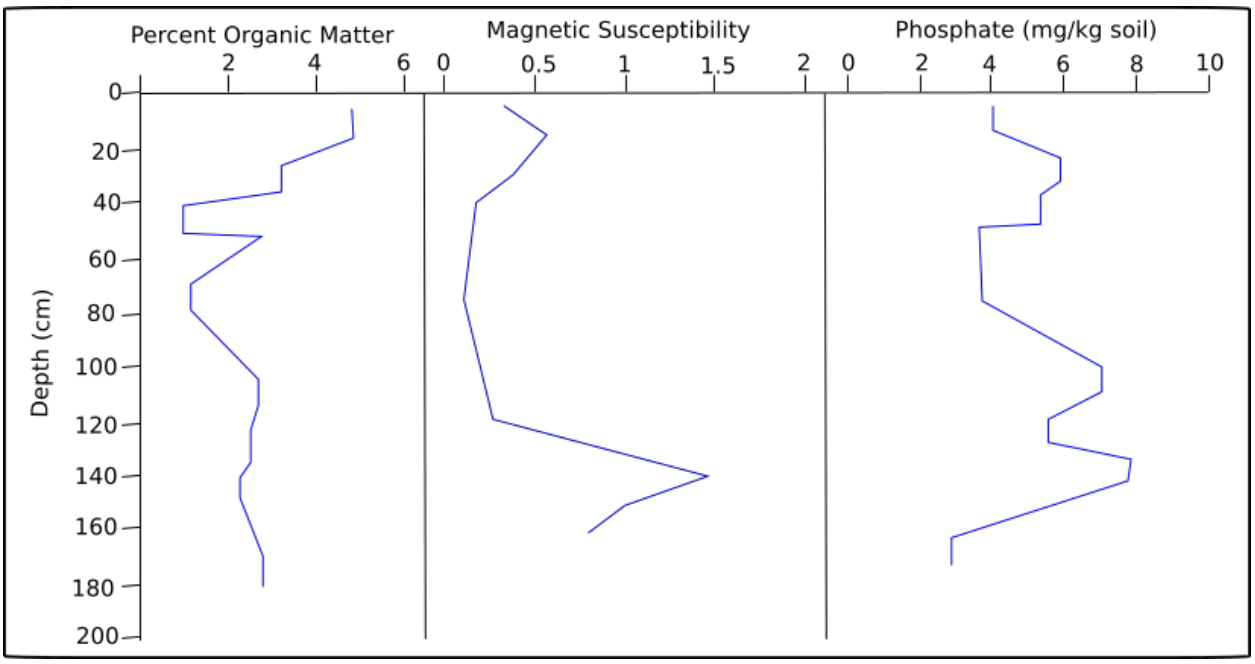

Figure 5.27: Profile C-SL loss-on-ignition, magnetic susceptibility, and phosphate results.

H-BVC

Profile H-BVC is located at coordinates N 17° 8’ 10.8’’, W 89° 7’ 57”, downslope from the archaeological site of Buena Vista at the edge of what I hypothesize to be a paleochannel (Figures 5.27, 5.28, 5.29, 5.30). The profile extends from 0 to 238 cm (Table 5.8), at which point we encountered the water table and therefore stopped digging. The A1 horizon extends from 0-15 cm and is composed of brown fine, granular sandy, clayey silt. The A2 horizon begins at 15 cm and continues to 35 cm. It’s made up of light brown coarse, structureless sandy silt. This is followed by a series of C horizons extending from 60 cm to the bottom of the profile at C5. They are all composed of a mix of light red-brown loose, sand, silt, and clay, with clay increasing near the bottom of the profile. From 213 to 238 cm the sediment becomes wet gleyed clay sitting just above the water table.

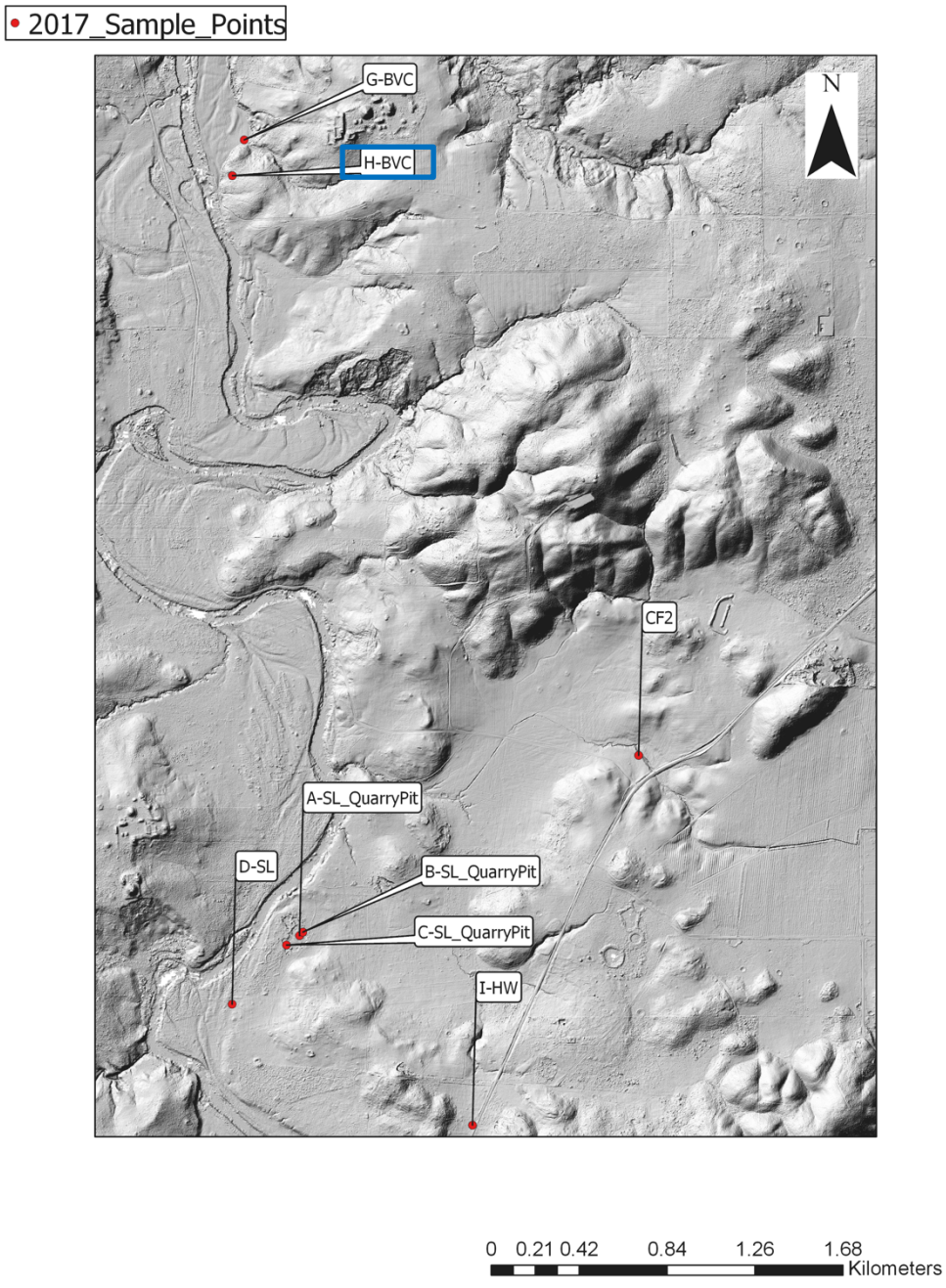

Figure 5.28: Profile H-BVC location map

Figure 5.29: Profile H-BVC

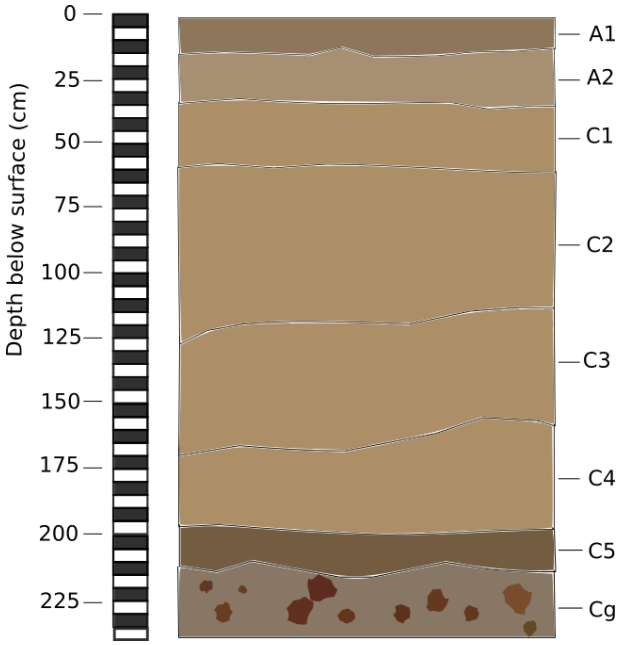

Figure 5.30: Profile H-BVC

Depth (cm)	Horizon	Description
0-15	A1	Fine sandy clayey silt, granular, 10YR 5/3
15-35	A2	Coarse sandy silt, no structure, 10YR 6/3
35-60	C1	Fine sandy silt, loose, 10YR 6/4
60-125	C2	Fine silty sand, loose, 10YR 6/4
125-168	C3	Silty coarse sand, loose, 10YR 6/4
168-198	C4	Sandy silty clay, 10YR 6/4
198-213	C5	Sandy clay, moist, 10YR 4/3
213-238	Cg	Sandy clay with abundant gravel-cobbles, wet, 10YR 5/2

Table 5.8: Profile H-BVC soil log

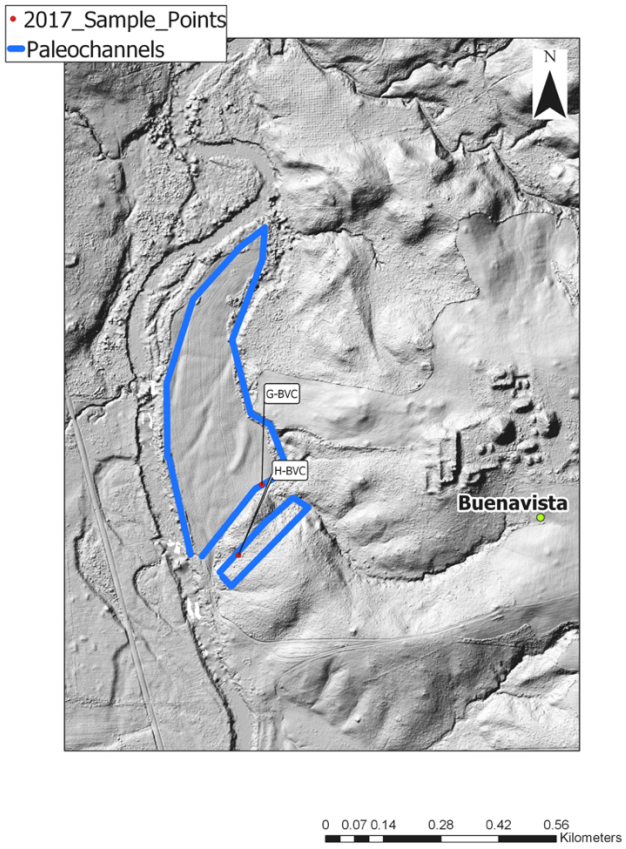

Figure 5.31: Paleofloodplain features visible in the LiDAR imagery near the Buena Vista series soil profiles.

No potential dark-colored Ab horizon was observed in the field, and this profile was completely sterile of artifacts, excluding a single piece of very rounded ceramic in the Cg horizon. This ceramic had probably been transported some distance by the paleoriver; the Cg horizon likely represents a paleochannel. Loss-on-ignition, magnetic susceptibility, and phosphorus results for this profile do not indicate likely presence of Ab horizon (Figure 4.55). There is no significant increase in percent of organic matter at any point in the profile, other than at the surface. Magnetic susceptibility shows an increase, based on a single data point, around 160 cm. This number seems to occur at the same depth as the Ab horizon in profile B-SL, and the possible Ab profile in profile C-SL. However, since profile H-BVC is located in a different area than the San Lorenzo profiles, and there is only one line of evidence indicating a possible Ab horizon around 160 cm, I can't draw any valid conclusions. More research is needed in the Buena Vista floodplain area, as well as in the area between San Lorenzo and Buena Vista.

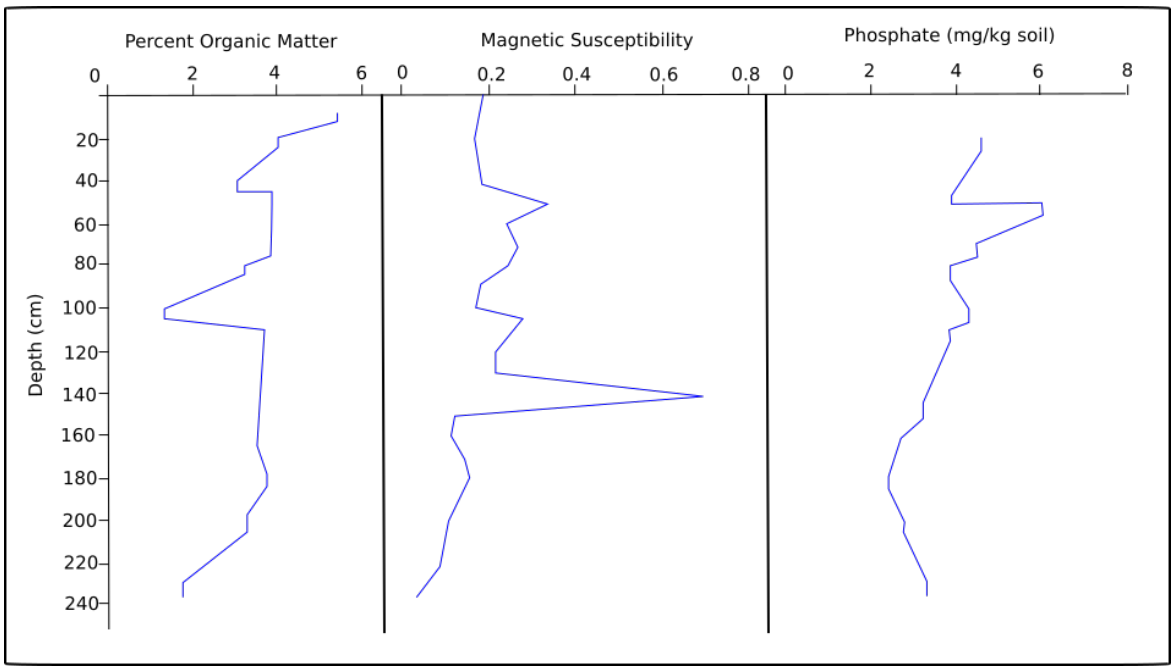

Figure 5.32: Profile H-BVC loss-on-ignition, magnetic susceptibility, and phosphate results.

CF2

Profile CF2 is located at coordinates N 17° 6’ 40.3’’, W 89° 6’ 52” (Figure 5.32, 5.33, 5.34) in a deep gully through which a seasonal stream flows, roughly in between the San Lorenzo and Buena Vista profiles. The profile is along the wall of the gully, on an actively eroding and slanted surface, making it fairly difficult to accurately describe depths. The following description is based on approximate depths (Table 5.9). The described profile extends to a depth of 400 cm, beginning with an A-horizon composed of brown clayey silt. Next is a hypothesized Ab horizon, beginning at 180 cm and extending to 300 cm. It is made up of black clayey silt and was very obvious in the profile. From 300 to 400 cm the sediment is composed of light brown-red silty clay with some red and grey mottling. This is likely a C-horizon. Magnetic susceptibility values do not reflect the hypothesized Ab horizon (Figure 5.35), but it may be that I was not getting an accurate signal because of all the erosion and downward movement of sediment. I was not able to clean the profile because the landowner specifically requested that I only look at the soil, and not disturb it in any way because he was concerned about further erosion.

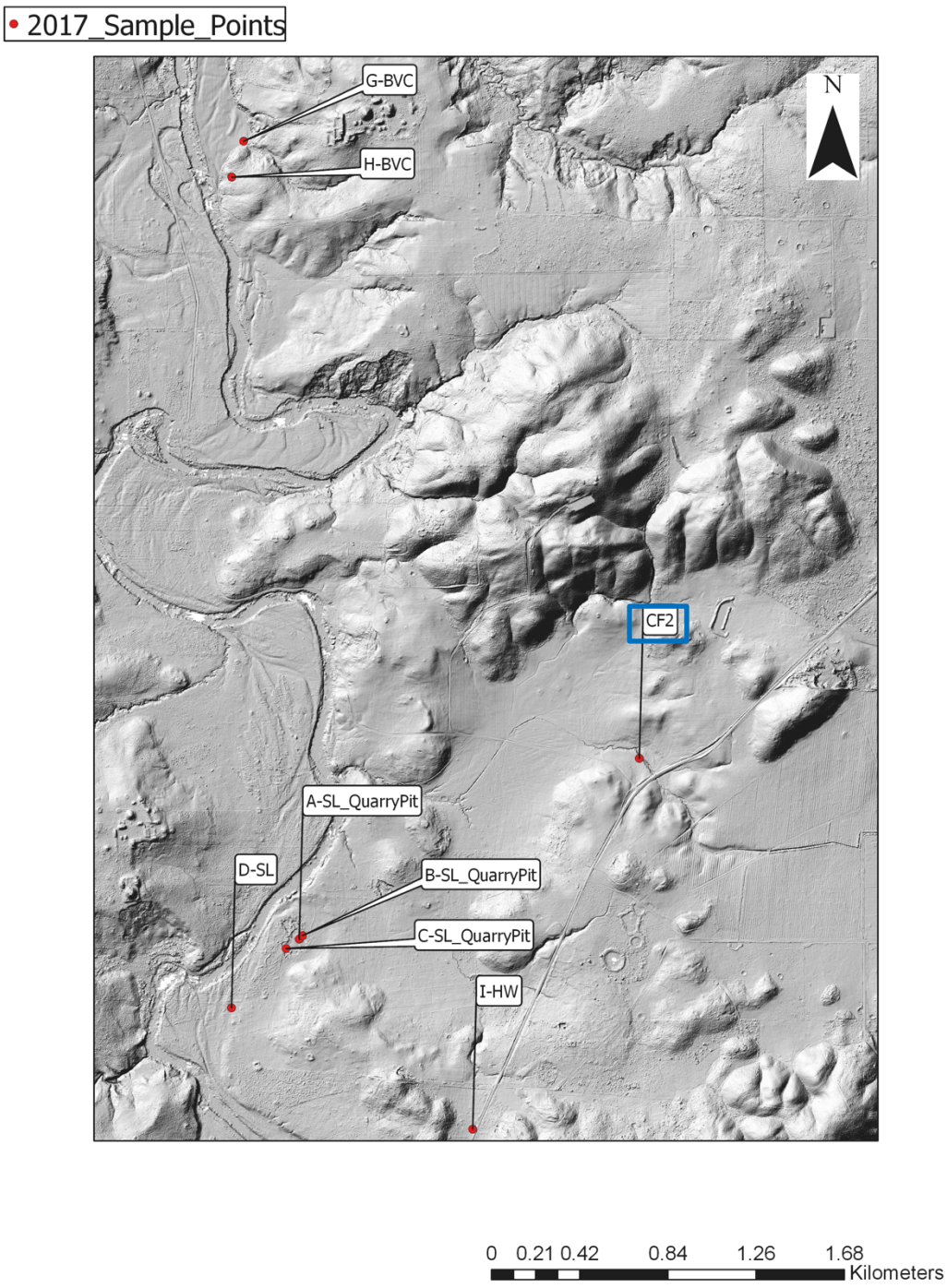

Figure 5.33: Profile CF2 location map

Figure 5.34: Profile CF2

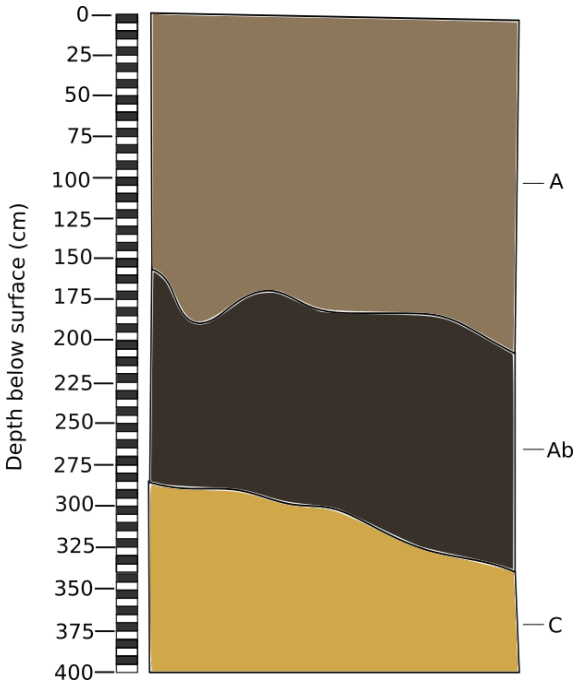

Figure 5.35: Profile CF2

Depth (cm)	Horizon	Description
0-180	A	Clayey silt, 10YR 5/3
180-300 cm	Ab	Silty clay, 10YR 2/1
300-400	C	Silty clay, 2.5Y 7/8 with some red and grey mottling

Table 5.9: Profile CF2 soil log

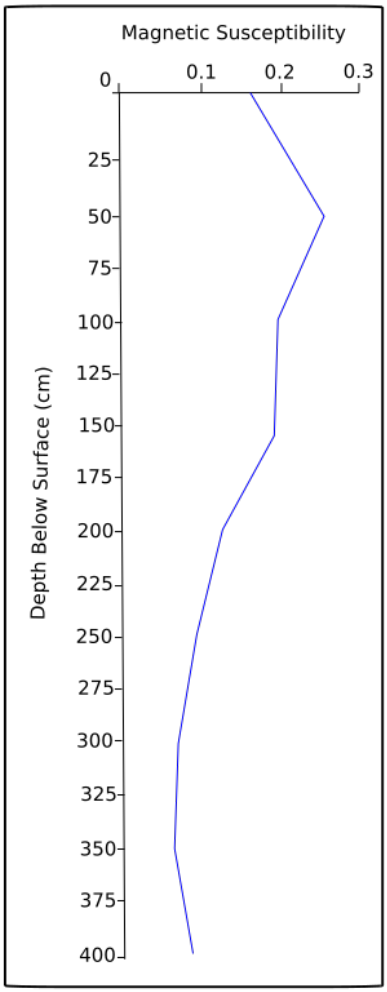

Figure 5.36: Profile CF2 magnetic susceptibility results.

G-BVC

Profile G-BVC is located at coordinates N 17° 8’ 15’’, W 89° 7’ 52.9” (Figures 5.36, 5.37), within a Mennonite field. After lab analyses and study of dates on profile G-BVC, we think that the profile is fill material (Table 5.9), possibly emplaced during Mennonite field building operations. Radiocarbon dates, loss-on-ignition, phosphorus, and magnetic susceptibility results support this hypothesis (Figure 5.38). The three dates I have are all historic to modern, and they are nearly identical down the profile. Loss-on-ignition, phosphorus, and magnetic susceptibility results show no defined patterns or trends, which is not what I would expect to see in a 300-cm-deep profile.

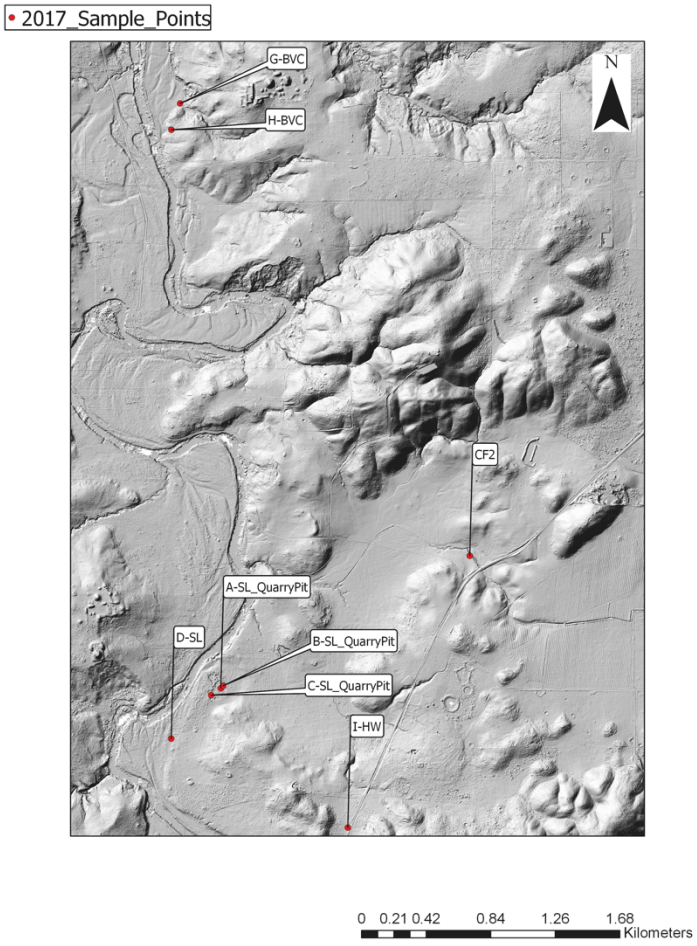

Figure 5.37: Profile G-BVC location map

Figure 5.38: Profile G-BVC

Depth (cm)	Possible Horizon	Description
0-20	Ap	Granular, 10YR 5/2
20-40	A2	Granular, moist, 10YR 5/2
40-70	C	10YR 6/3 mixed with white ash or calcium carbonate
70-80	Charcoal	Charcoal with visible structure
80-90	C/Ck	Clay mixed with white ash or calcium carbonate, 10YR 5/3
90-96	Burn Layer	Oxidized, probably burn surface, 2.5YR 4/6
96-120	C	Clay, 10YR 5/3
120-130	?	White ash or calcium carbonate
130-185	Ab	Clay, abundent ceramics, 10YR 3/3
185-236	Bt	Sandy-silty loam, 5YR 5/6
236-246	?	Sandy loam, 10YR 7/4
246-260	?	Gravely clay mixed with sandy loam, redoxomorphic, 10YR 7/4
260-320	?	Subangular gravely clay, colluvium, 10YR 7/4
320-330	?	Clay mixed with chert gravel to cobbles, abundant ceramics at 330, 10YR 7/4

Table 5.10: Profile G-BVC soil log

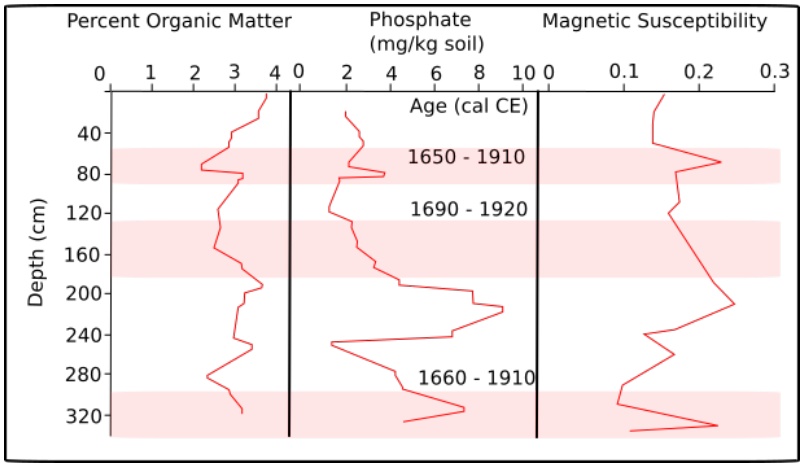

Figure 5.39: Profile G-BVC loss-on-ignition, magnetic susceptibility, and phosphate results.

I-HW

Profile I-HW is located at coordinates N 17° 5’ 37.6’’, W 89° 7’ 20.9” (Figure 5.39. 5.40, 5.41). This profile is located along the Western Highway just west of the driveway to camp. It was exposed as part of a construction project to build a gas station. The gas station has since been completed and the profile is no longer there. This profile is well upslope from the river and is not a floodplain soil, as indicated by the reddish coloration of the profile. It provides a non-floodplain soil to compare with the floodplain soils discussed in this thesis. The profile is 230 cm in depth (Table 5.10), and begins with an A1 horizon from 0 to 10 cm. The O-horizon was present in a few places, but most of it had been burned off as part of the construction project. The A1 horizon is composed of 10YR 3/2 mottled with 10YR 3/3 granular silt with limestone nodules. The A2 horizon extends from 10 to 30 cm and is made up of a similar grain size with a blocky texture and darker color of 10YR 4/4. The B1 horizon is beneath that, extending to 60 cm. It is composed of 10YR 4/4 structureless clay with limestone nodules. There are a series of Bt horizons over the next 100 cm, ending at 160. These are composed of clay and silt with manganese nodules and sediment coloration indicating redoximorphic processes. The C horizon extends from 160 to 210 and is composed of 10YR 7/6 mottled with 10YR 6/8 and 10YR 6/4 silty clay with calcite and manganese nodules. There is a Ck horizon from 210 to the bottom of the profile. Loss-on-ignition results indicate no zones of high organic matter other than the A horizon (Figure 5.42). Phosphorus results show a couple of increases in the Bt horizons.

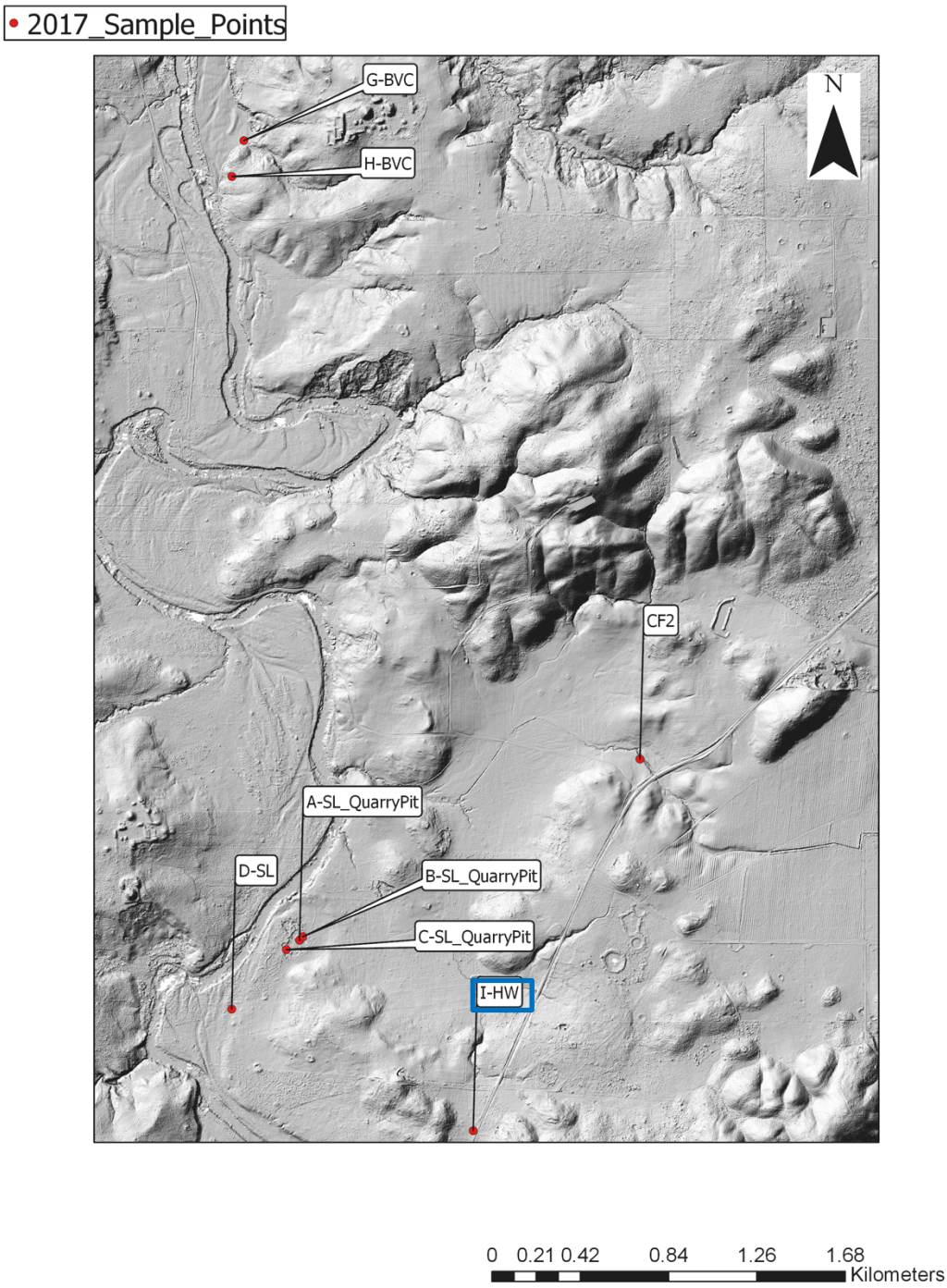

Figure 5.40: Profile I-HW location map

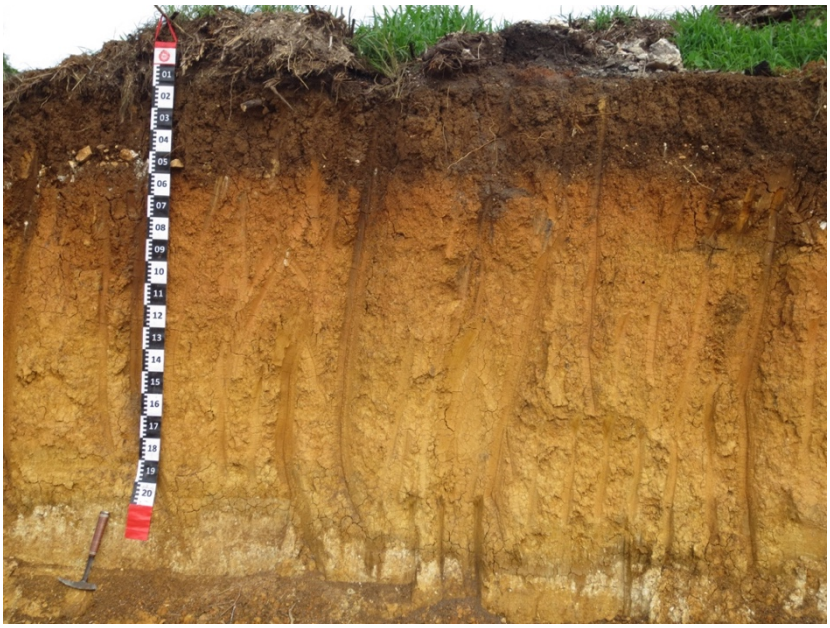

Figure 5.41: Profile I-HW

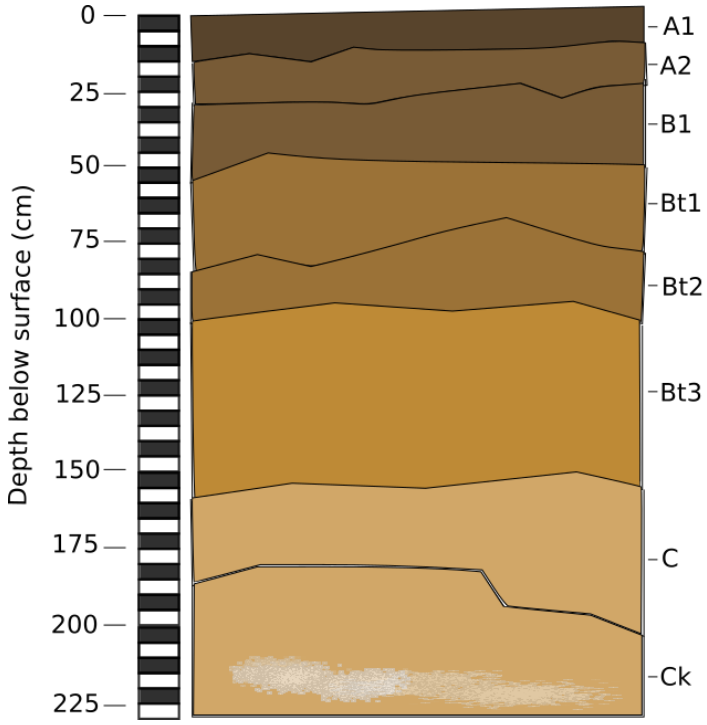

Figure 5.42: Profile I-HW

Depth (cm)	Horizon	Description
0-10	A1	Silt with limestone nodules, granular, mottled 10YR 3/2 with 10YR 3/3
10-30	A2	Silt with limestone nodules, blocky, 10YR 4/4
30-60	B1	Clay with limestone nodules, structureless, 10YR 4/4
60-83	Bt1	Silt, structureless, 10YR 5/6
83-100	Bt2	Clayey silt, structureless, 10YR 5/6
100-160	Bt3	Clayey silt with manganese nodules and oxidation staining, mottled 10YR 6/8 with 10YR 4/4
160-210	C	Silty clay with clacite nodules and some managnese nodules, moddled 10YR 7/6, 10YR 6/8 and 10YR 6/4
210-230	Ck	SAA with calcium carbonate throughout

Table 5.11: Profile I-HW soil log

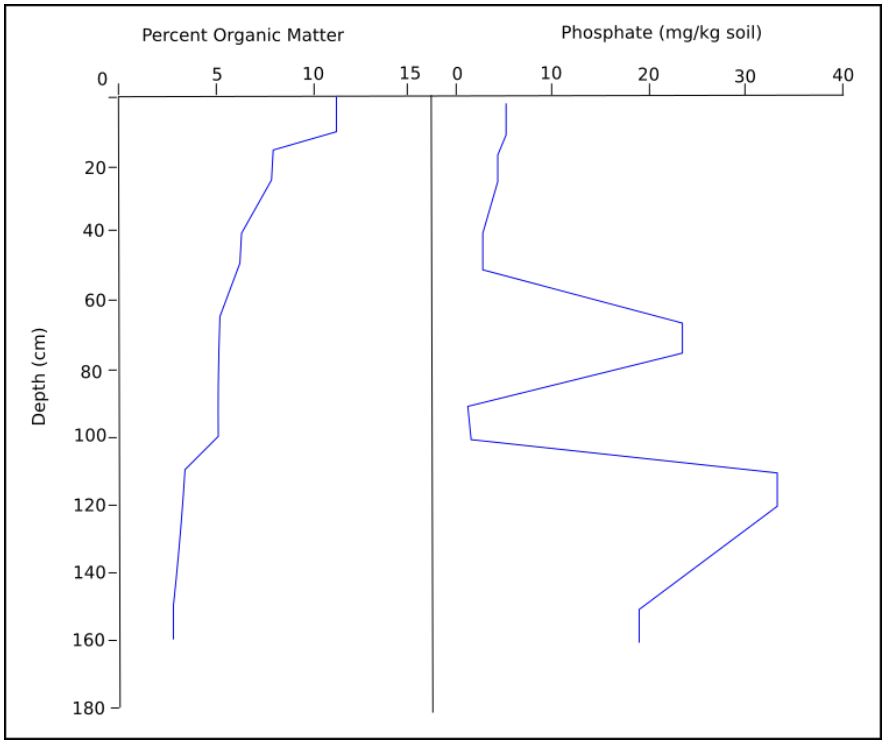

Figure 5.43: Profile I-HW loss-on-ignition and phosphate results.

PALEOSOL IDENTIFICATION AND RESULTS SYNTHESIS

I hypothesize that there is a paleosol (Ab horizon) located from around 150 cm to 200 cm, though in some areas it begins a bit shallower or extends deeper. This paleosol represents the stable land surface that the Maya were living on somewhere between 2000 and 1000 cal BCE (Early Preclassic). The hypothesized paleosol is intermingled with sediments deposited by flooding and high energy riverine environments. These flood sediments may be the result of flooding caused by Maya land use for construction and agriculture, however at this point I do not have enough data to draw this conclusion. Further dates are needed to develop and refine this chronology. This horizon is generally clayey in composition across all profiles. Profiles B-SL, D-SL, and A-SL all have a dark-colored soil that occurs around 150 to 200 cm. (Figure 5.44). Loss-on-ignition, magnetic susceptibility, and phosphorus results all increase in this zone in profile B-SL. In profiles D-SL and A-SL, magnetic susceptibility and loss-on-ignition results increase through this zone. Elemental concentrations also show a general increase at 150 cm in profile B-SL, and phosphorus and sulfur also show an increase around this depth in profile D. Though I did not field-observe a potential Ab horizon in profile C-SL, magnetic susceptibility and phosphorus results show elevated values from 100 to 160 cm. At 160 cm, profile H-BVC shows and increase in magnetic susceptibility, and profile CF2 has a very dark-colored clayey horizon from 180 to 300.

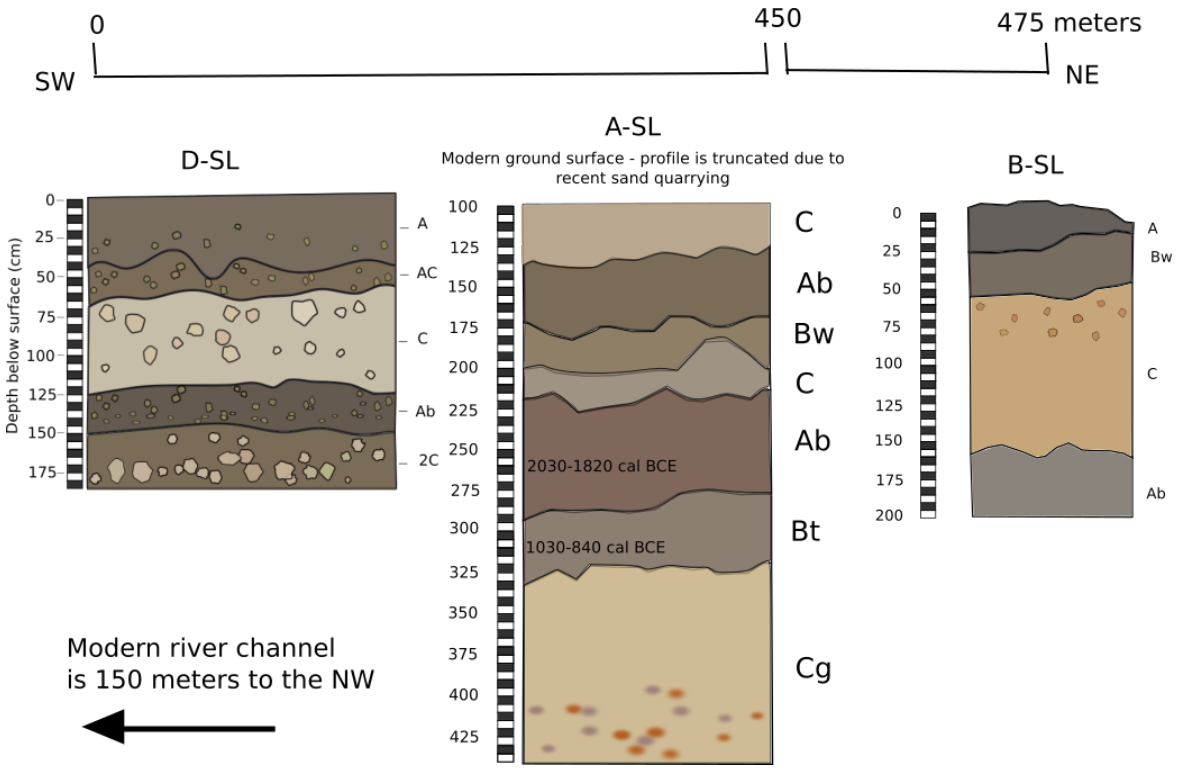

Figure 5.44: Cross section of profiles D-SL, A-SL, and B-SL

GIS Results

The next step of this research is to identify additional sites that will provide records of flooding over time and I have therefore applied my GIS method of flood mapping to the modern channel. For future sampling efforts I will focus on areas that would have been flooded at stages of 3 meters (Figure 5.45). As I continue to sample and describe sediments, I can identify profiles that were likely to have been deposited by the paleo-river. Combining these data with paleochannels that are clearly visible in the LiDAR, I should be able to map the paleo-river. From there, the next step will be to develop a flood map based on the paleo-river and floodplain.

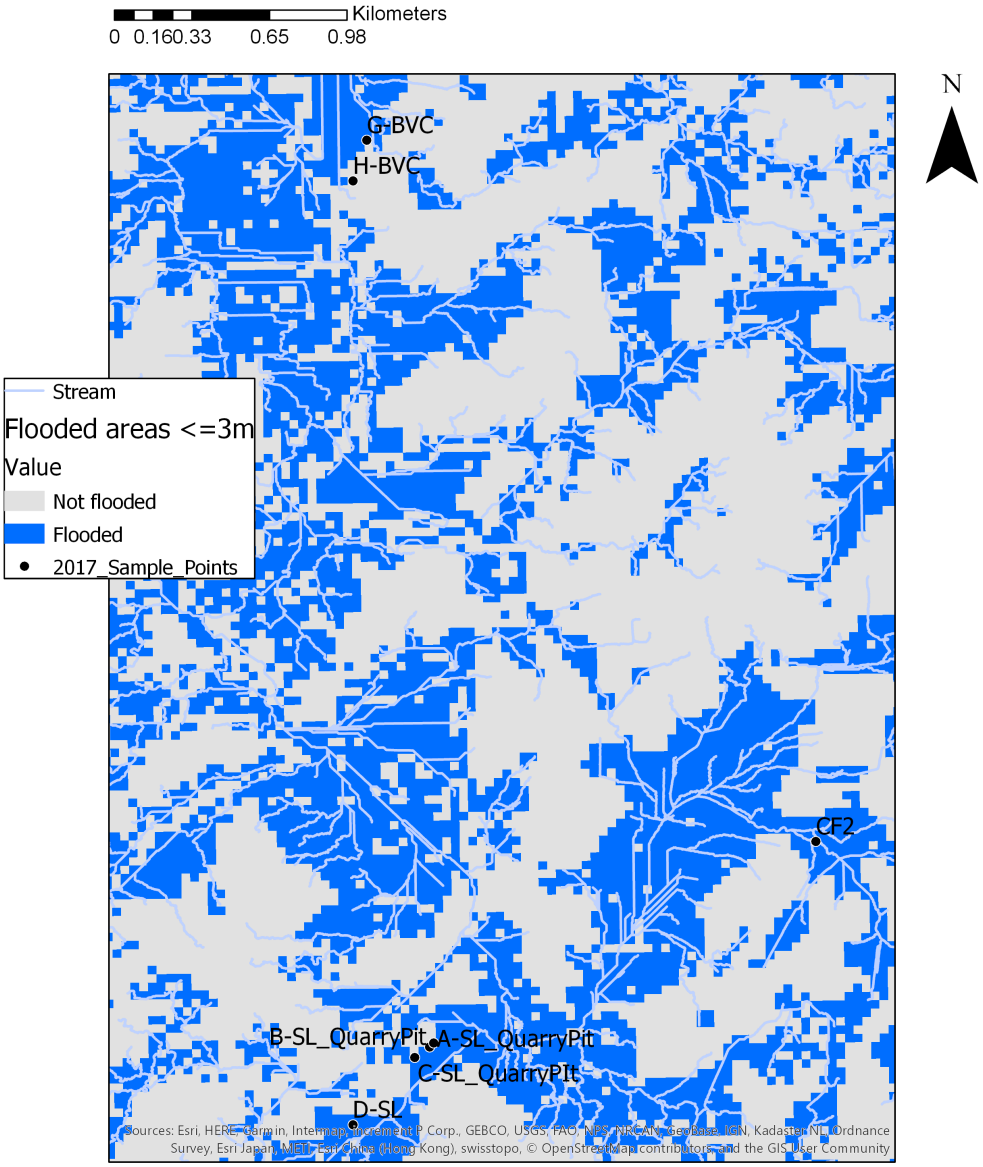

Figure 5.45: Flood map at stage of 3 meters.

Chapter 6: Conclusion

This thesis addresses the hypothesis that as the Maya were deforesting their landscape for construction and for agriculture they were causing erosion. This erosion changed the Mopan River's sediment budget, which in turn altered the flood frequency thus resulting in the floodplain landscape as it exists today. Data indicates presence of a paleosol from the Early Preclassic (2000 – 1000 BCE) , a time period during which Maya chronology indicates that abundant erosion took place. Therefore, we would expect the sediment record to show erosion, and therefore flooding activity, increasing. Coarse sediments that are indicative of flooding do seem to correspond to presence of the paleosol, however we do not have enough data to conclude whether ancient Maya landscape alterations or other drivers were responsible for floods. Nonetheless, it is clear from this thesis that the Maya were altering their landscape, and that fluvial activity changed over time. This type of work requires many years of interdisciplinary research in order to study many deep sediment sequences and produce a long-term chronology of landscape formation. It is interesting to note that even the deepest sequences studied in this thesis did not produce dates that were as old as would be expected. The oldest dates in these sequences correspond to the Early Preclassic.

We need more research to address questions brought up by this thesis. First, we need more dates from the exposures discussed in this thesis. This will help us to refine the chronology of deposition and erosion. More dates will also provide us with insight into why such deep sequences show younger than anticipated dates. It may be that the river has experienced a huge amount of aggradation over the time that the Belize River Valley has had people living in it. However, we need more dates to address this idea. Additionally, we need many more deep exposures

accompanied by thorough dates, chemical analysis, and particle size analyses. Next steps should also include carbon isotope analyses for the soil samples that we have already collected, as well as for any new soil samples. This will enable us to correlate our dates with a chronology of land use and land cover patterns. We have described a new sequence of soil profiles and produced data that provides the foundation for this future work and development of a conceptual model.

References

Albert, D., MacLeod, B. 1971. "Caving in British Honduras." *National Speleological Society News* 29(1): 6-9.

Anselmetti, F.S., Hodell, D.A., Ariztegui, D., Brenner, M., Rosenmeier, M.F. 2007. "Quantification of soil erosion rates related to ancient Maya deforestation." *Geology* 35: 915-918.

Bateson, J.H. 1972. New interpretation of Maya Mountains, British Honduras. *American Association of Petroleum Geologists Bulletin* 56(5): 956-963.

Beach, T., Dunning, N., Luzzadder-Beach, S., Cook, D.E., Lohse, J. 2006. "Impacts of the ancient Maya on soils and soil erosion in the central Maya Lowlands." *Catena* 65: 166-178.

Beach, T. 2017. "Morals to the Story of the "Mayacene" from Geoarchaeology and Paleoecology." In: Exploring Frameworks for Tropical Forest Conservation: managing production and consumption for sustainability. UNESCO.

Beach, T., Luzzadder-Beach, S., Cook, D., Krause, S., Doyle, C., Eshleman, S., Wells, G., Dunning, N., Brennan, M.L., Brokaw, N., Cortes-Rincon, M., Hammond, G., Terry, R. Trein, D., Ward, S. 2018a. "Stability and instability on Maya Lowlands tropical hillslope soil. *Geomorphology* 305: 185-208.

Beach, T., Luzzadder-Beach, S., Krause S., Doyle, C. 2018b. "An Early Anthropocene Analog: The Geomorphology and Hydrology of the Rio Bravo Watershed in the Belize Tropics." Springer-Nature First International Conference of the Arabian Journal of Geosciences.

Beach, T., Luzzadder-Beach, S., Dunning, N., Jones, J., Lohse, J., Guderjan, T., Bozarth, S., Millspaugh, S., Bhattacharya, T. 2009. "A review of human and natural changes in Maya Lowland wetlands over the Holocene." *Quaternary Science Reviews* 28: 1710-1724.

Beach, T., Luzzadder-Beach, S., Dunning, N., Cook, D. 2008. "Human and natural impacts on fluvial and karst depressions of the Maya Lowlands." *Geomorphology* 101: 308-331.

Beach, T., Luzzadder-Beach, S., Krause, S., Walling, S., Dunning, N., Flood, J., Guderjan, T., Valdez, F. 2015. "'Mayacene' floodplain and wetland formation in the Rio Bravo Watershed of northwestern Belize." *The Holocene* 25: 1612-1626.

Belize Natural Resources Ltd. 1995. "Gladden Basin Offshore, Belize, CA." Unpublished farm-out Brochure.

Beresford-Jones, D., Lewis, H., Boreham, S. 2009. "Linking cultural and environmental change in Peruvian prehistory: Geomorphological survey of the Samaca Basin, Lower Ica Valley, Peru. *Catena* 78: 234-249

Birchall, C.J., Jenkin, R.N. 1979. "The Soils of the Belize Valley, Belize; Volume 1. Prepared by the Foreign and Commonwealth Office, Overseas Development Administration of the Land Resources Development Centre in Surrey, England. Supplementary Report 15.

Brown, A., Toms, P., Carey, C., Rhodes, E. 2013. "Geomorphology of the Anthropocene: Time-transgressive discontinuities of human-induced alluviation." *Anthropocene* 1: 3-13.

Burt, R. (Ed.), 2014. Soil Survey Laboratory Methods Manual. Soil Survey Investigations

Butzer, K. 1973. "Spring sediments from the Acheulian Site of Amanzi (Uitenhage District, South Africa)." *Quaternaria* 17: 299-319.

Butzer, K. W. 2008. “Challenges for a cross-disciplinary geoarchaeology: The intersection between environmental history and geomorphology. *Geomorphology* 101: 402-411.
Chase, A.F., Chase, D.Z. 2008. “Scale and intensity in Classic Period Maya agriculture: terracing and settlement at the “Garden City” of Caracol, Belize.” *Culture and Agriculture* 20: 60-77.
Chase A.F., Chase, D.Z., Weishampel, J.F., Drake, J.B., Shrestha, R.L., Slatton, K.C., Awe, J.J., Carter, W.E. 2011. “Airborne LiDAR, archaeology, and the ancient Maya landscape at Caracol, Belize.” *Journal of Archaeological Science* 38:387–398.
Chase, A.F., Chase, D.Z., Fisher, C.T., Leisz, S.J., Weishampel, J.F. 2012. “Geospatial revolution and remote sensing LiDAR in Mesoamerican archaeology.” *Proceedings of the National Academy of Science* 109: 12916-12921
Cherrington, E.A., Cho, P.P., Waight, I., Santos, T.Y., Escalante, A.E., Nabet, J., Usher, L. 2010. “Forest Cover and Deforestation in Belize: 1980-2010.” *Technical Report.*
Chevron Overseas Petroleum Company. 1975. “Belize Tectonic Map, structural elements overlay, scale 1:200,000.”
Cordova, C.E., Porter, J.C., 2015. The 1930s Dust Bowl: Geoarchaeological lessons from a 20th century environmental crisis. *The Holocene* 25: 1707-1720.
Dalan, R.A. 2006. “A geophysical approach to buried site detection using down-hole susceptibility and soil magnetic techniques.” *Archaeological Prospection* 13: 182–206.
Day, M. 1987. “Slope form, erosion, and hydrology in some Belizean karst depressions. *Earth Surface Processes and Landforms* 12: 497-505.
Day, M. 1993. “Resource use in the tropical karstlands of central Belize.” *Environmental Geology* 21: 122-128.
Day, M. 1996. ‘Karst and land use in central Belize’, *Proceedings 9th International Speleological Congress*, 1, 221 -223.
Denommee, K.C., Bentley, S.J., Droxler, A.W. 2014. “Climatic controls on hurricane patterns: a 1200-y near-annual records from Lighthouse Reef, Belize.” *Scientific Reports* 4: 3876.
Dillon, W.P., Vedder, J.G. 1973. Structure and Development of the Continental Margin of British Honduras. *Geological Society of America Bulletin* 84: 2713-2732.
Dixon, C.B. 1955. Geology of Southern British Honduras. Belize, Government Printer, 92 pp.
Dotterweich, M. 2013. “The history of human-induced soil erosion: Geomorphic legacies, early descriptions and research, and the development of soil conservation –A global synopsis.” *Geomorphology 201*: 1-34.
Douglas, P.M.J., Demarest, A.A., Brenner, M., Canuto, M.A. 2016. “Impacts of Climate Change on the Collapse of Lowland Maya Civilization.” *Annual Review of Earth and Planetary Sciences* 44: 613-645.
Dunning, N., Scarborough, V., Valdez, F., Luzzadder-Beach, S., Beach, T., Jones, J.G. 1999. “Temple mountains, sacred lakes, and fertile fields: ancient Maya landscapes in northwestern Belize. *Antiquity* 73: 650-660.
Dunning, N.P., Luzzadder-Beach, S., Beach, T., Jones, J.G., Scarborough, V., Culbert, T.P. 2004. “Arising from the Bajos: The Evolution of a Neotropical Landscape and the Rise of Maya Civilization.” *Annals of the Association of American Geographers* 92: 267-283.
Ebert, C.E., Culleton, B.J., Awe, J.J., Kennett, D. 2016. “AMS^{14} dating of Preclassic to Classic period household construction in the ancient Maya community of Cahal Pech, Belize.” *Radiocarbon* 58: 69-87.

Faust, D., Zielhofer, C., Baena Escudero, R., Diaz del Olmo, F. 2004. "High-resolution fluvial record of late Holocene geomorphic change in northern Tunisia: climatic or human impact?" *Quaternary Science Reviews* 23: 1757–1775.

Fedick, S. L. 1991. "The managed mosaic: ancient Maya agriculture and resource use." Papers presented at the Conference on Ancient Maya Agriculture and Biological Resource Management: 424 p.

Fedick, Scott. 1994. "Ancient Maya Agricultural Terracing in the Upper Belize River Area." *Ancient Mesoamerica* 5: 107-127.

Fernandez-Diaz, J.C., Carter, W.E., Shrestha, R.L., Glennie, C.L. 2013. "Lidar remote sensing." In: Handbook of Satellite Applications." Pp. 758-771, eds. J.N., Madry, S., Camacho-Lara, S. Springer Science + Business Media, New York.

Fleming, Steve, Madden, Marguerite, Leigh, David, Jackson, Phyllis, Menhart, Dustin, Peralta, Rodney. 2011. "Technical Analysis and Characterization of Southern Cayo, Belize, for Tropical Testing and Evaluation of Foliage Penetration Remote Sensing Systems." Produced by the Center for Environmental and Geographic Sciences in the Department of Geography and Environmental Engineering at the United States Military Academy and the Center for Remote Sensing and Mapping Science at the University of Georgia.

Flores, G. 1952. Geology of Northern British Honduras. *American Association of Petroleum Geologists Bulletin* 36(2): 404-413.

Gischler, E. 2003. "Holocene lagoonal development in the isolated carbonate platforms off Belize." *Sedimentary Geology 159*: 113-132.

Gischler, E., Hudson, J.H. 2004. "Holocene development of the Belize Barrier Reef." *Sedimentary Geology* 164: 223-236.

Graham, E. 2004. "Lamanai reloaded: Alive and Well in the Early Postclassic." *Research Reports in Belizean Archaeology* 1: 223-241.

Graham, E. Jones, G.D., Kautz, R.R. 1985. "Archaeology and ethnohistory on a Spanish colonial frontier: the Macal-Tipu project in western Belize." In: *The Lowland Maya Postclassic: Questions and Answers* (ed. A.F. Chase Rice, P.). Pp. 206-214. University of Texas Press.

Gran, K. B., Finnegan, N., Johnson, A.L., Belmont, P., Wittkop. C., Rittenour, T. 2013. "Landscape evolution, valley excavation, and terrace development following abrupt postglacial base-level fall." *GSA Bulletin* 125: 1851-1864.

Hach DR/850 Procedures Manual. Hach Co., 2013.

Hammond, G. 2016. "Water, stone and soil: a preliminary investigation into the location of selected sites in far northwest Belize to critical natural resources. In: *The ancient Maya city of Blue Creek. Wealth, social organization and ritual*. T. Guderjan (Ed.), BAR Press, Oxford, UK, pp. 17-29.

Hoggarth, J.A., Culleton, B.J., Awe, J.J., Kennett, D.J. 2014. "Questioning Postclassic continuity at Baking Pot, Belize, using direct AMS ^{14}C dating of human burials." *Radiocarbon* 56: 1057-1075.

Holley, George R., Woods, William I., Dalan, Rinita A., Watters, Harold W. 2000. "Implications of a buried Preclassic site in western Belize." In: *Mounds, Modoc, and Mesoamerica: Papers in Honor of Melvin L. Fowler*. Pp. 111-124. SR Ahler (Ed.). Illinois State Museum Scientific Papers, Vol XXVIII. Springfield.

Holliday, V.T., Gartner, W.G. 2007. "Soil phosphorus and archaeology: a review and comparison of methods." *Journal of Archaeological Science* 34: 301–333.

Jacob, John S. 1995. “Ancient Maya Wetland Agricultural Fields in Cobweb Swamp, Belize: Construction, Chronlogy and Function.” *Journal of Field Archaeology* 22: 175-190.
Kirke, CM St G. 1980. “Prehistoric agriculture in the Belize River valley.” *World Archaeology* 11: 281-286.
Knox, J.C. 2006. Floodplain sedimentation in the Upper Mississippi Valley: Natural versus human accelerated. *Geomorphology* 79: 286-310.
Krause, S.M. 2018. “Wetland Agroecosystems in the Maya Lowlands of Belize: LiDAR and Multi-Proxy Environmental Change.” *Doctoral Dissertation for the Department of Geography and the Environment at the University of Texas at Austin.*
Kwan, P., Eagles, P.F.J., Gebhardt, A. 2010. “Ecolodge patrons’ characteristics and motivations: a study of Belize.” *Journal of Tourism* 9: 1-20.
LacCore. 2013. Loss-on-Ignition Standard Operating Procedure. National Lacustrine Core Facility.
Lachniet, M.S., Patterson, W.P. 2009. “Oxygen isotope values of precipitation and surface waters in northern Central America (Belize and Guatemala) are dominated by temperature and amount effects. *Earth and Planetary Science Letters* 284: 435-446.
Lentz, D.L., Dunning, N.P., Scarborough, V.L., Magee, K.S., Thompson, K.M., Weaver, E., Carr, C., C., Terry, R.E., Islebe, G., Tankersley, K.B., Sierra, L.G., Jones, J.G., Buttles, P., Valdez, F., Ramos Hernandez,C.E. 2014. “Forests, fields, and the edge of sustainability at the ancient Maya city of Tikal.” *Proceedings of the National Academy of Sciences* 111: 18513-18518.
Luzzadder-Beach S., Beach, T. 2008. “Water Chemistry Constraints and Possibilities for the Ancient and Contemporary Maya Wetlands.” *The Journal of Ethnobiology*. 28: 211-230.
Luzzadder-Beach S., Beach, T. 2009. “Arising from the Wetlands: Mechanisms and Chronology of Landscape Aggradation in the Northern Coastal Plain of Belize.” *Annals of the Association of American Geographers*. 99:1-26.
Luzzadder-Beach, S., Beach, T.P., Dunning, N.P. 2012. "Wetland fields as mirrors of drought and the Maya abandonment." *Proceedings of the National Academy of Sciences*. 109(10):3646-3651.
Luzzadder-Beach, S., Beach, T., Hutson, S., Krause, S. 2016. “Sky-earth, Lake-sea: climate and water in Maya history and landscape.” *Antiquity*. 90:426-442.
Maidment, David R. 2002. *Arc hydro: GIS for water resources*. Redlands, Calif: ESRI Press.
McGovern, J.O. 1993. “Survey and excavation at Actuncan.” In *Xunantunich Archaeological Project 1993 Field Season*, ed. By R.M. Leventhal pp. 100-127
Meerman, J., Clabaugh, J. 2017. Biodiversity and Environmental Resource Data System of Belize. Online. http://www.biodiversity.bz
Mehlich, A. 1984. “Mehlich 3 soil test extractant: a modification of Mehlich 2”. *Communications in Soil Science and Plant Analysis* 15: 1409–1416.
Metcalfe, S., Davies, S. 2007. “Deciphering recent climate change in central Mexican lake records.” *Climatic Change* 83: 169-186.
Miller, J.B. 1966. “Photogeology, detailed landform and primary features, northern British Honduras.” 1:200,000 scale map, Chevron Exploration Company.
Miller, T. 1996. “Geologic and Hydrologic Controls on Karst and Cave Development in Belize.” *Journal of Cave and Karst Studies* 58: 100-120.
Miller, T.E. 2006. “Integration of a large tropical cave network in brecciated limestone: Caves Branch, Belize.” *Geological Society of America Special Paper 404*

Muhs, Daniel, Kautz, Robert R., MacKinnon, J. Jefferson. 1985. "Soils and the Location of Cacao Orchards at a Maya Site in Western Belize." *Journal of Archaeological Science* 12: 121-137.

Munsell, A.H. 2010. Munsell Soil Color Charts: with Genuine Munsell Color Chips. Grand Rapids, MI.

Nobre, A.D., Cuartas, L.A., Hodnett, M., Renno, C.D., Rodrigues, G., Silveira, A., Waterloo, M., Saleska, S. 2011. "Height Above the Nearest Drainange – a hydrologically relevant new terrain model." *Journal of Hydrology* 404: 13-29.

Ower, L.H. 1928. Geology of British Honduras. *Journal of Geology* 36: 494-509.

Pohl, M.D., Pope, K.O., Jones, J.G., Jacob, J.S., Piperno, D.R., deFrance, S.D., Lentz, D.L., Gifford, J.A., Danforth, M.E., Kathryn Josserand, J. 1996. "Early agriculture in the Maya lowlands." *Latin American Antiquity* 7: 355-372.

Pope, K.O., Ocampo, A.C., Fischer, A.G., Alvarez, W., Fouke, B.W., Webster, C.L., Vega, F.J., Smit, J., Fritsche, A.E., Claeys, P. 1999. "Chicxulub impact ejecta from Albion Island, Belize." *Earth and Planetary Science Letters* 170: 351-364.

Prufer, K., Thompson, A. E., Kennett, D. J. 2015. "Evaluating airborne LiDAR for detecting settlements and modified landscapes in disturbed tropical environments at Uxbenka, Belize." *Journal of Archaeological Science* 51: 1-13.

Purdy, E., Gischler, E. 2003. "The Belize margin revisited: 1. Holocene marine facies." *International Journal of Earth Sciences* 92: 532-551.

Roberts, P., Hunt, C., Arroyo-Kalin, M., Evans, D., Boivin, N. 2017. "The deep human prehistory of global tropical forests and its relevance for modern conservation." *Nature Plants* 3: 17093.

Robin, C. 1994. "Form, Function, and Meaning: 1994 Excavations on El Castillo, Structure A-6." In *Xunantunich Archaeological Project: 1994 Field Season*, ed. by R.M. Leventhal and W. Ashmore, pp. 48-64.

Roering, J.J., Mackey, B.H., Marshall, J.A., Sweeney, K.E., Deligne, N.I., Booth, A.M., Handwerger, A.L., Cerovski-Darriau, C. 2013. "'You are HERE': Connecting the dots with airborne lidar for geomorphic fieldwork." *Geomorphology* 200: 172-183.

Rosenmeier, M.F., Hodell, D.A., Brenner, M., Curtis, J.H., Guilderson, T.P. 2002a. "A 4000-year lacustrine record of environmental change in the southern Maya lowlands, Petén, Guatemala." *Quaternary Research* 57: 183-190.

Rosenmeier, M.F., HOdell, D.A., Brenner, M., Curtis, J.H. Martin, J.B., Anselmettic, F.S., Ariztegui, D., Guilderson, T.P. 2002b. "Influence of vegetation change on watershed hydrology: Implications for paleoclimatic interpretation of lacustrine $\delta^{18}O$ records." *Journal of Paleolimnology* 27: 117-131.

Saleska, S. 2011. "Height Above the Nearest Drainage – a hydrologically relevant new terrain model." *Journal of Hydrology* 404: 13-29.

Schlezinger, D.R. Howes, B.L. 2000. "Organic phosphorus and elemental ratios as indicators of Prehistoric Human Occupation." *Journal of Archaeological Science* 27: 479-492.

Schuldenrein, J. 2007. "A reassessment of the Holocene stratigraphy of the Wadi Hasa Terrace and Hasa Formation, Jordan." *Geoarchaeology* 22: 559–588.

Smith, A. Sampson, C., Bates, P. 2014. "Regional Flood Frequency Analysis at the Global Scale." *Water Resources Research* 51: 539-553.

Smith, J. 1998. “Geology and Carbonate Hydrogeochemistry of the Lower Mopan and Macal River Valleys, Belize.” *Master’s Thesis for the Department of Geology at the University of Pennsylvania*. Pp. 1-94.
Soil Survey Staff. 1975. “Soil Taxonomy: A Basic System of Classification for Making and Interpreting Soil Surveys.” Agriculture Handbook No. 436. Washington: US Government Printing Office.
Soil Survey Staff. 1999. Soil taxonomy: A basic system of soil classification for making and interpreting soil surveys. 2nd edition. Natural Resources Conservation Service. U.S. Department of Agriculture Handbook 436.
Stemp, W.J., Awe, J.J., Prufer, K.M., Helmke, C.G.B. 2016. “Design and function of Lowe and Sawmill points from the preceramic period of Belize.” *Latin American Antiquity* 27: 279-299.
Taschek, J.T., Ball, J.W. 1986. “Guerra: A Late Classic suburban paraje of Buena Vista del Cayo, Belize.” Paper presented at the 51st Annual Meeting of the Society for American Archaeology, New Orleans.
Terry, R. E., Fernandez, F. G., Parnell, J. J., and Inomata, T. 2004. “The story in the floors: chemical signatures of ancient and modern Maya activities at Aguateca, Guatemala.” *Journal of Archaeological Science* 31: 1237-1250.
Trigg, M., Smith, A., Sampson, C. 2016. “CHaRIM Project (www.charim.net) Belize National Flood Hazard Mapping Methodology and Validation Report (FINAL VERSION).” *Caribbean Handbook on Risk Information Management*
USDA. Report No. 42. USDA-NRCS. National Soil Survey Center, Lincoln, NE.
Van Wambeke, A. 1987. “Soil moisture and temperature and moisture regimes of Central America, Caribbean, Mexico.” *USDA Soil Management Support Services Technical Monograph*, vol. 16, Department of Agronomy, Cornell University, Ithaca, N.Y.
Verstraeten, G., Broothaerts, N., Van Loo, M., Notebaert, B., D’Haen, K., Dusar, B., De Brue, H. 2017. “Variability in fluvial geomorphic response to anthropogenic disturbance.” *Geomorphology* 294: 20-39
Walter, R.C., Merritts, D.J. 2008. “Natural streams and the legacy of water-powered mills.” *Science* 31: 299–304
Wells, E. C. 2004. “Investigating ancient patterns in prehispanic plazas: weak acid extraction ICP-AES analysis of anthrosols at classic period El Coyote, Northwestern Honduras.” *Archaeometry* 46: 67-84.
Williams, N. 1996. “An introduction to cave exploration in Belize.” *Journal of Cave and Karst Studies* 58: 69-75.
World Bank Group. 2018. Climate Change Knowledge Portal. http://sdwebx.worldbank.org/climateportal/index.cfm?page=country_historical_climate&ThisCCode=BLZ
Xiaorong, W., Mingde, H., Mingan, S. 2007. “Copper fertilizer effects on copper distribution and vertical transport in soils.” *Geoderma* 138: 213-220.
Yaeger, J. 1997. “The 1997 Excavations of Plaza A-III and Miscellaneous Excavation and Architectural Clearing in Group A.” In *Xunantunich Archaeological Project: 1997, the Final Field Season*, ed. by R.M. Leventhal and W. Ashmore, pp. 24-55.
Yaeger, J. 2000. “Changing patterns of social organization: The Late and Terminal Classic communities at San Lorenzo, Cayo District, Belize.” Dissertation, Department of Anthropology at the University of Pennsylvania.

Vita

Leila Dolce Donn received a BS in Geology from Sewanee: The University of the South in 2011. After graduation, she worked as a professional geologist and environmental scientist for five years. During these five years, she worked at an exploration phase mine in northern Alaska, for Baker Hughes and Exxon on an offshore drill ship, for ARCADIS environmental consulting, and for the State of Tennessee. While in these positions she logged soil, performed analyses and created maps using ArcGIS, and completed soil and groundwater field and lab work. Leila began her MA at UT Austin in 2011 and is continuing her dissertation at UT with Dr. Timothy Beach. Her dissertation will focus on developing a machine-learning method of identifying cave entrances using LiDAR imagery, and then using this method to find caves that may contain stalagmite climate records in the Maya Lowlands of Petén, Guatemala.

Permanent address (or email): <leiladonn@utexas.edu

This thesis was typed by Leila Dolce Donn